

HETEROPOLYACID CATALYSTS FOR ETHERIFICATION OF ISOOLEFINS

A THESIS SUBMITTED TO
THE GRADUATE SCHOOL OF NATURAL AND APPLIED SCIENCES
OF
THE MIDDLE EAST TECHNICAL UNIVERSITY

BY

ZEYNEP OBALI

IN PARTIAL FULFILLMENT OF THE REQUIREMENTS FOR THE DEGREE OF
MASTER OF SCIENCE
IN
THE DEPARTMENT OF CHEMICAL ENGINEERING

SEPTEMBER 2003

Approval of the Graduate School of Natural and Applied Sciences

Prof. Dr. Canan Özgen
Director

I certify that this thesis satisfies all the requirements as a thesis for the degree of Master of Science.

Prof. Dr. Timur Doğu
Head of Department

This is to certify that we have read this thesis and that in our opinion it is fully adequate, in scope and quality, as a thesis and for the degree of Master of Science.

Prof. Dr. Timur Doğu
Supervisor

Examining Committee Members

Prof. Dr. A. Tülay Özbelge

Prof. Dr. Timur Doğu

Prof. Dr. Güzide Çalık

Assoc. Prof.Dr. Gürkan Karakaş

Assoc. Prof. Dr. Pınar Çalık

ABSTRACT

HETEROPOLYACID CATALYSTS FOR ETHERIFICATION OF ISOOLEFINS

Obalı, Zeynep

M.Sc. in Chemical Engineering

Supervisor: Prof. Dr. Timur Doğu

September 2003, 116 pages

Due to the water pollution problems created by MTBE, significant research was focused on the production of alternative oxygenates, such as ethyl *tert*-butyl ether (ETBE), *tert*-amyl-methyl-ether (TAME) and *tert*-amyl-ethyl-ether (TAEE) as octane enhancing gasoline blending components. These oxygenates are expected to improve the burning characteristics of gasoline and reduce exhaust emissions of CO and hydrocarbons. Generally, macroreticular acidic resin catalysts (Amberlyst-15) are used for the etherification reactions between C₅ iso-olefins (2M1B/2M2B) and alcohols (ethanol/methanol). But in recent years, heteropoly acid compounds are being used in the production of *tert*-ethers to replace those macroreticular acidic resin catalysts. HPAs are known to be active catalysts for many of homogeneous and heterogeneous acid catalyzed reactions.

These compounds have high acidity, high catalytic activity but they are highly soluble in polar solvents such as water, alcohol when they are used in bulk form.

In this research, applicability of bulk heteropoly acid (HPA) and its supported form, to the gas-phase etherification reaction of iso-olefin (2-methyl-2-butene) with ethyl alcohol in a continuous differential reactor was investigated. The heteropoly acid ($H_3PW_{12}O_{40} \cdot xH_2O$) was supported on activated carbon, at two different loading levels, by aqueous impregnation technique. After catalyst characterization, kinetic experiments were done in a temperature range between 80°C-97°C with a feed concentration of 30 vol.% 2M2B+70 vol.% ethanol. Supported HPA catalysts yielded lower conversion and rate of reaction than the bulk HPA. After that, to make a comparison, same experiments have been carried out with Amberlyst-15 and a different HPA ($H_3PMo_{12}O_{40} \cdot xH_2O$) at 90°C. The results showed that, at this temperature, bulk tungstophosphoric acid ($H_3PW_{12}O_{40} \cdot xH_2O$) was highly active among the other catalysts. Moreover, the deactivation of bulk and supported HPA were investigated and found that partial deactivation occurred when they were reused, without any treatment. In the final part of the study, the activity of alcohol-treated supported HPA catalyst and formation of side products, dimethyl or diethyl ether, at 90°C were investigated. When the supported catalyst was treated with alcohol, before utilizing in the experiments, lower conversion was obtained with respect to the conversion value obtained in the presence of fresh catalyst. The studies done on the formation of side product showed that, no side product was formed at this working temperature.

Key Words: Octane enhancer, 2M2B, Ethanol, TAEE, Catalyst, Heteropoly Acid, Activated Carbon, Impregnation Technique, Supported Heteropoly Acid

ÖZ

İZOOLEFİNLERİN ETERİFİKASYONUNDA KULLANILAN HETEROPOLİASİT KATALİZÖRLERİ

Obalı, Zeynep

Yüksek Lisans, Kimya Mühendisliği

Tez Yöneticisi: Prof. Dr. Timur Doğu

Eylül 2003, 116 sayfa

MTBE'in neden olduğu çevresel problemler nedeniyle alternatif oktan yükseltici bileşikler konusundaki araştırmalar, etil tersiyer-bütül eter (ETBE), tersiyer-amil metil eter (TAME) ve tersiyer-amil etil eter (TAEE) üretimine yönelmiştir. Bu eterler, yakıtın yanma özelliklerini arttırmanın yanısıra karbon monoksit ve yanmamış hidrokarbon emisyonunu azaltmaktadır. C₅ izoolefinlerinin (2M1B/2M2B), alkolle(etanol/metanol) eterleşme reaksiyonlarında genellikle makroretiküler asidik reçine katalizörleri(Amberlit-15) kullanılmaktadır. Fakat, son yıllarda tersiyer eter üretiminde bu reçine katalizörleri yerine heteropoli asit (HPA) katalizörleri kullanılmaya başlanmıştır. Heteropoliasit katalizörlerinin birçok homojen ve heterojen reaksiyonda aktif olduğu bilinmektedir Bu bileşikler yüksek aktiflik ve asitliğe sahiptirler ancak saf halde kullanıldıkları zaman polar çözücülerde (su ve alkol gibi) çözünmektedirler.

Bu çalışmada, sürekli bir diferansiyel reaktörde, izo-olefinin (2-metil-2-büten) etil alkolle gaz fazında eterleşme reaksiyonlarına heteropoliasit bileşiklerinin, saf ve destekli şekliyle, uygulanabilirliği çalışılmıştır. Destekli heteropoliasit ($H_3PW_{12}O_{40} \cdot xH_2O$) katalizörü, saf heteropoliasidin aktif kömür üzerine, ağırlıkça iki farklı yükleme seviyesinde, emdirme tekniği kullanılarak yüklenmesiyle hazırlanmıştır. Katalizör karakterizasyonu yapıldıktan sonra 80°C-97°C sıcaklık aralığında kinetik çalışmalar yapılmıştır. Besleme karışımı içerisindeki 2M2B yüzdesi 30, etanol yüzdesi ise 70 olarak alınmıştır. Destekli HPA katalizörü, saf heteropoliaside göre daha düşük dönüşüm ve reaksiyon hız değerleri vermiştir. Daha sonra bir karşılaştırma yapabilmek için, aynı deneyler Amberlit-15 ve başka bir heteropoliasit katalizörü ($H_3PMo_{12}O_{40} \cdot xH_2O$) ile 90°C' de tekrarlanmış ve saf heteropoliasidin, bu sıcaklıkta, diğer katalizörlerden daha yüksek aktivite gösterdiği saptanmıştır. Bunlara ilaveten, aynı sıcaklık aralığında saf ve destekli heteropoliasitin deaktivasyonu çalışılmış ve kısmen deaktive olduğu gözlemlenmiştir. Çalışmanın son kısmında, 90°C de, alkolle muamele edilmiş destekli heteropoliasidin aktivitesinin incelenmesinin yanısıra yan ürün, dimetil veya dietil eter oluşup oluşmadığı incelenmiştir. Bu çalışma sıcaklığında, alkolle muamele edilmiş katalizör, işlem görmemiş destekli katalizöre göre daha az dönüşüm değeri vermiş ve ayrıca, bu sıcaklıkta herhangi bir yan ürün oluşumuna rastlanmamıştır.

Anahtar Kelimeler: Oktan yükseltici, 2M2B, Etanol, TAEE, Katalizör, Heteropoliasit, Aktif kömür, Emdirme tekniği, Destekli heteropoliasit

To my Family and Friends,

ACKNOWLEDGEMENTS

First, I would like to express my sincere appreciation to Prof. Timur Dođu for his guidance, support and encouragement throughout this study. Also, thanks are extended to Prof. Gölşen Dođu and Gazi University Research Group for their support in this study.

I would like to thank here my family, my mother Olcay Obalı, my father Metin Obalı, for their big supports, patience and faith in me, in every moment throughout my education. Thanks for their big love...

I would like to thank Dilek Varıřlı. Thanks for loving, supporting and helping me all time. I want to send my best wishes and my loves to my dearest friends, Almıla Bahar, İsmail Dođan, Özge Ođuzer, Alp Yürüm, Deđer Şen, Yalçın Yıldız, Berker Fıçıcılar, Başak Kurbanođlu and Onur Diri for their good friendship and for their support while writing this thesis. Also I want to send my best wishes to far away from here to Işıl Severcan and Mustafa Tekin Dokucu hoping to see them in a very short time.

I would like to thank Nezahat Boz, for giving support and sharing her ideas with me during our studies.

Finally, I would also like to thank all other people whom I could not name here, for being near me in these years.

TABLE OF CONTENTS

ABSTRACT.....	iii
ÖZ	v
DEDICATION.....	vii
ACKNOWLEDGEMENTS	viii
TABLE OF CONTENTS	ix
LIST OF TABLES	xiii
LIST OF FIGURES	xv
NOMENCLATURE.....	xvi
CHAPTER	
1 INTRODUCTION.....	1
2 OXYGENATES	4
2.1 HISTORICAL DEVELOPMENT OF FUEL OXYGENATES	4
2.2 PROPERTIES AND PRODUCTION OF OXYGENATES.....	7
2.2.1 Methanol	8
2.2.2 Ethanol.....	8
2.2.3 MTBE (Methyl <i>tert</i> -Butyl Ether)	8
2.2.4 ETBE (Ethyl <i>tert</i> -Butyl Ether)	10
2.2.5 TAME (<i>tert</i> - Amyl Methyl Ether)	12
2.2.6 TAEE (<i>tert</i> - Amyl Ethyl Ether)	14
2.2.7 DIPE (Diisopropyl ether)	17
2.3 CATALYST USED IN THE ETHERIFICATION REACTIONS.....	18
3 HETEROPOLY ACIDS	22

3.1 PREPARATION OF HETEROPOLY ACIDS.....	23
3.2 STRUCTURAL CHARACTERISTICS	24
3.2.1 Molecular Structure	24
3.2.2 Proton Structure	28
3.2.3 Surface Area and Pore Structure	29
3.2.4 Thermal Stability and Water Content.....	29
3.2.5 Pseudo-liquid Phase.....	30
3.3 ACIDIC PROPERTIES.....	31
3.3.1 Heteropoly Acids in Solution	33
3.3.2 Solid Heteropoly Acids	35
3.4 REDOX PROPERTIES	35
3.5 SUPPORTED HETEROPOLY ACIDS	36
3.5.1 HPA on Silica	36
3.5.2 HPA on Mesoporous Molecular Sieve	37
3.5.3 HPA on Carbon	38
3.5.4 HPA on Ion-Exchange Resins	38
3.5.5 Other Supported HPA Catalysts.....	38
3.6 HETEROPOLY ACID SALTS	39
3.7 HOMOGENEOUS CATALYSIS	40
3.7.1 Hydration of Olefins.....	42
3.7.2 Esterification and Related Reactions.....	43
3.7.3 Condensation	45
3.8 BIPHASIC CATALYSIS	46
3.8.1 Polymerization of Tetrahydrofuran	46
3.8.2 Esterification	47
3.8.3 Other Reactions	47
3.9 HETEROGENEOUS CATALYSIS.....	48
3.9.1 Paraffin Alkylation	48

3.9.2	Friedel-Crafts and Related Reactions.....	49
3.9.3	Esterification, Hydrolysis, and Related Reactions.....	50
4	EXPERIMENTAL	52
4.1	CHEMICALS AND CATALYSTS.....	52
4.2	EXPERIMENTAL SET-UP.....	53
4.3	EXPERIMENTAL PROCEDURE.....	55
4.3.1	Preparation of Supported Heteropoly Acid Catalysts	55
4.3.2	Characterization of Catalysts	56
4.3.3	Catalytic Reactions.....	56
4.3.4	Analytical Method.....	59
5	RESULTS AND DISCUSSION.....	61
5.1	CATALYST CHARACTERIZATION	62
5.1.1	Determination of Water of Crystallization.....	62
5.1.2	Determination of Surface Area and Pore Diameter	63
5.1.3	Determination of Porosity of Activated Carbon.....	64
5.1.4	Determination of Calcination Temperature of Catalysts	64
5.2	CATALYTIC REACTIONS	66
5.2.1	Catalytic Activity of Bulk Heteropoly Acid.....	66
5.2.2	Catalytic Activity of Supported Heteropoly Acid.....	70
5.2.3	Comparison of Catalysts.....	75
5.2.4	Deactivation of Bulk and Supported Heteropoly Acid.....	77
5.2.5	Catalytic Activity of Alcohol-treated Supported Heteropoly Acid	78
5.2.6	Side Product Formation Reactions.....	79
6	CONCLUSIONS AND RECOMMENDATIONS	80
	REFERENCES	82
	APPENDICES.....	88
A	GAS CHROMATOGRAPH CALIBRATION FACTORS	88
A.1	Sample Calculation for Finding Calibration Factors.....	89

A.2	Sample Calculation for Finding Concentration from GC	90
B	CALCULATIONS	92
B.1	Calculation of Vapor-Phase Equilibrium Constants	92
B.2	Calculation of Vapor-Phase Equilibrium Conversions	95
B.3	Calculation of Reaction Rate in a Continuous Differential Reactor	97
B.4	Calculation of Volume Fraction from Experimental Data.....	98
B.5	Calculation of Molar Flow Rate	98
B.6	Calculation of Initial Molar Concentration (Theoretical).....	99
C	EXPERIMENTAL DATA.....	100
C.1	Experimental Data for 1.Experiment (Bulk TPA)	100
C.2	Experimental Data for 2.Experiment (Bulk TPA-reproduced)	101
C.3	Experimental Data for 3.Experiment (25-wt%TPA/AC, $T_{\text{calc.}}$:120°C) .	102
C.4	Experimental Data for 4.Experiment (25-wt%TPA/AC, $T_{\text{calc.}}$:180°C) .	103
C.5	Experimental Data for 5.Experiment (31-wt% TPA/AC)	104
C.6	Experimental Data for 6.Experiment (25-wt%TPA/AC, $T_{\text{calc.}}$:120°C) .	105
C.7	Experimental Data for 7.Experiment (25-wt%TPA/AC, $T_{\text{calc.}}$:180°C) .	106
C.8	Experimental Data for 8.Experiment (25-wt%TPA/AC, $T_{\text{calc.}}$:120°C) .	107
C.9	Experimental Data for 9.Experiment (25-wt%TPA/AC, $T_{\text{calc.}}$:180°C) .	108
C.10	Experimental Data for 10.Experiment (31-wt% TPA/AC).....	109
C.11	Experimental Data for 11.Experiment (Amberlyst-15)	110
C.12	Experimental Data for 12.Experiment (Bulk MPA)	111
C.13	Experimental Data for 13.Experiment (Bulk TPA).....	112
C.14	Experimental Data for 14.Experiment(25-wt%TPA/AC, $T_{\text{calc.}}$:120°C) 113	
C.15	Experimental Data for 15.Experiment (31-wt% TPA/AC).....	115
C.16	Experimental Data for 16.Experiment (Bulk TPA).....	116

LIST OF TABLES

2.1 Oxygenates for reformulated gasoline	7
2.2 Properties of some hydrocarbons and oxygenates	16
2.3 Typical composition of FCC light gasoline	17
3.1 Advantage of Solid Heteropoly Catalysts.....	23
3.2 Hammett acidity function for some solid acid catalysts	33
3.3 Dissociation Constants for Heteropoly Acids in Acetone at 25°C.....	34
3.4 Properties of Heteropoly Acid Salts	40
3.5 Some Homogeneous Reactions Catalyzed by HPA	42
4.1 Physical Properties of the Amberlyst-15 Catalyst	52
4.2 Properties of Chemicals Used in the Experiments	53
4.3 The outline of the experiments.....	58
4.4 Calibration Factors for reactants and products	60
5.1 Equilibrium Conversion Values at Different Temperatures.....	70
5.2 Comparison of conversion values obtained at 90°C (w=0.2g).....	76
5.3 Comparison of reaction rates obtained at 90°C (w=0.2g)	76
A.1 The evaluation of calibration factor α for 2M2B.....	90
B.1 Enthalpy of vaporization values at 298 K	93
B.3 Liquid-phase heat capacity equation constants	94
B.4 Vapor and Liquid-Phase Equilibrium Constants	95
B.5 Equilibrium Conversion vs. Temperature.....	97
C.1 By-pass data of 1.Experiment (w=0.2 g)	100
C.2 Experimental data for 1.Experiment.....	101
C.3 By-pass data of 2.Experiment (w=0.2 g)	101
C.4 Experimental data for 2.Experiment.....	102
C.5 By-pass data of 3.Experiment (w=0.2 g)	102
C.6 Experimental data for 3.Experiment.....	103
C.7 By-pass data of 4.Experiment (w=0.2 g)	103
C.8 Experimental data for 4.Experiment.....	104
C.9 By-pass data of 5.Experiment (w=0.2 g)	104
C.10 Experimental data for 5.Experiment.....	105

C.11 By-pass data of 6.Experiment (w=0.2 g)	105
C.12 Experimental data for 6.Experiment	106
C.13 By-pass data of 7.Experiment (w=0.2 g)	106
C.14 Experimental data for 7.Experiment	107
C.15 By-pass data of 8.Experiment (w=0.8 g)	107
C.16 Experimental data for 8.Experiment	108
C.17 By-pass data of 9.Experiment (w=0.8 g)	108
C.18 Experimental data for 9.Experiment	109
C.19 By-pass data of 10.Experiment (w=0.644 g)	109
C.20 Experimental data for 10.Experiment	110
C.21 By-pass data of 11.Experiment (w=0.2 g)	110
C.22 Experimental data for 11.Experiment	111
C.23 By-pass data of 12.Experiment (w=0.2 g)	111
C.24 Experimental data for 12.Experiment	111
C.25 By-pass data of 13.Experiment (w=0.2 g)	112
C.26 Experimental data for 13.Experiment (1.run)	112
C.27 Experimental data for 13.Experiment (2.run)	113
C.28 By-pass data of 14.Experiment (w=0.2 g)	113
C.29 Experimental data for 14.Experiment (1.run)	114
C.30 Experimental data for 14.Experiment (2.run)	115
C.31 By-pass data of 15.Experiment (w=0.644 g)	115
C.32 Experimental data for 15.Experiment	116
C.33 Experimental data of 16.Experiment (methanol)	116
C.34 Experimental data of 16.Experiment (ethanol)	116

LIST OF FIGURES

3.1 Heteropolyanion with the Keggin structure.....	25
3.2 Heteropolyanion with Wells – Dawson structure.....	26
3.3 Heteropolyanion with Anderson structure.....	27
3.4 An example of the secondary structure $H_3PW_{12}O_{40} \cdot 6H_2O$	28
4.1 Experimental Set-Up	54
5.1 TGA result of bulk tungstophosphoric acid	62
5.2 TGA result of bulk molybdophosphoric acid	63
5.3 TGA result of 25-wt% TPA/AC catalyst	65
5.4 TGA result of 31-wt% TPA/AC catalyst	66
5.5 Variation of conversion with temperature in the presence of bulk tungstophosphoric acid (Exp.#: 1-2)	68
5.6 Variation of reaction rates with temperature in the presence of bulk tungstophosphoric acid (Exp.#: 1-2)	68
5.7 Variation of conversion with temperature in the presence of three different supported catalysts (Exp.#: 3-5)	71
5.8 Variation of reaction rates with temperature in the presence of three different supported catalysts (Exp.#:3-5).....	71
5.9 Variation of conversion with temperature in the presence of 25-wt% TPA/AC (reproducibility check)	72
5.10 Variation of reaction rate with temperature in the presence of 25-wt% TPA/AC (reproducibility check) (Exp.#: 6-7)	72
5.11 Comparison of bulk and supported tungstophosphoric acid catalysts ($w_{total}=0.2$ g) (Exp.#: 1,3-5)	73
5.12 Variation of conversion with temperature at different levels of catalyst loading to reactor (Exp.#: 8-10)	74
5.13 Deactivation of bulk TPA (Exp.#:13)	77
5.14 Deactivation of 25-wt%TPA/AC(T_{calc} : 120°C)(Exp.#:14)	78

NOMENCLATURE

a_i	Activity of species i
K_j	Equilibrium Constant for reaction j
y_i	Mole Fraction of species i in the mixture
X_{Af}	Total Conversion of Olefin to TAE
m	Mass of the catalyst, g
F_{A0}	Initial Molar Flow Rate of specie A, mol/s
R	Gas Constant, J/mol.K
ΔH_{vJT}	Enthalpy of Vaporization of j , kJ/mol
MW_i	molecular Weight of species i , g/mol

Abbreviations:

2M2B	2-methyl-2-butene
2M1B	2-methyl-1-butene
MTBE	Methyl <i>tert</i> -butyl ether
ETBE	Ethyl <i>tert</i> -butyl ether
TAME	<i>tert</i> -amyl methyl ether
TAE	<i>tert</i> -amyl ethyl ether
DIPE	Diisopropyl ether
TBA	<i>tert</i> -butyl alcohol
IPA	isopropyl alcohol
FCC	Fluid Catalytic Cracking
HPA	Heteropoly acid
TPA	Tungstophosphoric acid
MPA	Molybdophosphoric acid
AC	Activated carbon
FID	Flame Ionization Detector
BET	Brunauer-Emmett-Teller
TGA	Thermal Gravimetric Analysis

Greek Letters

α_I	Gas Chromatography calibration factor for ith species
ϵ	Porosity
ϕ_i	Fugacity coefficients of species i
ν_i	Stoichiometric coefficients of species i in reaction
ρ_i	Density of species i

CHAPTER 1

INTRODUCTION

Environmental considerations have become by far the most substantial drive in product reformulation for transportation fuels. The late 80's and early 90's have shown public awareness and concern in environmental issues. Governments and regulatory agencies all over the world have by now been sensitized to these issues and are taking legislative steps that affect rather profoundly the refining industry. Regulations aimed to reduce the impact of transportation fuels on the ecosystem and especially on human health [1].

Correlation of gasoline physical properties and their impact on human health, air quality and the environment, is the issue of great relevance. For the definition of proper quality standards, which could really affect the end result of the legislation, in spite of the great deal of work in this area, it is still difficult to establish relationships and effect between all the variables. Smylie *et.al.*[2] reviewed the impact on air quality of gasoline reformulation efforts. These gasoline would usually differ from "conventional" fuels at least three features: lower volatility, presence of an oxygenate and lower aromatics.

In the early 1980's, as demand for unleaded gasoline grew, oxygenated fuel components received attention. Their combustion properties allow them to suppress the undesirable phenomenon known as engine knock. Lead -

containing additives had traditionally played this role, and, with their use being restricted or eliminated by regulations and laws, the use of oxygenates as gasoline blend components increased [3].

Two classes of oxygenates are of primary interest as fuel blending components, alcohols and ethers. The alcohols include methanol and ethanol, and the ethers include methyl *tert*-butyl ether (MTBE), ethyl *tert*-butyl ether (ETBE), *tert*-amyl methyl ether (TAME) and *tert*-amyl ethyl ether (TAEE). MTBE is the most popular oxygenate but it creates water pollution problems and is thought to be carcinogenic. ETBE is a good alternative to MTBE since it is produced by the reaction of olefin and ethanol. Producing oxygenates from Fluid Catalytic Cracking (FCC) olefins have several advantages. It allows higher levels of oxygenate production, which lowers the proportion of olefins in the gasoline pool and maximizes the use of FCC olefins [4]. TAME and TAEE are produced by C₅ reactive olefins, which is present in FCC light gasoline at a 13-weight percentage.

Generally, macroreticular acidic resin catalysts are used for the etherification reactions between C₄ and C₅ iso-olefins and alcohols. But in recent years, heteropoly acid compounds are being used in the production of *tert*-ethers to replace those macroreticular acidic resin catalysts.

Heteropoly acids, their salts and supports are known to be active catalysts for many homogeneous and heterogeneous acid catalyzed reactions [5-7]. A growing interest has been developed related with the chemical, physical and the activity of these compounds, such as; very strong Brønsted acidity, approaching to superacid region, fairly high stability, structure with high proton mobility and high solubility in polar solvents, high catalytic activity and pseudo-liquid phase behavior, in which solid heteropoly acids behave like concentrated solutions

toward polar substances. So, reaction proceeds not only on the surface but also in the bulk of the crystalline heteropoly acid.

In this research, applicability of bulk heteropoly acid and its supported form, to the etherification reaction of isoamylene (2-methyl-2-butene) with ethyl alcohol in a continuous differential reactor was investigated. The effect of temperature and the effect of loading amount of heteropoly acid on the conversion and reaction rate were studied. Tungstophosphoric ($\text{H}_3\text{PW}_{12}\text{O}_{40}\cdot x\text{H}_2\text{O}$) acid (TPA) type of heteropoly acid was used as active solid acid catalysts and impregnated on the activated carbon (AC). Also, to make a comparison of activity of that pure and supported heteropoly acid, same studies, at a fixed temperature, were done with a macroreticular acidic resin (Amberlyst-15) and bulk molybdophosphoric acid ($\text{H}_3\text{PMo}_{12}\text{O}_{40}\cdot x\text{H}_2\text{O}$), which is another heteropoly acid type. Moreover, the deactivation of supported catalyst (TPA on AC) and of bulk tungstophosphoric acid was investigated. After that, the catalytic activity of alcohol treated supported tungstophosphoric acid was investigated at a fixed temperature of 90°C.

CHAPTER 2

OXYGENATES

Periodical oil crises, environmental issues, and energy consumption optimization brought oxygenated compounds into consideration as fuel additives with the role of enhancer and/or octane booster. Light alcohols and ethers offer different and specific advantages in meeting the clean fuel requirements. Methyl *tert*-butyl ether (MTBE) was preferred product up to now; positive future perspectives can be envisaged for the less volatile ethyl *tert*-butyl ether (ETBE), *tert*-amyl methyl ether (TAME) and *tert*-amyl ethyl ether (TAE).

2.1 HISTORICAL DEVELOPMENT OF FUEL OXYGENATES

At the end of the 1950s, petroleum refinery seemed to have reached a satisfactory technological level representing a good energy / economy balance. However, great increase in energy consumption and deterioration of the environment led to the recognition during the 1960s that energy production and automotive transportation were major causes of air-quality deterioration. By the 1970s it became clear that petroleum refining had to meet a new goal: energy, economy, and environment together [8].

The most publicized environmental measure adopted in the 1970s was the progressive phasing-out of lead additives in motor fuels and the introduction of

severe emission limits for 1975 that could be met only by the application of catalytic converters for the oxidation of CO and hydrocarbons in automobile exhaust. By 1978, NO_x emissions had to be reduced drastically, which brought about the development of the three-way catalytic converter, allowing a simultaneous reduction of CO, hydrocarbons and NO_x.

The complete removal of lead additives from gasoline was necessary for the technical operability of catalytic converters because the catalysts are intolerant of lead that causes them to deactivate rapidly. An important technical consequence of the reduction of lead concentration in gasoline was a notable drop in gasoline octane number, which could not be tolerated by millions of automobiles designed for high-octane-number fuel. The immediate solution for the problem was to raise octane number with increasing concentrations of butanes and aromatics in gasoline. Since aromatics were known as carcinogenic species, a second and more innovative solution was developed. It was the use of a new class of high-octane oxygenated compounds, called oxygenates.

According to the ASTM D 4814 'Standard Specification for Automotive Spark-Ignition Engine Fuel' an oxygenate is defined as *an oxygen containing, ashless organic compound, such as an alcohol or ether, which can be used as a fuel or fuel supplement.*

Oxygenates began to be added to gasoline and to play an increasingly important role in gasoline formulation, as octane booster replacing alkyl lead, from 1973. During the oil crises of the early 1970s, oxygenates originating from sources partially alternative to crude oil, played also a role as volume extenders.

The oxygenate market was dominated by methyl *tert*-butyl ether (MTBE), due to its octane blending value, relatively low volatility, complete miscibility

with gasoline, low susceptibility to phase separation in the storage and distribution system and low tendency to undergo peroxidation. MTBE became the fastest growing chemical of the 1980s [8].

Starting in 1975, the entire US production of new cars had catalytic converters and was run with unleaded gasoline. But, the unleaded gasoline/catalytic converter solution did not completely solve the car emission abatement. At the end of 1980s, the public concern about the winter high CO concentration and summer ozone levels brought to consideration a reformulation in gasoline and diesel fuel composition as an essential mean to low road pollution.

A new more global approach was introduced by the Amendments of Clean Air Act, issued in 1990 (1990 CAAA) [9]. It was designed to control air pollution problems nationwide at affordable costs. Specifications for gasoline and diesel fuel were enforced by CAAA and two new fuels were mandated:

- ❖ Oxygenated gasoline during the winter months in areas that do not comply with CO emission standard.
- ❖ Reformulated gasoline (RFG) all year around in areas that do not comply with ozone emission standard.

Both 'oxygenated gasoline' and RFG require certain oxygen content. The CAAA gave to oxygenates the new role of clean air additives, advancing that of octane supplier.

Despite the controversial future of oxygenates as 'clean air additive', they are expected to maintain and extend the role of 'octane supplier' to replace butanes and aromatics.

2.2 PROPERTIES AND PRODUCTION OF OXYGENATES

Fuel oxygenates improve the hydrocarbon burning efficiency of gasoline and reduce CO emissions. They also help to reduce atmospheric ozone resulting from gasoline evaporative emissions due to their lower volatility and atmospheric characteristics in comparison with hydrocarbon constituents of the refinery gasoline they replace. Due to the oxygenates clean burning characteristics, they are expected to play a significant role in most of the countries in the world, where clean burning light octane fuels are needed.

Table 2.1 lists some high-octane ethers and alcohols [8,10]. Those currently used in refinery blending for gasoline formulation are MTBE – ETBE – TAME – ethanol. Methanol, *tert*-butyl alcohol (TBA) are presently discontinued; diisopropyl ether (DIPE) and *tert*-amyl ethyl ether are possible future candidates.

Table 2.1 Oxygenates for reformulated gasoline [8]

	Blend ON (R*+M**)/2	Blend RVP (psi)	Boiling Point (°C)	Oxygen (wt. %)
<i>Ethers</i>				
MTBE	109	8	55	18
ETBE	110	4	72	16
TAME	104	4	86	16
TAAE	105	1	101	14
DIPE	105	5	68	16
<i>Alcohols</i>				
Methanol	116	60	65	50
Ethanol	113	18	78	35
TBA	101	13	83	22

*R : Research octane number , **M : Motor octane number

Among the oxygenates for reformulated gasoline, ethers are advantageous over alcohols, because of their lower Reid vapor pressure (RVP; fuel's vapor pressure at 37.7°C). Also they avoid phase separation in the presence of water, which accounts for their full compatibility with the petroleum refining and distribution systems.

2.2.1 Methanol

It was available at the pumps in the early 1980s blended with higher alcohol to improve the water stability. The high methanol volatility blending, due to azeotrope formation with hydrocarbon, caused the refusal of the market. Presently methanol is one of the reactants to produce MTBE and other methyl ethers [8].

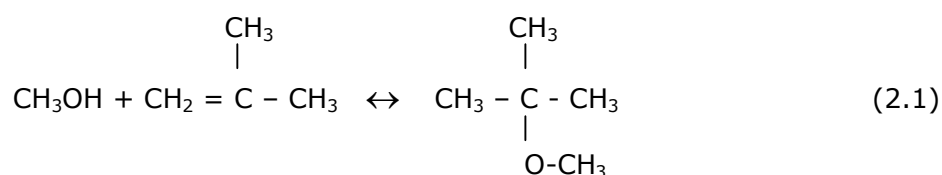
2.2.2 Ethanol

It is produced by fermentation of biomass and put on the market in an anhydrous form. Presently, the production cost starting from corn or other valuable biomass does not allow ethanol to be competitive on fuel market [8]. The use of cellulose as raw material and an integrated scheme allowing the recovery of the produced CO₂ and other fermentation byproducts could greatly improve ethanol economics.

Ethanol, besides being used as direct blending agent, is a raw material for ETBE production and it is expected to maintain such a dual status if a favorable legislation toward renewable oxygenates will be maintained.

2.2.3 MTBE (Methyl *tert*-Butyl Ether)

It is produced by the reaction of isobutene with methanol. The reaction is given in Equation 2.1. This is a reversible, exothermic reaction, which may take place in gas or liquid phase depending on the system pressure. In the liquid phase, the reaction proceeds selectively and with high conversion if the equilibrium is attained at low temperatures (40 - 60°C) [11].



Some side reactions, however can accompany the formation of MTBE, such as the isobutene dimerization to 2,4,4-trimethyl-1-pentene and 2,4,4-trimethyl-2-pentene and methanol dehydration to dimethyl ether (DME). Traces of water found in the reactants lead to the formation of TBA due to the competitive addition of water to isobutene. This reaction proceeds to equilibrium conversion. However, because of the low amount of water in the reactants, TBA does not, generally, reach a concentration level above 0.5 – 1% in MTBE.

The thermodynamics of the reaction was first studied by Colombo *et.al.*[12]. Also, Rehfinger *et.al.* [13], Izquierdo *et.al.* [14] and Zhang and Datta [15] proposed different correlations for the equilibrium constant, K vs. temperature for MTBE synthesis reaction in the liquid phase. Equilibrium constants calculated through the Colombo expression meet quite well those of Rehfinger and Hoffmann at low temperatures. It become progressively more favorable as the temperature increases.

Considering the nature of the reaction, the selection of the catalyst for this reaction was oriented to acid substrates. All the industrial plants built till today have used acidic cation exchange resins as catalysts. Related to ion exchange resin catalysts used for this reaction, a fundamental work was given in the early work of Ancillotti *et.al.* [16].

The increasing demand of MTBE has for a long time been conditioned by the isobutene availability. In the 1970s industrial quantities of isobutene were coming from C₄ streams of catalytic cracking processes from gasoline production and of ethylene manufacture. The availability of methanol is a key element in MTBE manufacture, but, unlike isobutene, methanol is extensively produced in many sites from inexpensive natural gas or other carbon sources. Methanol shortage, if any, will depend on delay in investing or other market upset.

In 1998, MTBE's total worldwide production was 6.6 billion gallons, with the US consuming the most, about 4.3 billion gallons annually [17]. When it is released to the air, the greater part will exist in the atmosphere, with small amounts entering soil and water, with chemical degradation being the major removal source from air [17]. When MTBE released into water, a significant amount remains dissolved on the surface of water, with some partitioning into air and a much smaller amount into soil [18]. Due to its high solubility, once released it moves through the soil and into ground water more rapidly than the other chemicals present in the gasoline. It is slowly biodegraded and is more persistent than other gasoline-related compounds. Therefore, the potential exposure for humans to MTBE is considerable. These exposures generally occur through inhalation.

2.2.4 ETBE (Ethyl *tert*-Butyl Ether)

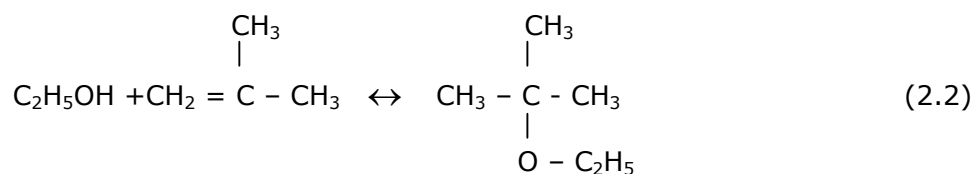
The main oxygenates used today are MTBE and ethanol to eliminate the leaded octane enhancers such as tetramethyl lead and tetraethyl lead. MTBE, thus, has a dual environmental advantage.

In Europe, MTBE is mainly used as an octane booster in high-octane gasoline and to achieve the specified oxygen content requirements, 5-15% MTBE in gasoline is required [19]. Due to the high concentrations of these ethers in gasoline, human exposure to these compounds is likely during production, blending, refueling and by evaporation [20]. EPA based on animal studies which looked primarily at inhalation effects, concluded that MTBE poses a potential for carcinogenicity to humans at high doses. Concern over ground and surface water contamination caused by persistent MTBE has lead the Environmental Protection Agency (EPA) to propose reducing or eliminating its use as a gasoline additive.

The major potential alternatives to MTBE are other forms of ethers such as ethyl *tert*-butyl ether (ETBE) or *tert*-amyl methyl ether (TAME) [17].

ETBE has a slightly higher octane number and lower blending RVP and it is produced from renewable ethanol. Moreover, there has been no evidence that ETBE is carcinogenic [21]. Thus, ETBE is a good alternative to MTBE in spite of its higher cost at present. Recent advances in ethanol production from biomass may decrease the price of ethanol and the cost of ethanol-based ethers may become comparable to the cost of MTBE in the near future [11].

The formation of ETBE from ethanol and isobutene is an acid catalyzed, reversible and moderately exothermic reaction. The reaction is given in Equation 2.2. The reaction is equilibrium limited in the industrially significant ranges of temperatures so that the equilibrium conversion from a stoichiometric mixture of reactant at 70°C is only 84.7% [22].



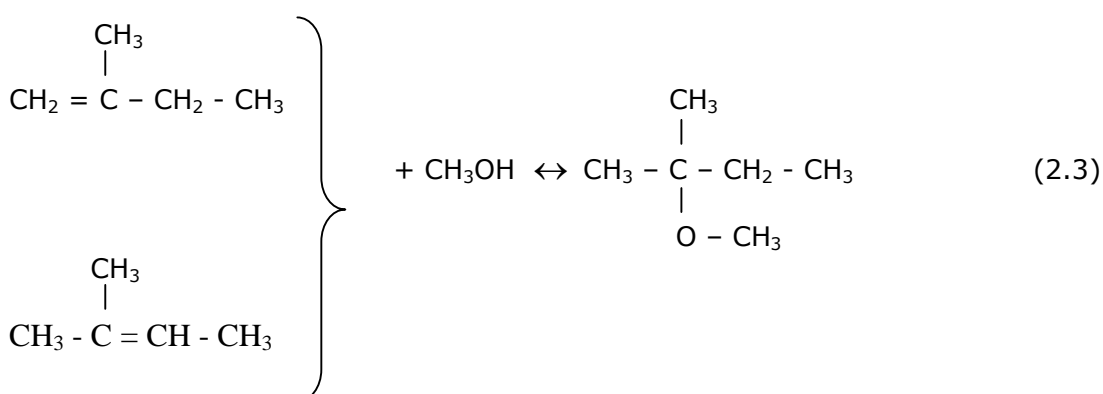
As for MTBE, the used catalysts appear to be the acidic macroreticular ion exchange resins. Tau and Davis [23] studied the synthesis of ETBE in liquid and vapor phases on acid resins (A15, A35, phenylphosphoric acid, fluorocarbonsulphuric acid polymer, etc.) and on zeolites (ZSM-5 and S115 of Union Carbide). In the vapor phase Amberlyst-15 was found to be the most active catalyst. In the liquid phase, FCSA and ZSM-5 showed performances near to those of Amberlyst-15 but at much higher temperatures. This prevents to attain equilibrium conversion at the more favorable lower temperatures. The

selectivity is high, but some byproducts such as diisobutene and diethyl ether may appear if the temperature is high enough and the ethanol / isobutene molar ratio is far from the stoichiometric ratio. It is worth noting that the water impurity accompanying ethanol can be higher than with methanol, therefore the competitive formation of TBA is a more important side reaction in ETBE synthesis[8].

2.2.5 TAME (*tert* - Amyl Methyl Ether)

This compound received serious consideration as an oxygenate in the early 1990s, in spite of its lower octane content than other ethers, as it compares favorably for vapor pressure, boiling point and water mixability [24].

TAME is obtained by reacting methanol with one of the two-branched C₅ olefins (2-methyl-2-butene, 2M2B, and 2-methyl-1-butene, 2M1B). The third C₅ branched olefin, 3-methyl butene-1, is completely inert toward the reaction with methanol. Some amount of *tert*-amyl alcohol can be present in the reaction product if water is an impurity of the reactants. The reaction is given in Equation 2.3. Like MTBE and ETBE, TAME synthesis is an acid catalyzed reversible reaction. The catalyst is a macroreticular ion exchange resin as in MTBE and ETBE synthesis.



Krause and Hammarström [25] investigated the reaction giving the limits of the thermodynamic equilibrium at various temperatures and pressures. Rihko *et.al.*[26] experimentally measured the reaction equilibrium in the liquid phase.

The isoamylenes reactivity toward the methanol addition was first investigated by Ancillotti *et.al.*[27]. They evidenced that 2M2B and 2M1B react giving both methanol addition and double bond isomerization. The initial rate of double bond isomerization is faster than methanol addition, so two isoamylenes equilibrate before TAME equilibrium is achieved.

Differently from MTBE and in spite of the good octane quality, TAME is not a true 'octane supplier' because it is normally produced from two high-octane olefins present in the gasoline pool, coming from the front end of catalytic cracking gasoline. The net TAME octane contribution corresponds therefore to the difference between the octane contribution of TAME produced and the loss of the octane contribution of reacted isoamylenes.

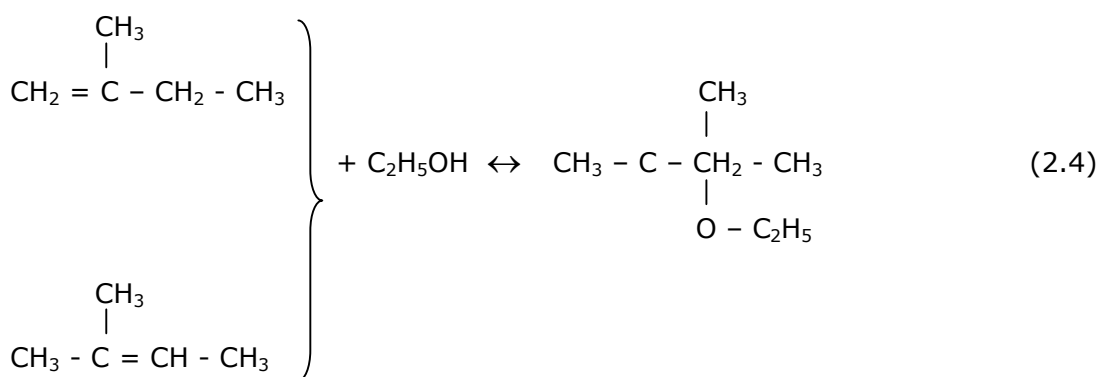
Notwithstanding its minor octane contribution, TAME is important as a 'clean air additive' contributing to meet three important requirements of reformulation: introduction of oxygen, reduction of volatility and removal of highly volatile and photochemically reactive olefins [8].

The TAME potential capacity is strictly related to the reactive isoamylenes present in the light gasoline catalytic cracking plants. Availability that will be to a some extent influenced by the evolution of catalytic cracking system. An additional minor contribution to TAME capacity can arise from C₅ coming from naphtha steam cracking for ethylene manufacture, after a selective hydrogenation to remove dienes.

Compared with MTBE, ETBE is less economical to produce, and TAME is more toxic [17].

2.2.6 TAE (tert- Amyl Ethyl Ether)

Tertiary amyl ethyl ether, which is obtained by reacting ethanol with one of the isoamylenes, 2M1B or 2M2B, has been identified as a suitable additive to gasoline in order to reduce pollution and to enhance octane ratings. The reaction scheme is given in Equation 2.4.



Kinetic studies on the production of TAE are very few. Major kinetic studies on TAE synthesis have been using isoamylenes from fuel cracking streams, and ethanol as reactants have been carried out by Rihko and Krause [28], Rihko, Linnekoski & Krause [26], Kitchaiya & Datta [29], Linnekoski, Krause & Struckmann [30], Oktar *et.al.* [31].

Kitchaiya and Datta [29] studied experimentally this reaction in a wide range of compositions and temperatures. They reported a thermodynamic analysis of the liquid phase synthesis of TAE and of accompanying mutual isomerization of the two olefins. The etherification reactivity of isoamylenes with ethanol in liquid phase has been studied by Rihko and Krause [28], the liquid phase equilibrium by Rihko *et.al.* [26] and Kitchaiya and Datta [29].

Oktar *et.al.* [31] studied the reactivities of 2-methyl-2-butene (2M2B) and 2-methyl-1-butene (2M1B) in the etherification reaction with ethanol catalyzed by a strongly acidic molecular resin catalyst in a temperature range of 333-360 K using liquid phase differential flow reactor. They showed that 2M1B was more active than 2M2B and its activation energy was lower in the etherification reaction.

A particular advantage of TAE is that ethanol can be produced by fermentation from renewable resources, such as molasses, sugarcane, sugar, corn, etc. Although ethanol is higher in price than methanol, using less pure ethanol that is an azeotropic or sub-azeotropic mixture of ethanol and water could diminish the difference [30].

TAE represents lower blending RVP (< 5.3 kPa) and lower solubility in water than in other oxygenates. Despite the positive convenience for hot places and underground water contamination, TAE is not in the market presently [8].

Ethyl ethers show slightly better blending octane properties than methyl ethers and lower blend RVP that favors the blending with more low cost butanes. The alternative use of methyl or ethyl ethers will mainly depend on availability and price of two alcohols.

Producing oxygenates from all potential FCC tertiary olefins is one of the most economic methods for reducing olefins and Reid vapor pressure in motor gasoline. This route allows a higher level of oxygenates production, thereby lowering RVP and the proportion of olefins in the gasoline pool and maximizing the use of FCC olefins [4]. Higher ethers (TAME and TAE) can be used to meet the amended blend RVP levels, and the limits on the olefin content of the reformulated gasoline. They have lower blend RVP than the isoamylenes from

which they are produced (Table 2.2). Therefore, production of TAME and TAE from isoamylenes reduces the olefin content of the light FCC gasoline.

Table 2.2 Properties of some hydrocarbons and oxygenates [8]

Compound	Octane Number (R+M)/2	Atmospheric reactivity	Blending RVP (psi)
Isobutene		55	66
2M2B	91 pure	85	15
	158 blend		
2M1B	92 pure	70	19
Methanol	116 blend	1	60
Ethanol	113 blend	3.4	18
MTBE	109 blend	2.6	8
ETBE	110 blend	8.1	4
TAME	104 blend	7.9	4
TAE	105 blend		1

The FCC unit can be identified as a major issue because almost all light olefins and a large proportion of aromatics comes from here. The typical composition of FCC light gasoline is given in Table 2.3.

The FCC unit, however, can play the role of problem-solver as well. By using all the components produced by an FCC efficiently, many gasoline problems can be solved. Isobutene is converted to MTBE, C₃ / C₄ olefins are converted to alkylate and C₅ tertiary olefins can be converted to TAME. All of these are preferred components for gasoline quality. But, little attention has been given to the fact that FCC light gasoline contains much more reactive olefins that can be converted to ethers. This way, more octanes are produced and less octanes from reformat are required. Therefore, olefins and aromatics content of the gasoline pool can be reduced. The trend in FCC development allows much deeper conversion to light olefins and lower amounts of aromatics – rich FCC heavy gasoline. By producing more oxygenates like MTBE, TAME and heavier ethers, a refinery can be sufficient in blending reformulated gasoline and oxygenates need to be purchased. The olefin content in the FCC light gasoline

soluble and explosive peroxides [8], The tendency to peroxidation is due to the presence of two tertiary hydrogens in α position to the ethereal oxygen atom.

Problems could arise however, in the storage and handling of net DIPE. They appear to be overcome in a captive production but unlikely in a merchant production. As far as the feedstock is concerned, DIPE process competes with alkylation and polymerization, both producing components for gasoline. Due to its totally olefinic nature poly gasoline is expected to decrease in importance as long as reformulated gasoline market will climb, so, at least C₃ stream used as poly feed could be diverted to DIPE [8].

2.3 CATALYST USED IN THE ETHERIFICATION REACTIONS

Ancillotti and Fattore [8] reviewed the catalysts used in the etherification reactions. In this section, some important results will be given.

Ancillotti *et.al.* [16] has done a fundamental study about ion exchange resins as catalyst for the production of MTBE, firstly. Amberlyst-15 is a macroreticular sulfonic resin manufactured by Rohm and Haas. It is sulphonated copolymer of styrene and divinylbenzene. Its surface area is 45m² /g and ion exchange capacity is 4.8 mequiv. of H⁺ / g dry, as reported by Kunin *et.al.* [32]. In the study of Oktar *et.al.* [31] a detailed information about the pore size distribution, average particle diameter (7.4×10^{-4} m), average macropore diameter (2.28×10^{-8} m), porosity ($\epsilon_a = 0.32$) and surface area (59.2 m² / g) were reported.

The morphology and the active sites were mentioned in the work of Ancillotti and Fattore [8]. Differently from gel type resins where the polymeric gel phase occupies, as a continuum, all the physical volume of the particles, the

macroreticular porous resins are structurally composed of small microgel particles to form clusters bonded at the interfaces. The geometry of microgel tends toward spherical symmetry and the diameter of the individual microgel can range from 0.01 to 15 μm [8]. In the study of Dođu *et.al.* [33], the average particle radius of the resin used was 0.037 μm and they estimated the average micrograin diameter of the catalyst as 8.2×10^{-8} m from the SEM photographs. The porosity arises from the void spaces between and within the clusters. The void region is a continuous open-celled system with essentially all the pores are interconnected. The gel phase is also continuum, so that a macroreticular porous polymeric particle is constructed of two phases: a continuous pore phase and a continuous gel phase. The pore system makes macroreticular resins suitable for anchoring catalytic sites, namely SO_3H groups that can lie either on the surface microspheres or inside the gel phase. Porous macroreticular resins generally show an enhanced catalytic activity compared with nonporous gel polymers of the same level of crosslinking but an increase in porosity and in area surface of a functionalized macroreticular polymer does not univocally result in an increased catalytic activity. In fact, the most part of sulfonic groups in macroreticular resins are located inside the gel phase, more than 95% for Amberlyst-15, and such a situation remains also increasing the surface area unless very high surface areas are obtained [8].

It is clear that, when most part of the catalytic sites are inside the microgel particles, the gel phase is the working one. The macroreticular resins, when the gel phase is the working one, have advantage on gel type polymer due to the smaller dimensions and enhanced accessibility of the gel domine. If the gel phase has sufficient penetrability for the molecules involved in reaction, macroreticular resins with the gel phase working represent the best solution, since sulfonic groups in the gel portion are more active than those on the

surface. This is due to the environment within the gel portion that gives rise to a higher Hammett acidity with respect to that found on the surface and to a more stabilized activated complex [34].

Resins such as Amberlyst-15, having a large number of interior catalytic sites, would represent the best catalytic solution for MTBE synthesis, provided that the gel phase is easily penetrable by methanol and isobutene. Macroreticular ion exchange resins actually represents the chosen class of catalyst for MTBE synthesis. Other acidic materials were tried.

The first synthesis of MTBE and similar ethers were done using inorganic catalyst as mineral acids. Sulphuric acid was active but not selective, favouring the formation of dehydrated by-products, dimethyl ether, and oligomers of the olefin. Moreover, the use of soluble inorganic acids makes the separation and purification of ethers a rather complex operation [8].

Attention to complex alumino silicates (like montmorillonites and bentonites), with defined structure and ion exchanged to introduce acidity and metal ions, was given by Adams *et.al.* [35]. Catalytic activity and / or selectivity of these catalysts resulted always lower compared to macroreticular acid resins. Better results, yet still not at the same level of those given by resins, were reached when operating in certain reaction conditions; addition of water to the reacting feed, different solvent (1,4-dioxan) [35]. In conclusion, all these catalysts represent an interesting effort to introduce easily regenerable substrates but they are penalized by limited yields in comparison to resin-based catalysts.

Synthetic zeolites were demonstrated to be good catalysts in different reactions requiring acidic properties. Chu and Kuhl [36] studied zeolites for

MTBE synthesis in vapor phase conditions. Their work considered large (Y, mordenite, etc.), medium (ZSM5 and 11) and small (ferrierites) pore zeolites. All zeolites tested were shown to be less active than resins and the optimum performances were given at higher temperature (80° - 110°C instead of 60° - 90°C).

Chu and Kuhl [36] utilized the most promising zeolites selected (namely ZSM5 and ZSM11) in liquid phase reaction conditions and made a comparison with Amberlyst-15. The results are quite near to those of A15 and the authors claim higher thermal stability, regenerability by calcination, low sensitivity to methanol/isobutene ratio and higher productivity.

The heteropoly acid (HPA) possesses strong acidity to be applicable to several acid-catalyzed reactions in the liquid phase at moderate temperatures. Heteropoly acids and their salts catalyze the MTBE synthesis much more effectively than the ordinary protonic acids. It was proposed that high catalyst efficiency of heteropoly acids is due to those specific properties of heteropoly anions that can be characterized by very weak basicity and great softness, in addition to a large molecular size of polyhedral heteropoly anion [37]. Major problem of using heteropoly acids in such etherification reactions is their solubility in polar solvents, such as alcohols, etc. Detailed information about heteropoly acids and their uses will be given in the next chapter.

CHAPTER 3

HETEROPOLY ACIDS

Catalysis by heteropoly acids (HPAs) and related polyoxometalate compounds is a field of increasing importance, attracting increasing attention worldwide, in which many new and exciting developments are taking place in both research and technology [5]. They have high capability in practical uses. On the other hand, heteropoly acids have a very strong, approaching the superacid region, Brønsted acidity; on the other, they are efficient oxidants, exhibiting fast reversible multielectron redox transformations under rather mild conditions. Their acid – base and redox properties can be varied over a wide range by changing the chemical composition.

The catalytic function of heteropoly acids has attracted much attention particularly in the last two decades [7]. They are used in solution as well as in the solid state as acid and oxidation catalysts. The reason why heteropoly catalysts are attractive is their variety and high potential as catalyst. The advantageous characteristics of heteropoly compounds as heterogeneous catalysts are listed in Table 3.1.

Table 3.1 Advantage of Solid Heteropoly Catalysts [7]

1. Catalyst design based on acidic and redox properties.
These two important properties can be controlled by the constituent elements of polyanions and countercations.
2. Molecularity
Molecular design of catalysts
3. Unique reaction field
 - a. Pseudoliquid phase
Bulk-type and surface-type reactions
 - b. Complex formation
Polyanions are soft bases which stabilize the reaction intermediates in the pseudoliquid phase.

3.1 PREPARATION OF HETEROPOLY ACIDS

Preparation of heteropoly acids is getting more and more important for their applications. Such heteropoly acids as $\text{H}_3\text{PW}_{12}\text{O}_{40}$, $\text{H}_4\text{SiW}_{12}\text{O}_{40}$, and $\text{H}_3\text{PMo}_{12}\text{O}_{40}$ are commercially available as crystalline hydrates. The simplest way to prepare heteropoly acids involves the acidification of an aqueous solution containing the oxoanions and the heteroatom:



Control of the pH and the ratio of central atom to metal atom (X/M) is necessary in order to obtain the desired structure. Acidification is achieved by direct addition of a mineral acid. Isolation of the heteropoly acid can be obtained by extracting with ether (etherate method). If the aqueous acid solution is shaken with an excess of diethylether, three phases separate: an aqueous layer, which is drawn off and treated again with ether to recover as much as possible of the heteropoly acid, an upper layer containing excess ether, and an intermediate heavy oily etherate, which contains a complex between the ether and the heteropoly acid. This etherate complex can be hydrolyzed by addition of

a controlled amount of water; then the ether is removed, and the concentrated aqueous solution of the heteropoly acid is evaporated until crystallization occurs[38].

Alternatively, the excess ether in the etherate complex is removed by evaporation, and the ether complex is thermally decomposed to yield the solid acid by drying at 80 - 100°C. The etherate method suffers from disadvantages because of the low yield achievement and of the large amount of waste product formation.

The acid can be exchanged with other metal ions by dissolution in aqueous solutions and addition of the proper metal salt. If the salt or mixed acid/salt obtained is soluble, it has to be recovered by the evaporation of water.

3.2 STRUCTURAL CHARACTERISTICS

3.2.1 Molecular Structure

Acidification of the Mo^{6+} or W^{6+} solutions in the presence of other anions leads to the incorporation of the latter anion at the center of the polyanion, with formation of the so-called *heteropolyanions* (or heteropolyoxometalates, or heteropolycompounds, HPCs). Many different ions can be heteroatoms in heteropolycompounds: Be, B, Al, Si, Ge, Sn, P, Te, and the entire first row transition elements. The heteroatom can adopt either tetrahedral or octahedral co-ordination. The atomic ratio between the atoms in peripheral position and the heteroatom can be 12, 11, 9 or 6 [38].

There exist a large number of different HPCs, but the most important heteropolyoxometalates are classified as follows:

i. Keggin HPCs, with general formula



where X is the central atom (Si^{4+} , Ge^{4+} , P^{5+} , As^{5+} , etc.), n the degree of its oxidation, and M is molybdenum or tungsten, which can be partly replaced by other metals [39].

The structure of Keggin compounds, shown in Figure 3.1, comprises four trigonal groups of edge-sharing MO_6 octahedra, each group sharing corners with neighboring groups and with the central tetrahedron (α -structure). In each octahedron the metal is displaced towards the terminal oxygen atoms. This structural arrangement leads to the formation of a spherical polyanion.

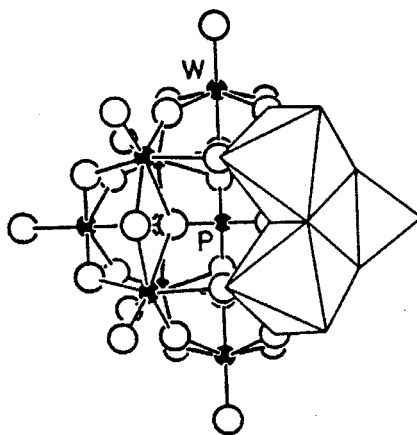


Figure 3.1 Heteropolyanion with the Keggin structure [40]

The first characterized and the well known heteropolycompound is the one having Keggin structure which is fairly stable and easily available, so investigations of catalytic properties in the solid state have been mostly devoted to this group [40].

ii. Wells – Dawson HPCs, with general formula



where X is P^{5+} , S^{6+} , As^{5+} and M may be either W^{6+} or Mo^{6+} . These HPCs are formed via dimerization of $\alpha\text{-PM}_9\text{O}_{34}$ moieties, thus under conditions of pH at which the parent Keggin compound forms the corresponding tri-lacunary compound by the loss of MO groups. The structure of Wells – Dawson compounds is shown in Figure 3.2.

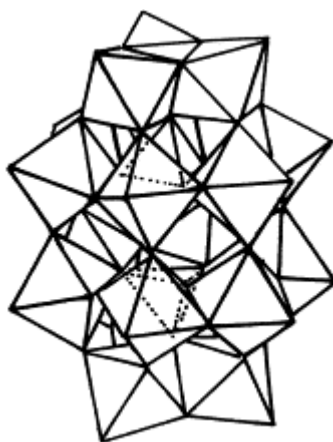


Figure 3.2 Heteropolyanion with Wells – Dawson structure [38]

iii. Anderson HPCs, with general formula



where X is Mn^{4+} , Ni^{4+} , Pt^{4+} , Te^{6+} and M may be either W^{6+} or Mo^{6+} . The structure is planar in which, each MoO_6 octahedron has two terminal oxygens and the heteroatom X adopts the octahedral coordination. Anderson anions are usually obtained from aqueous solutions at a pH of 4-5. Their structure is shown in Figure 3.3.

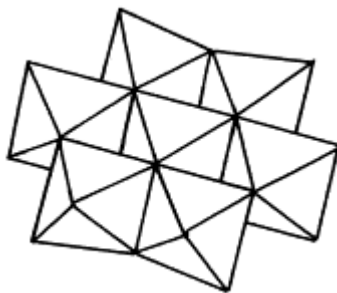


Figure 3.3 Heteropolyanion with Anderson structure [38]

Generally, heteropolycompounds in the solid state are composed of heteropolyanions, cations (protons, and metal or onium ions), and water of crystallization. Sometimes in addition they contain neutral (or protonated) organic molecules. It is very important for the understanding of the heterogeneous catalysis of heteropolycompounds to make a clear distinction between the primary and the secondary structure. Heteropolyanions are the primary structures, and the three - dimensional arrangements of the polyanions, cations, and other components are regarded as the secondary structures [40]. These structures are very variable, whereas the primary structure is stable. The flexibility of the secondary structure is an important feature of heteropolycompounds when they are used as solid acids.

There exist different types of secondary structures for Keggin heteropolyacids; e.g., the body-centered cubic lattice, which is the structure met in $\text{H}_3\text{PW}_{12}\text{O}_{40}\cdot 6\text{H}_2\text{O}$, and the face-centered cubic lattice which is less compact than the previous one, and can accommodate up to 30 water molecules per anion like in $\text{H}_3\text{PW}_{12}\text{O}_{40}\cdot 29\text{H}_2\text{O}$. As an example, the secondary structure of $\text{H}_3\text{PW}_{12}\text{O}_{40}\cdot 6\text{H}_2\text{O}$ is shown in Figure 3.4. Other lattices may be formed by Keggin anions, depending on both the number of hydration water molecules and the anion charge.

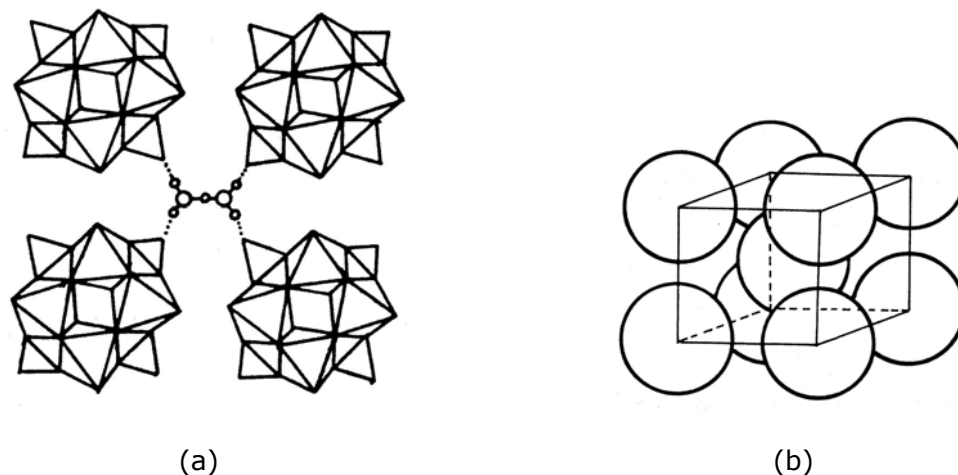


Figure 3.4 An example of the secondary structure $H_3PW_{12}O_{40} \cdot 6H_2O$ ($= H_5O_2 \cdot 3PW_{12}O_{40}$). Each $H_5O_2^+$ bridges four polyanions as shown in (b). The bcc packing of polyanions is illustrated in (b). [40]

3.2.2 Proton Structure

Structural characterization of HPA proton sites is an important step towards understanding the catalytic activity [5].

Keggin anions have three types of outer oxygen atoms as potential protonation centers. One type of terminal oxygen $M=O$ and two types of bridging oxygens $M-O-M$, edge sharing and corner sharing, respectively [6].

Bond length – bond strength correlations indicate that in the free polyanions in solution, the bridging oxygen atoms, having a higher electron density than the terminal oxygen atoms, are protonated. In the free Keggin anion, edge-bridging $M-O-M$ oxygens are assumed to be the predominant protonation sites, but on the other side, in the solid HPAs, the protons take part in the formation of the heteropolyacid crystal structure, linking the neighboring heteropolyanions. In this case the more accessible terminal oxygens can be protonated.

3.2.3 Surface Area and Pore Structure

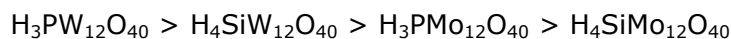
Hydrogen forms and group A salts (e.g. Na, Mg, Cu), which are prepared from aqueous solutions, have low surface areas (1 – 15 m²/g), reflecting their high solubility in water. On the other hand, the surface areas of group B salts, which consist of larger ions such as Cs⁺, Ag⁺, NH₄⁺, etc., are much higher (50 – 200 m²/g). Very fine particles are instantaneously precipitated when these cations are titrated to aqueous solutions of H₃PW₁₂O₄₀ and H₃PMo₁₂O₄₀, in which their surface areas vary depending on the precipitation and the drying process.

The surface areas of Cs_xH_{4-x}SiW₁₂O₄₀ were reported to be 9.0, 23,49 and 83 m² g⁻¹ for x = 0, 2, 2.5, and 3, respectively, and those of Cs_xH_{3-x}PW₁₂O₄₀ 6.0, 1.0, 1.2, 135, and 156 m² g⁻¹ for x = 0, 1, 2.5, and 3, respectively [7].

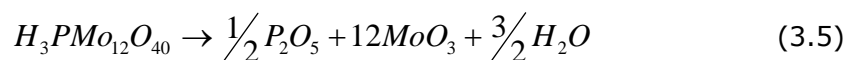
The high surface area is likely to be due to the very small size of the primary particles and is not due to the presence of micropores (pore diameter < 2nm) in the crystal structure. Considering the size and shape of the Keggin anion and the crystal structure of cesium salts, there are no open pores in the crystal structure through which nitrogen can penetrate. However, by proposing a different interpretation, it was found that the micropore structure (>0.59 nm) could be controlled by the partial substitution of H by Cs⁺ or NH₄⁺. The pore size of acidic Cs salts (Cs_xH_{3-x}PW₁₂O₄₀) could be controlled by the Cs content.

3.2.4 Thermal Stability and Water Content

The thermal stability of heteropolyacids is fairly high and this stability change depends very much on the kind of HPAs [7]. The thermal stability of hydrogen forms of heteropolyacids changes with heteroatom, polyatom, and polyanion structure as follows:



Above 350°C, decomposition of the Keggin structure occurs which also causes the loss of acidity; the decomposition is believed to be as follows:



This decomposition proceeded via $\text{PW}_{12}\text{O}_{38.5}$ in the case of $\text{H}_3\text{PW}_{12}\text{O}_{40}$ [41]. The thermal stability of heteropolycompounds depends on the environment; in a reducing atmosphere they decompose more rapidly. In the presence of water vapor and oxygen, the thermal stability of heteropolycompounds increases.

As a rule, HPAs readily soluble in water and water – containing solvents, but the solubility falls sharply when dehydrated HPA and thoroughly dried non – aqueous solvents are used. Heteropolyacids do not dissolve in solvents such as benzene, petroleum ether, and chloroform [39].

Moreover, the thermal stability of metal salts can be discussed in two main categories. The first group consists of the salts of small ions like Na^+ and Cu^{2+} are readily soluble in water and in the other group, the salts of larger ions such as Cs^+ , Ag^+ , etc., are included. Salts of small metal ions resemble the acid forms in several aspects. Water evolving near 200°C for divalent metal salts might be due to water coordinated to metal ion. For the larger ions, water content is low and is released at a lower temperature [40].

3.2.5 Pseudo-liquid Phase

Due to the flexible nature of the certain heteropolyacids like $\text{H}_3\text{PW}_{12}\text{O}_{40}$ and $\text{H}_3\text{PMo}_{12}\text{O}_{40}$ easily absorb a large amount of water, alcohols, and ethers in the solid state, although their surface areas are very low. This is not adsorption in

micropores; rather molecules are absorbed between the lattice polyanions, expanding the lattice.

Heteropolyacids that have absorbed a significant amount of polar molecules behave in a sense like concentrated solution and the reaction takes place in the solid bulk. This state is called as "*pseudo-liquid phase*" [42-44].

The pseudo-liquid phase behavior apparently brings about high catalytic activities for reactions of polar molecules at low temperatures especially when the sorption of the substrate in the catalyst bulk is rather high. Beside these, unique selectivities are also achieved.

The tendency to form a pseudo-liquid phase depends on the kind of heteropolycompound, particularly on the counteranion, and on the molecules to be absorbed. Acid forms absorb polar molecules like alcohols and amines into their solid bulk, but nonpolar molecules like hydrocarbons can be only adsorbed on the surface of the heteropolycompound. On the other hand, in the case of Cs salt, since the secondary structure is rigid the polar molecules are not absorbed. The rate of absorption varies in a similar way, depending on the basicity of the molecule and on the molecular size. The rate of absorption depends also on the water content of heteropolycompounds. Temperature, partial pressure, and molecules coexisting in the system are also influential.

3.3 ACIDIC PROPERTIES

The acid – base properties of heteropolycompounds can be modified by the choice of the heteroatom, of the oxometal in the primary structure, and of the cation [38].

The acidity can be generated by the protons which act as counteractions in heteropolyacids (i.e., in $H_3PMO_{12}O_{40}$) and in mixed acidic salts (for instance, in $Cs_xH_{3-x}PW_{12}O_{40}$) There are two types of protons in crystalline HPA: (i) non – localized hydrated protons bound to one HPAN as a whole and rapidly exchanging with the protons of the water molecules in the hydration shell of the acid; (ii) non – hydrated protons localized at the peripheral oxygen atoms of the polyanion [39].

All heteropolyacids are strong acids, much stronger than conventional solid acids such as $SiO_2 - Al_2O_3$, H_3PO_4 / SiO_2 , and HY and HX zeolites and mineral acids as H_2SO_4 , HCl, p – toluene sulfonic acid etc. They are completely dissociated in aqueous solutions and partly dissociated in organic solvents. This strong acidity can be attributed to the delocalization of surface charge density throughout the large sized polyanion, leading to a weak interaction between the protons and the anion.

The acid strength can be expressed by the Hammett acidity function H_0 :

$$H_0 = pK_{BH^+} - \log\left(\frac{[BH^+]}{[B]}\right) \quad (3.6)$$

where $[B]$ is the concentration of the indicator B, $[BH^+]$ is the concentration of the conjugated acid and K_{BH^+} is the equilibrium constant for the reaction:



The $[BH^+] / [B]$ ratio can be determined by spectroscopy in the UV and visible bands, or can be measured more roughly by visually observing the point in the titration at which the color changes.

The H_0 value of 100% H_2SO_4 (-11.94) is taken as a reference number. The acids with values lower than -12 are classified as *superacids* [45]. Superacids with H_0 values of -20 (that is 10^8 times stronger than 100% H_2SO_4), such as $HSO_3F - SbF_5$, are able to protonate methane. The values of the Hammett function for a number of solid acids, including $H_3PW_{12}O_{40}$ are given as follows:

Table 3.2 Hammett acidity function for some solid acid catalysts[45]

Solid acid	H_0
Nafion	-12
$H_3PW_{12}O_{40}$	-13,2
$AlCl_3 - CuCl_2$	-13,7
$SbF_5/SiO_2 - Al_2O_3$	-13,7
SO_4^{2-} / TiO_2	-14,5
SO_4^{2-} / ZrO_2	-16,1

According to this scale heteropolycompounds can be classified as *superacid* compounds. This extraordinarily high acidity has led to increasing interest in the possibility of using them as alternative catalysts for acid - catalyzed transformations which employ environmentally homogeneous liquid acids like HF, $AlCl_3$ or H_2SO_4 . On the other hand, a very high acidity may be responsible for undesired side - reactions, and for quick deactivation phenomena due to the formation of heavy by - products.

3.3.1 Heteropoly Acids in Solution

In solutions, the acid properties of heteropoly acids are quite well documented in terms of dissociation constants and Hammett acidity function [39]. They have very high solubilities in polar solvents such as water, lower alcohols, ketones, ethers, etc. On the other hand, they are insoluble in nonpolar solvents.

In aqueous solution, heteropoly acids such as $H_3PW_{12}O_{40}$, $H_4SiW_{12}O_{40}$ and $H_3PMo_{12}O_{40}$ are fully dissociated. The stepwise character of the dissociation is not observable as a consequence of the leveling influence of the solvent.

Table 3.3 Dissociation Constants for Heteropoly Acids in Acetone
at 25°C [39].

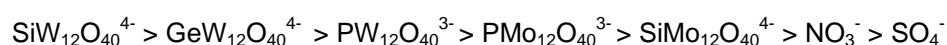
Acid	pK ₁ *	pK ₂	pK ₃
H ₃ PW ₁₂ O ₄₀	1.6	3	4
H ₄ PW ₁₁ VO ₄₀	1.8	3.2	4.4
H ₄ SiW ₁₂ O ₄₀	2	3.6	5.3
H ₃ PMo ₁₂ O ₄₀	2	3.6	5.3
H ₄ SiMo ₁₂ O ₄₀	2.1	3.9	5.9
H ₂ SO ₄	6.6		
HCl	4.3		
HNO ₃	9.4		

*pK₁ = -logK₁, pK₂ = -logK₂, pK₃ = -logK₃

Heteropoly acids in solution are stronger than the usual mineral acids such as H₂SO₄, HCl, etc. as shown in Table 3.3. The strength of the Keggin heteropoly acid depends weakly on their composition and the tungsten acids are remarkably stronger than molybdenum ones. The acidity of HPA concentrated solutions in terms of the Hammett acidity function also weakly depends on their composition and is stronger than that of equimolar solutions of H₂SO₄.

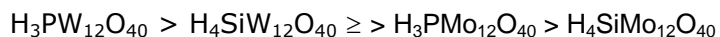
Although the acid strength and catalytic activity of Brönsted acids are best quantified in terms of their dissociation constants and Hammett acidity function, other characteristics, namely the hardness of the acid or the softness of the corresponding base, are the key parameters of the hard and soft acid-base theory, which are related to the polarizability and generally applied to Lewis acids and bases [6].

Keggin anions can be characterized as having a very weak basicity and great softness [37]. The softness of the heteropoly anions is assumed to play an important role in stabilizing organic intermediates. The order of softness of heteropoly anions in aqueous solution was estimated as follows:



3.3.2 Solid Heteropoly Acids

They possess purely Brönsted acidity and are stronger than such conventional acids like $\text{SiO}_2 - \text{Al}_2\text{O}_3$, $\text{H}_3\text{PO}_4/\text{SiO}_2$, and HX and HY zeolites. The acid strength of crystalline heteropoly acids decreases in the order of

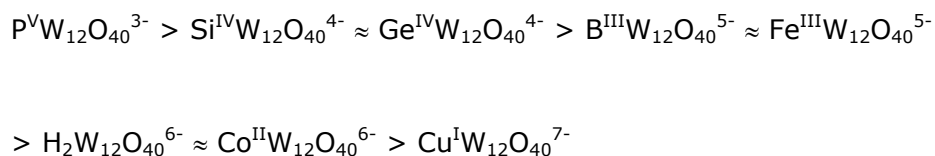


Usually, relative catalytic activities of heteropoly acids are consistent with this order both in homogeneous and in heterogeneous systems.

3.4 REDOX PROPERTIES

In solutions, the reduction potentials of heteropolyanions containing Mo and V are high as these ions are easily reduced. Oxidative ability decreases generally in the order: V- > Mo- > W- containing heteropolyanions, which means that the vanadium-containing heteropoly compounds are the strongest oxidants[46].

The nature of the heteroatom affects the overall charge of the polyanion. An increase in the charge leads to a decrease in the oxidation potential for the $\text{W}^{6+} / \text{W}^{5+}$ couple in:



Also the effect of the countercation can be significant. When the cation is easily reducible, the redox properties of the heteropoly compound are parallel to those of the cation. When the cation is not reducible, like alkali metals, the reducibility of the metal in the primary structure is nevertheless affected by the

nature of the cation [38]. The oxidizing ability has been estimated from the rate of reduction of heteropoly compounds by H_2 , CO, and organic compounds, but sometimes the data appear inconsistent, due to the difference in the kind of reductant, inhomogeneity, non-stoichiometry, decomposition of the catalysts[47].

3.5 SUPPORTED HETEROPOLY ACIDS

Dispersing heteropoly acids on solid supports with high surface areas is important for catalytic application because the surface area of unsupported heteropoly acids are usually low (1-10 m^2/g) [7]. Generally, heteropoly acids strongly interact with supports at low loading levels, while the bulk properties of heteropoly acids prevail at high loadings. Acidic or neutral substances like SiO_2 , active carbon, acidic ion-exchange resin, etc., are suitable supports, but on the other hand, solids having basicity like Al_2O_3 and MgO tend to decompose heteropoly acids [6].

3.5.1 HPA on Silica

SiO_2 is relatively inert toward heteropoly acids above a certain loading level. The thermal stability of heteropoly acid on silica seems to be comparable to or slightly lower than that of the parent heteropoly acid [40]. On the other hand, a thermally decomposed Keggin structure on the silica surface may be reconstructed on exposure to water vapor [48].

Impregnating silica with an aqueous solution of $H_3PW_{12}O_{40}$ gives catalysts with, in general, two heteropoly acid species with an intact Keggin structure and with a different structure and with a different structure which were assumed to be bulk crystalline $H_3PW_{12}O_{40}$ (A) and the interacting species $(SiOH_2^+)(H_2PW_{12}O_{40}^-)$ (B), respectively. The relative amount of species A and B

depends on HPA loading, with A dominating. At higher loadings, 30 – 50%, A is the only one present on silica surface, whereas at lower loadings, both species exist, the amount of $(\text{SiOH}_2^+)(\text{H}_2\text{PW}_{12}\text{O}_{40}^-)$ increasing as the HPA loading decreases.

When $\text{H}_3\text{PW}_{12}\text{O}_{40}$ was loaded on SiO_2 , the proton sites became weaker and less uniform. Like for bulk HPA, SiO_2 supported HPA strongly depends on the pretreatment temperature. According to the ammonia thermal desorption data [6], the acid strength of supported $\text{H}_3\text{PW}_{12}\text{O}_{40}$ decreases in the series of the carriers: $\text{SiO}_2 > \alpha\text{-Al}_2\text{O}_3 > \text{activated carbon}$ [5].

At low loadings, $\text{H}_3\text{PW}_{12}\text{O}_{40}$ and $\text{H}_4\text{SiW}_{12}\text{O}_{40}$ form finely dispersed species on the surface of silica and a heteropoly acid crystal phase is developed at heteropoly acid loading above 20-wt %. Silica-supported molybdenum HPAs like $\text{H}_3\text{PMo}_{12}\text{O}_{40}$ and $\text{H}_4\text{SiMo}_{12}\text{O}_{40}$, maintain the Keggin structure at high loadings but decompose at very low loadings because of the strong interactions with surface silanol groups.

3.5.2 HPA on Mesoporous Molecular Sieve

Incorporation of heteropoly acids into zeolite pores to obtain shape selective catalysts has long been a challenge. However, conventional zeolites are not suitable for this purpose due to their small pores to absorb large heteropoly acid molecules [6].

Recently, $\text{H}_3\text{PW}_{12}\text{O}_{40}$ supported on mesoporous pure-silica molecular sieve MCM-41 (BET surface area $1200\text{m}^2\text{g}^{-1}$, uniform pores 32 Å in size) was prepared and characterized by nitrogen physisorption, X-Ray Diffraction, Fourier-transform infrared spectroscopy and ^{31}P MAS NMR [5]. The $\text{H}_3\text{PW}_{12}\text{O}_{40}$ /MCM-41 compositions with loadings from 10 to 50 wt % have ~ 30 Å uniformly sized

mesopores. Heteropoly acids retain the Keggin structure on the MCM-41 surface at an HPA loading 20-wt %, on the other hand at lower loadings a partial decomposition of $\text{H}_3\text{PW}_{12}\text{O}_{40}$ was observed. Heteropoly acids form finely dispersed species on the MCM-41 surface. No HPA crystal phase was seen at HPA loadings as high as 50-wt %.

3.5.3 HPA on Carbon

While weaker acids, heteropoly acids supported on certain activated carbons are considered to be promising fixed-bed acid catalysts for liquid-phase reactions, because of their extraordinary stability toward HPA leakage from the carrier [49]. However, the acid strength of $\text{H}_3\text{PW}_{12}\text{O}_{40}$ is greatly reduced when loading on activated carbon [6]. When $\text{H}_3\text{PW}_{12}\text{O}_{40}$ and $\text{H}_4\text{SiW}_{12}\text{O}_{40}$ are supported on a chemically treated carbon, they retain their Keggin structure at the HPA loading above 5 wt %. On the other hand, they decompose at lower loadings [50]. Heteropoly acids form finely dispersed species on the carbon surface in which no heteropoly acid crystal phase is developed even at the HPA loading as high as 45 wt % [49].

3.5.4 HPA on Ion-Exchange Resins

Enhanced catalytic activity of heteropoly acids was found when they were supported on a strongly acidic ion-exchange resin, Amberlyst-15 [51]. The activity was much higher than those of Amberlyst-15 and of the acids supported on active carbon. This higher activity was explained by the synergism due to the interaction of the heteropolyanions and protons of the ion exchanger.

3.5.5 Other Supported HPA Catalysts

Pillaring hydrotalcite-type anionic clays by polyanions to form expanded layered catalysts for redox reactions have attracted interest in recent years.

These materials are often used as precursors for molecularly mixed oxide catalysts, which possess basic and/or redox properties and have been prepared by ion-exchange reactions with the Keggin type heteropoly anions [38]. Recently, variety of transition metal substituted polyoxometalates into ZnAl – NO₃ and MgAl – Cl host clays are also reported [6].

Heteropoly acids immobilized into an organic polymer, e.g., H₃PMo₁₂O₄₀ – polysulfone, H₃PMo₁₂O₄₀ – polyethersulfone, H₃PMo₁₂O₄₀ – polyacetylene, H₃PMo₁₂O₄₀ – polypyrrole and H₄SiW₁₂O₄₀ – aniline were prepared and characterized [6]. These are claimed to have an improved catalytic activity compared to bulk HPA in gas phase ethanol conversion.

3.6 HETEROPOLY ACID SALTS

The nature of counteraction in heteropoly acid salts is critical with respect to their acidity, solubility, porosity and thermal stability [6]. Salts with rather small cations resemble the parent heteropoly acids. They are readily soluble in water, nonporous, and possess surface areas under 10 m²g⁻¹ (Table 3.4). On the other hand, water-insoluble salts with large monovalent cations, such as NH₄⁺, K⁺, Cs⁺, etc., have rigid mesoporous/microporous structure and surface areas over 100 m²g⁻¹ [52]. Even if these solids are prepared by precipitation from aqueous solutions to be stoichiometric, residual quantities still remain which are apparently responsible for catalytic activity of these salts.

Misono *et al.* [45] showed that acidic Cs salt, Cs_{2.5}H_{0.5}PW₁₂O₄₀, has strong acid sites and high surface area (100 – 200 m²g⁻¹) and is an efficient solid acid catalyst for a variety of organic reactions. The pore size of Cs salts Cs_xH_{3-x}PW₁₂O₄₀ can be controlled by the Cs content [53].

Table 3.4 Properties of Heteropoly Acid Salts [6]

cation	ionic radius, A	solubility ^a	S _A , m ² g ⁻¹
Li ⁺	0,68	S	<10
Na ⁺	0,97	S	<10
Ag ⁺	1,26	S	<10
Mg ²⁺	0,66	S	<10
Ca ²⁺	0,99	S	<10
Cu ²⁺	0,72	S	<10
Zn ²⁺	0,74	S	<10
Al ³⁺	0,51	S	<10
Fe ³⁺	0,64	S	<10
La ³⁺	1,02	S	<10
Ce ³⁺	1,03	S	<10
K ⁺	1,33	N	>100
Rb ⁺	1,47	N	>100
Cs ⁺	1,67	N	>100
NH ₄ ⁺	1,43	N	>100

^aS : Soluble; N : Not Soluble

Izumi *et.al.* [54] reported that SiO₂ - bound Cs_{2.5}H_{0.5}PW₁₂O₄₀, is catalytically more active than Amberlyst -15 and H-ZSM-5, as based on the unit acid site. Catalysts obtained by loading HPAs on their insoluble salts have been studied and various methods for the preparation of bulk and supported HPA salt catalysts including characterization studies have been described [55-58].

3.7 HOMOGENEOUS CATALYSIS

Heteropoly acids catalyze a wide variety of reactions in homogeneous liquid phase offering strong options for more efficient and cleaner processing compared to conventional mineral acids [6]. In principle, mechanisms of homogeneous catalysis by heteropoly acids and by ordinary mineral acids are of the same origin. Both HPAs and mineral acids function as proton donors [5]. There are, however, some specific features in the HPA catalysis. First, being stronger acids, HPAs have significantly higher catalytic activity than mineral acids. In organic media, the molar catalytic activity of heteropoly acid is usually 100 – 1000 times

higher than that of H_2SO_4 (Table 3.5) [39]. This makes it possible to carry out the catalytic process at a lower catalyst concentration and/or at a lower temperature. Further, heteropoly acid catalysis lacks side reactions such as sulfonation, chlorination, etc., which occur with mineral acids. As stable, relatively nontoxic crystalline substances, HPAs are also preferable with regard to safety and ease of handling [6]

The relative activity of Keggin heteropoly acids depends primarily on their acid strength. Other properties such as the oxidation potential, the thermal and hydrolytic stability are also important factors. These properties for the most common heteropoly acids are summarized below:

Acid Strength: $\text{H}_3\text{PW}_{12}\text{O}_{40} > \text{H}_4\text{SiW}_{12}\text{O}_{40} \geq \text{H}_3\text{PMo}_{12}\text{O}_{40} > \text{H}_4\text{SiMo}_{12}\text{O}_{40}$

Oxidation Potential: $\text{H}_3\text{PMo}_{12}\text{O}_{40} > \text{H}_4\text{SiMo}_{12}\text{O}_{40} \gg \text{H}_3\text{PW}_{12}\text{O}_{40} > \text{H}_4\text{SiW}_{12}\text{O}_{40}$

Thermal Stability: $\text{H}_3\text{PW}_{12}\text{O}_{40} > \text{H}_4\text{SiW}_{12}\text{O}_{40} > \text{H}_3\text{PMo}_{12}\text{O}_{40} > \text{H}_4\text{SiMo}_{12}\text{O}_{40}$

Hydrolytic Stability: $\text{H}_4\text{SiW}_{12}\text{O}_{40} > \text{H}_3\text{PW}_{12}\text{O}_{40} > \text{H}_4\text{SiMo}_{12}\text{O}_{40} > \text{H}_3\text{PMo}_{12}\text{O}_{40}$

Generally, tungsten heteropoly acids are the catalysts of choice because of their stronger acidity, higher thermal stability, and lower oxidation potential compared to molybdenum heteropoly acids. Usually, if the reaction rate is controlled by the catalyst acid strength, $\text{H}_3\text{PW}_{12}\text{O}_{40}$ shows the highest catalytic activity in the Keggin series. However, in the case of less demanding reactions as well as in reactions at higher temperatures in the presence of water, $\text{H}_4\text{SiW}_{12}\text{O}_{40}$, having lower oxidation potential and higher hydrolytic stability, can be superior to $\text{H}_3\text{PW}_{12}\text{O}_{40}$.

Table 3.5 Some Homogeneous Reactions Catalyzed by HPA [6]

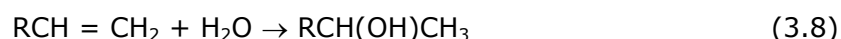
reaction	rate ratio ^a	T(C)
hydration of phenylacetylene	100	40
olefin+HOAc ---> ester	90	110
ester ---> olefin + carboxylic acid	100	128
styrene + HCHO (Prins reaction)	50	50

^aHPA/H₂SO₄(per proton)

The major problem, limiting the utility of homogeneously catalyzed processes, is the well-known difficulty in catalyst recovery and recycling. As the cost of the heteropoly acids is higher than mineral acids, the recycling of heteropoly acid catalysts is the key issue to their application. Only a few homogeneous reactions allow for easy heteropoly acid recycling like hydration of olefins. In some cases, HPA can be recovered from polar organic solution without neutralization by precipitating with a hydrocarbon solvent. HPA can also be extracted from an acidified aqueous solution of its salt with a polar organic solvent. Even though the neutralization of HPA is necessary, the amount of alkali needed and hence the amount waste formed thereupon is much less than with mineral acids. A more efficient way to overcome the separation problem is the use of biphasic systems or solid heteropoly acid catalysts [5,6]. Below are given selected examples of heteropoly acid catalyzed homogeneous reactions.

3.7.1 Hydration of Olefins

The heteropoly acid catalyzed hydration of C₃ – C₄ olefins is an industrially important reaction, and the hydration of propene being the first commercial process based on the heteropoly acid catalysis [59].



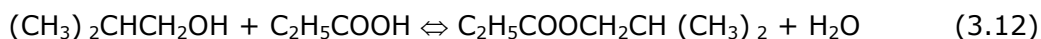
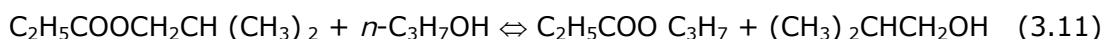
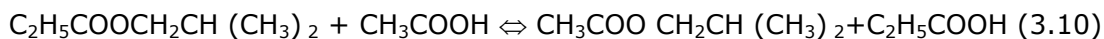
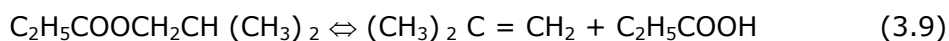
The hydration of isobutene is used for the separation of isobutene from the C₄ hydrocarbon stream produced by cracking. As the catalyst, a concentrated

aqueous solution of heteropoly acid is used. Compared to mineral acids, the heteropoly acid is 2–4 times more active per equal H_3O^+ concentration and shows a higher selectivity.

3.7.2 Esterification and Related Reactions

These reactions were extensively studied in the presence of Keggin and Dawson heteropoly acids as homogeneous catalysts [39, 60]. The catalytic activities of heteropoly acids usually follow the order of their acid strengths, as expected for Brønsted acid catalysis. However, Mo acids, having a higher oxidation potential than W ones, may exhibit a lower activity than expected from their acid strengths due to their reduction by the reaction medium.

Hu *et. al.* [60] studied a series of homogeneous reactions such as decomposition of isobutyl propionate (IBP), transesterification of IBP with acetic acid and *n* – propyl alcohol, and esterification of propionic acid with isobutyl alcohol.



In reaction (3.9), heteropoly acids are 60 – 100 times more active than H_2SO_4 and *p* – toluenesulfonic acid (TsOH). The activity is in the order $\text{H}_3\text{PW}_{12}\text{O}_{40} > \text{H}_4\text{SiW}_{12}\text{O}_{40} \geq \text{H}_4\text{GeW}_{12}\text{O}_{40} > \text{H}_6\text{P}_2\text{W}_{18}\text{O}_{62}$. The same activity pattern is observed for reaction (3.11) in the absence of water. In contrast to reaction (3.9), the addition of water accelerates reaction (3.10) and probably changes its course to proceed via the hydrolysis of isobutyl propionate to propionic acid and isobutyl alcohol, followed by the esterification of isobutyl alcohol with acetic acid. On the

other hand, for reactions (3.11) and (3.12) no significant difference in the activity between heteropoly acids and H_2SO_4 is observed due to the leveling effect of the reactant alcohols on the acid strength of the catalysts.

Synthesis of glycosides catalyzed by heteropoly acid is of industrial importance [59]. They are used as new effective and biodegradable surfactants. Heteropoly acid is several times more active than the conventional catalysts such as TsOH and ZnCl_2 . Acetylated monosaccharides interact readily with alcohols in a homogeneous phase in the presence of 2% HPA with respect to the sugar derivative at 70 - 130°C, yielding 70 - 90% of glycosides.

Methyl *tert* - butyl ether (MTBE) is produced by reacting isobutene with methanol in the presence of an acid catalyst, e.g., acidic ion - exchange resin. Heteropoly acids and their salts also catalyze the MTBE synthesis as homogeneous and heterogeneous catalysts. It is showed that, in the homogeneous reaction at 42°C, Keggin - type heteropoly acids such as $\text{H}_3\text{PW}_{12}\text{O}_{40}$ and $\text{H}_4\text{SiW}_{12}\text{O}_{40}$ are 2 - 4 times more active than the conventional catalysts in terms of the reaction rate per unit proton site [6]. Shikata *et.al.* [61] and Baronetti *et.al.*[62] studied gas phase synthesis of MTBE with several heteropoly acids and found that a Dawson - type HPA, $\text{H}_6\text{P}_2\text{W}_{18}\text{O}_{62}$, shows higher activity than the Keggin - type $\text{H}_3\text{PW}_{12}\text{O}_{40}$. Bielanski *et.al.* [63] showed that polyaniline supported HPA gave higher conversion when it was treated with air and lower conversion when it was treated with helium. Shikata *et.al.* [64] investigated that the silica-supported $\text{H}_3\text{PW}_{12}\text{O}_{40}$, $\text{H}_4\text{SiW}_{12}\text{O}_{40}$ and $\text{H}_6\text{P}_2\text{W}_{18}\text{O}_{62}$ exhibited high catalytic performance for gas-phase synthesis of MTBE. The activities were comparable to that of Amberlyst-15. Knifton and Edwards [65] demonstrated $\text{H}_3\text{PW}_{12}\text{O}_{40}$ and $\text{H}_3\text{PMo}_{12}\text{O}_{40}$, on Group III and IV oxide supports, such as titania, HF-treated montmorillonite clays, as well as mineral acid-activated clays to be effective for MTBE syntheses from methanol / *tert*-butanol

feed mixtures using a continuous, plug-flow, reactor system. An unexpected phase separation of the desired MTBE and isobutene products from aqueous methanol has been observed at high (>80%) *tert*-butanol conversion levels and operating temperatures $\geq 160^{\circ}\text{C}$.

3.7.3 Condensation

Heteropoly acids have long been known as catalysts for condensation reactions, e.g., the condensation of acetone to mesityl oxide and alkylbenzenes [39]. It has been shown that HPA is an efficient catalyst for condensations in the syntheses of vitamins E, K₁ and C [5].

H₃PW₁₂O₄₀ and H₄SiW₁₂O₄₀ catalyze the condensation of isophytol with 2,3,5 – trimethylhydroquinone (TMHQ) to α - tocopherol, that is the active form of vitamin E. Commercial synthesis of α - tocopherol is carried out with the use of H₂SO₄ or ZnCl₂ as catalysts. With ZnCl₂, which is the best catalyst, a high – quality product containing 95% vitamin E is obtained in an 80% yield. The drawback of this system is the high consumption of the catalyst and a large amount of waste products. With heteropoly acids, the yield of vitamin E is 10% higher and the quality of the product obtained is not lower than that obtained with ZnCl₂ [5].

Heteropoly acids catalyze the Prins reaction of alkenes with formaldehyde to yield 1,3 – dioxanes. In the reaction of styrene, Keggin – type HPAs are shown to be superior to H₂SO₄ and TsOH, the activity differing only slightly in the HPAs series.

3.8 BIPHASIC CATALYSIS

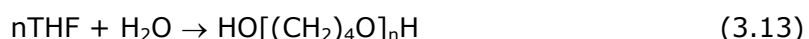
Separation of products and recovery and recycling of a catalyst often becomes much easier if a homogeneously catalyzed reaction can be performed in a biphasic system consisting of two immiscible liquid phases – a catalyst phase and a product / reactant phase – with intense mass transfer between them. Heteropoly acids, due to their special solubility properties, are suitable catalysts for operating under phase – transfer conditions.

There are two types of such biphasic systems: (1) initially homogeneous, a reaction system separates into two liquid phases in the course of the reaction; and (2) a reaction system is biphasic from the very beginning. The catalyst phase, usually the lower one, is a solution of heteropoly acid in a polar reactant. The reaction predominantly proceeds in the catalyst phase.

3.8.1 Polymerization of Tetrahydrofuran

Polymerization of tetrahydrofuran (THF) is used for the preparation of polyoxytetramethylene glycol (PTMG), which is used for the manufacturing spandex fibers and polyurethane.

Commercially, PTMG is produced by a two – step process, including ring – opening polymerization of THF with acetic anhydride catalyzed by HClO_4 , followed by hydrolysis of the terminal acetate groups in the prepolymer. Izumi *et. al.* [37] found that heteropoly acid is more active than HClO_4 in the polymerization of THF.



PTMG is obtained by ring opening THF with water in the presence of $\text{H}_3\text{PW}_{12}\text{O}_{40}$ at 60°C. The $\text{H}_2\text{O} / \text{H}_3\text{PW}_{12}\text{O}_{40}$ molar ratio is critical for the process,

controlling the reaction rate and molecular weight of polymer. When the $\text{H}_2\text{O} / \text{H}_3\text{PW}_{12}\text{O}_{40}$ molar ratio is above 15, a homogeneous phase forms, and no reaction takes place. When this ratio is below 15, the solution separates in two liquid phases – a THF (upper) phase and a $\text{H}_3\text{PW}_{12}\text{O}_{40}$ – THF – H_2O (lower) phase. The polymerization starts when the ratio is decreased below 10. The polymer is formed in the heteropoly acid phase and transferred to the THF phase.

3.8.2 Esterification

Esterification of *p* – nitrobenzoic acid is a step of the anesthetic synthesis. Ethyl *p* – nitrobenzoate is obtained in a 99% yield by esterification of *p* – nitrobenzoic acid with ethanol in the presence of $\text{H}_3\text{PW}_{12}\text{O}_{40}$ at 75°C [6]. Initially homogeneous, the reaction mixture becomes a two – phase system in the end of the reaction. The upper phase contains the product; the lower phase is a concentrated solution of heteropoly acid in ethanol.

Acetoxylation and hydration of dihydromyrcene (DHM) yield dihydromyrcenol (DHM – OH) and dihydromyrcenyl acetate (DHM – OAc), respectively, which are useful for perfume industry. These reactions occur simultaneously in a two – phase system in the presence of HPA at $14 - 30^\circ\text{C}$ [66]. The upper phase mainly consists of DHM and the lower phase is a concentrated solution of $\text{H}_3\text{PW}_{12}\text{O}_{40}$ in aqueous acetic acid.

3.8.3 Other Reactions

Sato *et.al.* [67] investigated various acetal formation reactions between monoalcohols or diols and a range of aldehydes or ketones catalyzed by a Keggin – type HPA in comparison with other acid catalysts. The catalyst activity was found to decrease in the order: $\text{H}_4\text{SiW}_{12}\text{O}_{40} > \text{H}_3\text{PMo}_{12}\text{O}_{40} > \text{H}_3\text{PW}_{12}\text{O}_{40} > \text{TsOH} > \text{H}_2\text{SO}_4$.

3.9 HETEROGENEOUS CATALYSIS

Solid heteropoly acids are more efficient than conventional solid acids, like zeolites, $\text{SiO}_2 - \text{Al}_2\text{O}_3$, etc. the ability to absorb large amount of polar molecules in the bulk, coupled with high proton mobility, leads to a high catalytic efficiency for liquid phase reactions, This behavior favors the reaction kinetics and the participation of all structural protons in the reaction [38]. This high activity allows the operation to be carried out at milder conditions than with other solid acids. Obvious advantage of heterogeneous systems over homogeneous is easy separation of a catalyst from reaction products.

Furthermore, since heteropoly acids are soluble only in wet polar solvents, their strong acidity cannot be utilized in homogeneous systems [6]. Therefore, heteropoly acids must be used as solid acid catalyst for catalyzing highly demanding reactions like Friedel – Crafts reaction. In order to enhance the acid strength, solid heteropoly acid catalysts are usually dehydrated by evacuating at 150 - 300°C for 1 – 2 h [39].

A serious problem with the solid heteropoly acid catalysts is their deactivation during organic reactions due to the coke formation on the catalyst surface, which remains to be solved to put heterogeneous heteropoly acid catalysis in practice. Instead of burning the coke as in the case of aluminosilicates and zeolites, supporting heteropoly acids on a carrier inhibits the formation of coke on the catalyst surface.

3.9.1 Paraffin Alkylation

The paraffin alkylation is used in industry to obtain higher-octane paraffins that are blended into gasoline. H_2SO_4 and HF are used as homogeneous catalysts in this process. $\text{H}_3\text{PW}_{12}\text{O}_{40}$ supported on a series of carriers, such as mesoporous

molecular sieve, MCM – 41, amorphous silica, and alumina resulted in higher olefin conversion about 87% for the isobutene to 2-butene alkylation [6].

3.9.2 Friedel-Crafts and Related Reactions

Heteropoly acids and their salts are promising solid acid catalysts for Friedel-Crafts reactions, to replace the conventional homogeneous catalysts such as AlCl_3 , BF_3 and H_2SO_4 , which bring about serious environmental and operational problems like high toxicity, corrosion, difficulty of separation and recovery, etc [6].

Silica supported $\text{H}_3\text{PW}_{12}\text{O}_{40}$ is a very active catalyst, superior to other HPAs for the alkylation of benzene with 1-octane. The catalytic activity depends on the pretreatment temperature and HPA loading [40,68]. In the acylation of *p*-xylene with benzoyl chloride, $\text{H}_3\text{PMo}_{12}\text{O}_{40}$ supported SiO_2 catalyst was found to decompose during the reaction [37]. Probably, the real active species is not the supported $\text{H}_3\text{PMo}_{12}\text{O}_{40}$, but some soluble species that might be formed by the interaction between $\text{H}_3\text{PMo}_{12}\text{O}_{40}$ and benzoyl chloride. On the contrary, $\text{H}_3\text{PW}_{12}\text{O}_{40}$ and $\text{H}_4\text{SiW}_{12}\text{O}_{40}$ both effectively catalyze the acylation and remain unchanged on the SiO_2 surface after the reaction. But in a more polar reaction medium, like in the acylation of chlorobenzene, even $\text{H}_4\text{SiW}_{12}\text{O}_{40}$ leaches from the silica support and decomposes in the course of the reaction like $\text{H}_3\text{PMo}_{12}\text{O}_{40}$.

Bulk $\text{H}_3\text{PW}_{12}\text{O}_{40}$ shows a better performance than liquid H_2SO_4 , CF_3COOH or solid Ambelyst-15, $\text{SiO}_2 - \text{Al}_2\text{O}_3$ catalysts for the selective alkylation of *p*-xylene with isobutene at 30°C to afford *tert*-butyl-*p*-xylene, an important precursor for liquid crystalline polymers, with 75% selectivity.

Insoluble $\text{Cs}_{2.5}\text{H}_{0.5}\text{PW}_{12}\text{O}_{40}$, which has a large surface area and strong acid sites, is a promising solid acid catalyst for Friedel-Crafts reactions [7]. In the

alkylation of 1,3,5-trimethylbenzene by cyclohexene, the cesium salt was found to be more active than the parent acid, $\text{H}_3\text{PW}_{12}\text{O}_{40}$. Higher hydrophobicity of the Cs salt compared to heteropoly acid is beneficial for the adsorption of nonpolar reacting molecules. Izumi *et.al.* [69] investigated that $(\text{NH}_4)_2\text{HPW}_{12}\text{O}_{40}$ worked as an efficient insoluble acid catalyst for the liquid-phase Friedel-Crafts alkylation of benzene and the acylation of *p*-xylene with benzoic anhydride or benzoyl chloride.

3.9.3 Esterification, Hydrolysis, and Related Reactions

There is a strong demand for new solid acid catalysts, having advanced characteristics, to replace conventional liquid and solid catalysts, such as sulfuric acid and ion exchange resins, in the reactions like esterification. Sulfuric acid, as already mentioned, poses serious environmental and operational problems. Acidic ion-exchange resins such as Amberlyst-15 are mostly used, but only at temperatures below 100°C due to their low thermal stability [6]. It is obvious that, in these reactions in which water participates as a reactant or a product, there are few solid acid catalysts that meet the criteria of activity and stability. Izumi *et.al.* [70] showed that certain supported heteropoly acid catalysts as well as insoluble heteropoly acid salts have advantages as catalysts for liquid-phase reactions in aqueous media because they are insoluble, thermally more stable than acidic resins and have strong acidity.

Active carbon strongly adsorbs a certain amount of heteropoly acid, and carbon - supported heteropoly acids thus obtained catalyze liquid - phase esterification and related reactions in polar media [6]. The carbon - supported $\text{H}_3\text{PW}_{12}\text{O}_{40}$ catalyze the formation of butyl *tert*-butyl ether from *n*-butyl alcohol and *tert*-butyl alcohol at 106°C and the esterification of acetic acid with *n*-butyl alcohol at 60°C. In all these reactions, the catalyst can be reused, no heteropoly

acid leaching from carbon being observed. However, the carbon-supported heteropoly acid catalysts have a rather low catalytic activity because of their weak acidity. In addition, since active carbon adsorbs polar organic molecules strongly, the work-up procedure becomes difficult.

Dupont and Lefebvre [71] studied the esterification of propanoic acid by butanol or 2-ethylhexanol catalyzed by $\text{H}_3\text{PW}_{12}\text{O}_{40}$ and $\text{H}_4\text{SiW}_{12}\text{O}_{40}$ pure or supported on carbon supports. As a result, $\text{H}_4\text{SiW}_{12}\text{O}_{40}$ showed slightly higher activity than $\text{H}_3\text{PW}_{12}\text{O}_{40}$. Carbon-supported heteropoly acids exhibits lower activity than the pure HPAs in all cases, the activity depending on the carbon support and the heteropoly acid loading. In addition, deactivation occurred during the recycling of these catalysts because of the leaching of HPA from the support.

Izumi *et.al.* [37] found that the insoluble $\text{Cs}_{2.5}\text{H}_{0.5}\text{PW}_{12}\text{O}_{40}$ is an active solid acid catalyst for esterification and hydrolysis, which is much more active than zeolite H-ZSM-5 for the hydrolysis of ethyl acetate and esterification of acetic acid with ethanol. However, $\text{Cs}_{2.5}\text{H}_{0.5}\text{PW}_{12}\text{O}_{40}$ consisting of very fine particles (~10 nm), form colloidal solution in water and alcohol, which makes it inseparable by filtration.

CHAPTER 4

EXPERIMENTAL

4.1 CHEMICALS AND CATALYSTS

In this study, tungstophosphoric acid ($\text{H}_3\text{PW}_{12}\text{O}_{40}\cdot x\text{H}_2\text{O}$) and molybdophosphoric acid ($\text{H}_3\text{PMo}_{12}\text{O}_{40}\cdot x\text{H}_2\text{O}$) from Acros Organics and Amberlyst-15 with an average particle diameter of 740 microns from Sigma [31] were used. The physical properties of Amberlyst-15 are given in Table 4.1. The activated carbon, which is used as the support material is from KUREHA (Japan) in granular form with mesh size of 40-50 (425-300 microns).

Table 4.1 Physical Properties of the Amberlyst-15 Catalyst [31]

Average particle diameter (m)	7.4×10^{-4}
Macroporosity, ε_p	0.32
Apparent density (g/cm^3)	0.99
Average macropore diameter (m)	2.28×10^{-8}
Surface area (m^2/g) (nitrogen adsorption)	39.2 ^a
(mercury porosimeter)	59.2 ^b

^a Corresponds to pores having diameter between 1.7×10^{-9} and 3×10^{-7}

^b Corresponds to pores having diameters greater than 6.7×10^{-9}

To prepare the impregnating solutions of tungstophosphoric acid (TPA), ethanol with a purity of 96 vol% from Birpa was used. In the etherification reaction experiments, 2-methyl-2-butene (2M2B) with a purity of 85% (the rest is 2M1B) from Merck and absolute ethanol (purity, min. 99.8 vol%) from Merck were used. In the side product formation reactions, besides ethanol, methanol from Merck was used. For the calibration of gas chromatography, beside 2M2B and ethanol, TAME (>97%) from Aldrich was used. The properties of the chemicals are listed in Table 4.2.

Table 4.2 Properties of Chemicals Used in the Experiments [72]

Chemical	Chemical Formula	Boiling Point (°C)	Purity	Density	Molecular Weight	Firm
2M2B	C ₅ H ₁₀	38	85%	0.66	70.14	Merck
Ethanol	C ₂ H ₅ OH	78-79	Min99.8 vol%	0.790	46.07	Merck
Ethanol	C ₂ H ₅ OH	78	96 vol%	0.800	46.07	Birpa
Methanol	CH ₃ OH	65	99.8 vol%	0.789	32.04	Merck
TAME	C ₆ H ₁₄ O	85-86	97 %	0.770	102.18	Aldrich

4.2 EXPERIMENTAL SET-UP

The experimental set-up consists of 9 main parts; a syringe pump, a vaporizer, a helium gas cylinder, a reactor, a constant temperature water bath, a condenser, a cold-water bath, a gas chromatograph equipment and flow lines. The schematic diagram is given in Figure 4.1.

Predetermined amounts of ethanol and 2M2B were mixed and fed to the system by the help of a syringe pump (Harvard Apparatus). The feed mixture leaving the pump was evaporated in a heated U-shaped glass tube, 13 cm. in length and 0.13 cm in outer diameter, filled with small glass pieces. This U-tube was heated by placing it into an oven (Fischer). In the vaporizer the feed

mixture was mixed with helium, which was used as the carrier gas in the system. Then, they were fed to the reaction section. This part of the apparatus was composed of a stainless-steel reactor that was 19 cm in length and 0.46 cm in inner diameter. The catalyst was placed into the reactor by using quartz wool supports at both ends and then the reactor was placed in a constant temperature water bath (Blue M). The outlet stream of the reactor was sent to the condenser in order to liquefy both the unreacted mixture and product. Samples were collected into small tubes and these tubes were immersed into an ice bath to avoid any loss of mixture.

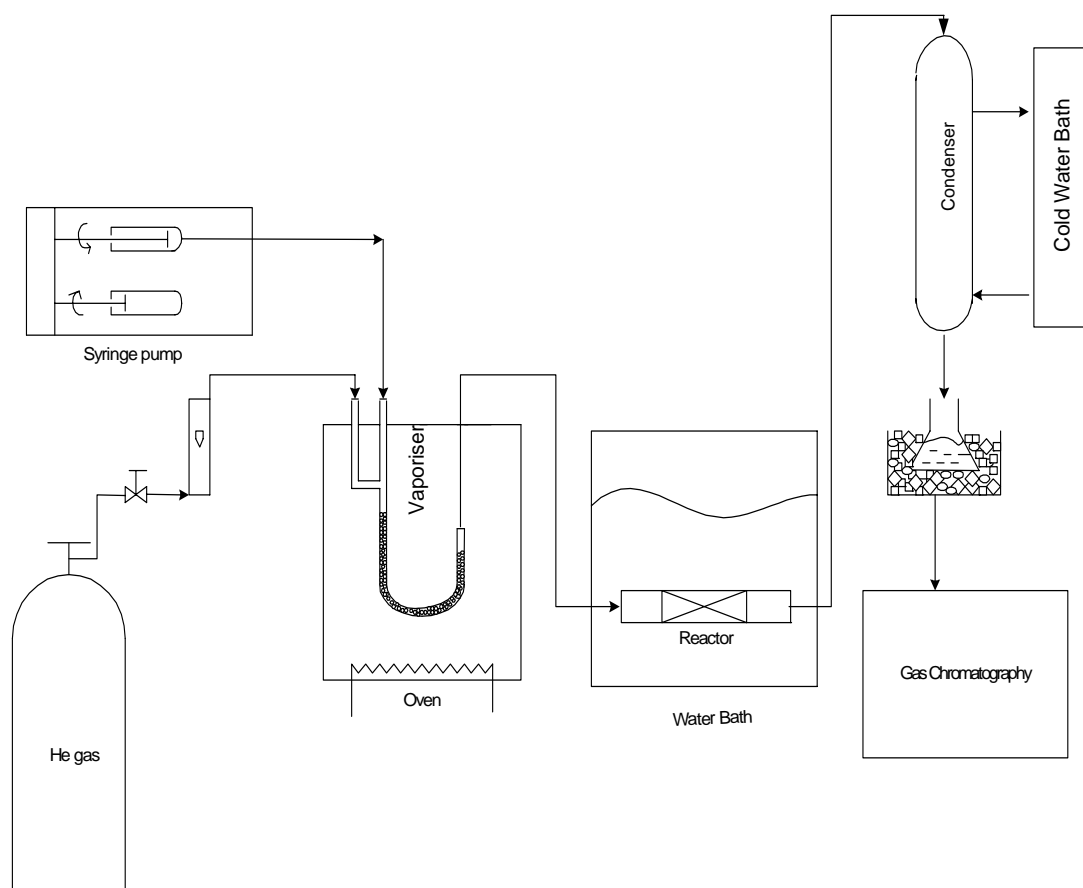


Figure 4.1 Experimental Set-Up

The samples taken from the condenser were injected into the chromatograph (Varian 2700 Aerograph). The column used in the system was packed with 15% FFAP on Chromosorb AW and the detector used was Flame Ionization Detector (FID).

Connection lines in the system were copper tubing. Starting from the outlet of the vaporizer to the condenser inlet all the lines were well heated by heating tapes in order to prevent any condensation of 2M2B and ethanol mixture as well as product.

4.3 EXPERIMENTAL PROCEDURE

4.3.1 Preparation of Supported Heteropoly Acid Catalysts

Before being utilized in impregnation experiments, the activated carbon (AC) was washed first in solution of 0.1 M NaOH, then in 0.1 M HCl to eliminate the soluble acidic and alkaline impurities. Finally, it was chemically treated in solution of HNO₃ (30 % w/w) heated by reflux for 2 hours to make the carbon more acidic [50].

After washing and acidification steps, two TPA solutions with different concentrations were prepared by using a mixture of demineralized water and ethanol (96%), in a volumetric ratio 1:1, as the solvent. These were supported on activated carbon by aqueous impregnation technique [50,52,64,73]. The loading amounts were 25 and 31-wt% TPA on activated carbon [50]. They were dried at 100°C overnight. After drying step, 25-wt% TPA/AC catalyst was calcined at two different temperatures, 120°C and 180°C for 4 hours and the other catalyst (31-wt%TPA/AC) was calcined at 130°C in a flow of air for 4 hours. These calcinations temperatures were decided according to the results of thermal analysis.

4.3.2 Characterization of Catalysts

The surface areas of catalysts and support used in the experiments were determined from N₂-Adsorption data at 77 K by using BET equation by a computerized surface area analyzer model ASAP 2000 of Micromeritics Co. Inc..

Thermogravimetric analysis of both bulk and supported heteropoly acids was carried out by using Dupont 951 Thermal Analyzer. The thermogravimetry experiments were performed under nitrogen, using 18-25 mg samples and a heating rate of 10°C/min. The studied temperature range was 30-800°C.

The bulk density of activated carbon was determined by mercury porosimetry using a commercial mercury porosimeter (Quantachrome Autoscan Mercury Porosimetry). Its solid density was determined by helium pycnometry using Micromeritics Multivolume Pycnometer 1305.

4.3.3 Catalytic Reactions

In our experiments, the feed concentration was 30 vol % 2M2B + 70 vol % ethanol and it was given to the system at a rate of 0.0477 ml/min. The flow rate of helium (carrier gas) was adjusted to 72.2 ml/min that was controlled by the help of a rotameter. In all experimental runs, these values were kept constant.

The experiments were carried out in seven parts. In the first part, the effect of temperature on the catalytic activity of bulk tungstophosphoric acid was investigated. 0.2 g of catalyst was placed into the reactor and the temperature range was taken between 80°-97°C. To check the reproducibility, the experiment was repeated with fresh catalyst under the same conditions.

In the second part of the experiments, the effect of temperature on the catalytic activity of supported tungstophosphoric acid was investigated. Also the

effect of loading amount and calcination temperature on the catalytic activity was studied. 0.2 g of 25-wt% TPA/AC calcined at 120°C was placed into the reactor and the temperature range was taken between 80°-97°C. After that, again to check the reproducibility, the experiment was repeated with unused catalyst under the same conditions. The same procedure was carried out for 25-wt% TPA/AC calcined at 180°C and 31-wt% TPA/AC and reproducibility check was done also for 25-wt% TPA/AC calcined at 180°C.

In the third part of the experiments, the same effects that were studied in the second part of the experiments were investigated. Here, the amounts of the supported catalysts loaded to the reactor were different, and the total tungsten concentration in the catalysts was fixed [50]. Therefore, for 25-wt% TPA/AC catalyst, 0.800 g of catalyst was loaded to the reactor and for 31-wt% TPA/AC catalyst, 0.644 g of catalyst was loaded to the reactor and in each run, the temperature range was taken between 80°-97°C.

In the fourth part of the experiments, the catalytic activity of alternative catalysts, Ambelyst-15 and molybdophosphoric acid (MPA), was investigated. In both runs, 0.2 g of catalyst was loaded to the reactor. Here, the experiments were performed at a fixed temperature of 90°C.

In the fifth part of the experiments, the deactivation of bulk tungstophosphoric acid and 25-wt% TPA/AC calcined at 120°C was studied. The amount of catalyst loaded to the reactor was 0.2 g and the temperature range was taken between 80°-97°C. The experiments were repeated under the same conditions without changing the catalyst inside the reactor.

In the sixth part of the experiments, the change in the activity of the supported TPA was investigated when it was kept in a polar medium before

utilizing in the experiments. For this purpose, 31-wt% TPA/AC catalyst was put into absolute ethanol and waited overnight. After that, 0.644 g of catalyst was loaded to the reactor and the experiment was done at 90°C.

In the seventh part of the experiments, formation of side products, diethyl ether and dimethyl ether, was studied. Here, only alcohol was used as the reactant. For diethyl ether formation, ethanol and for dimethyl ether formation methanol was used. 0.2 g of bulk TPA acid was loaded to the reactor and the temperature range was taken between 80°-97°C.

All the experiments carried out in this study are summarized in Table 4.3.

Table 4.3 The outline of the experiments

Run	Catalyst	Loading(g)	Temp. (°C)	Reactant
1	Bulk TPA	0.2	80-97	2M2B-EtOH
2	Bulk TPA	0.2	80-97	2M2B-EtOH
3	25-wt% TPA/AC($T_{calc.}=120^{\circ}C$)	0.2	80-97	2M2B-EtOH
4	25-wt% TPA/AC($T_{calc.}=180^{\circ}C$)	0.2	80-97	2M2B-EtOH
5	31-wt% TPA/AC	0.2	80-97	2M2B-EtOH
6	25-wt% TPA/AC($T_{calc.}=120^{\circ}C$)	0.2	80-97	2M2B-EtOH
7	25-wt% TPA/AC($T_{calc.}=180^{\circ}C$)	0.2	80-97	2M2B-EtOH
8	25-wt% TPA/AC($T_{calc.}=120^{\circ}C$)	0.8	80-97	2M2B-EtOH
9	25-wt% TPA/AC($T_{calc.}=180^{\circ}C$)	0.8	80-97	2M2B-EtOH
10	31-wt% TPA/AC	0.644	80-97	2M2B-EtOH
11	Amberlyst-15	0.2	90	2M2B-EtOH
12	Bulk MPA	0.2	90	2M2B-EtOH
13	Bulk TPA	0.2	80-97	2M2B-EtOH
14	25-wt% TPA/AC($T_{calc.}=120^{\circ}C$)	0.2	80-97	2M2B-EtOH
15	31-wt% TPA/AC	0.644	80-97	2M2B-EtOH
16	Bulk TPA	0.2	90	EtOH/MeOH

4.3.4 Analytical Method

The samples taken from the condenser were injected into the gas chromatograph (GC), as stated before, with a 5 μ l gas chromatograph syringe. The detector was Flame Ionization Detector (FID) and the column was packed with 15% FFAP on Chromosorb AW.

The column was operated using helium (He) as the carrier gas with a constant flow rate of 30 cc/min at a constant column temperature of 100°C. Before starting to analyze the samples, the column was conditioned for 3 hours with helium. Dry air and hydrogen were fed to the system for FID at a flow rate of 300 cc/min and 30 cc/min, respectively. Injector and detector temperatures were adjusted to 125 and 170°C, respectively.

With the data acquisition system connected to the chromatograph, the response peaks of the samples injected were analyzed with high precision. Before performing the experiments, for each component, chromatograph calibration factors (α) were evaluated. Sample calculation for finding calibration factor is given in Appendix A.1. When the response peaks of experiments were obtained, using the calibration factors, the mole fraction or concentration of the components were found for each sample taken. By this way, the errors due to injection and the probable errors coming from the detector were minimized. A sample calculation to find concentration from GC data is given in Appendix A.2.

In this study, the calibration factors for 2M2B and TAME were calculated to obtain quantitative results from the gas chromatograph trace. The calibration factor of ethanol was taken as unity and the calibration factors of the other species were determined relative to ethanol.

The calibration factors of 2M2B, EtOH and TAME used in the experimental calculations are given in Table 4.4.

Table 4.4 Calibration Factors for reactants and products

Component	Calibration factor. α
2-Methyl-2-butene. 2M2B	0.256
Ethanol, EtOH	1.000
Tert Amyl methyl Ether. TAME	0.318

CHAPTER 5

RESULTS AND DISCUSSION

In this study, applicability of pure heteropoly acid and its supported form, to the etherification reaction of isoamylene (2-methyl-2-butene) with ethyl alcohol in a continuous vapor phase differential reactor was investigated. The effect of temperature, the effect of loading level of heteropoly acid on activated carbon on the conversion and reaction rate were studied. Also the effect of catalyst amount loaded to the reactor was studied. Tungstophosphoric acid ($\text{H}_3\text{PW}_{12}\text{O}_{40}\cdot x\text{H}_2\text{O}$) type of heteropoly acid was used as active solid acid catalyst. Also, to make a comparison of activity of that pure and supported heteropoly acid, same studies, at a fixed temperature, were done with a macroreticular acidic resin (Amberlyst-15) and pure molybdophosphoric acid ($\text{H}_3\text{PMo}_{12}\text{O}_{40}\cdot x\text{H}_2\text{O}$), which is another type of heteropoly acid. Moreover, the deactivation of loaded catalyst (TPA on AC) and of pure tungstophosphoric acid was investigated. After that, formation of side products, in the presence of bulk tungstophosphoric acid, were studied and finally the catalytic activity of alcohol treated supported tungstophosphoric acid was investigated at a fixed temperature. All these studies were done at a fixed feed concentration.

5.1 CATALYST CHARACTERIZATION

5.1.1 Determination of Water of Crystallization

The amounts of water of crystallization found in the structure of $\text{H}_3\text{PW}_{12}\text{O}_{40}\cdot x\text{H}_2\text{O}$ and $\text{H}_3\text{PMo}_{12}\text{O}_{40}\cdot x\text{H}_2\text{O}$ were unknown. They were calculated according to the thermal gravimetric analysis (TGA) results. In bulk tungstophosphoric acid 11 moles and in bulk molybdophosphoric acid 16 moles of water of crystallization were found. The TGA results of bulk tungstophosphoric acid and molybdophosphoric acid were given in Figure 5.1 and in Figure 5.2, respectively.

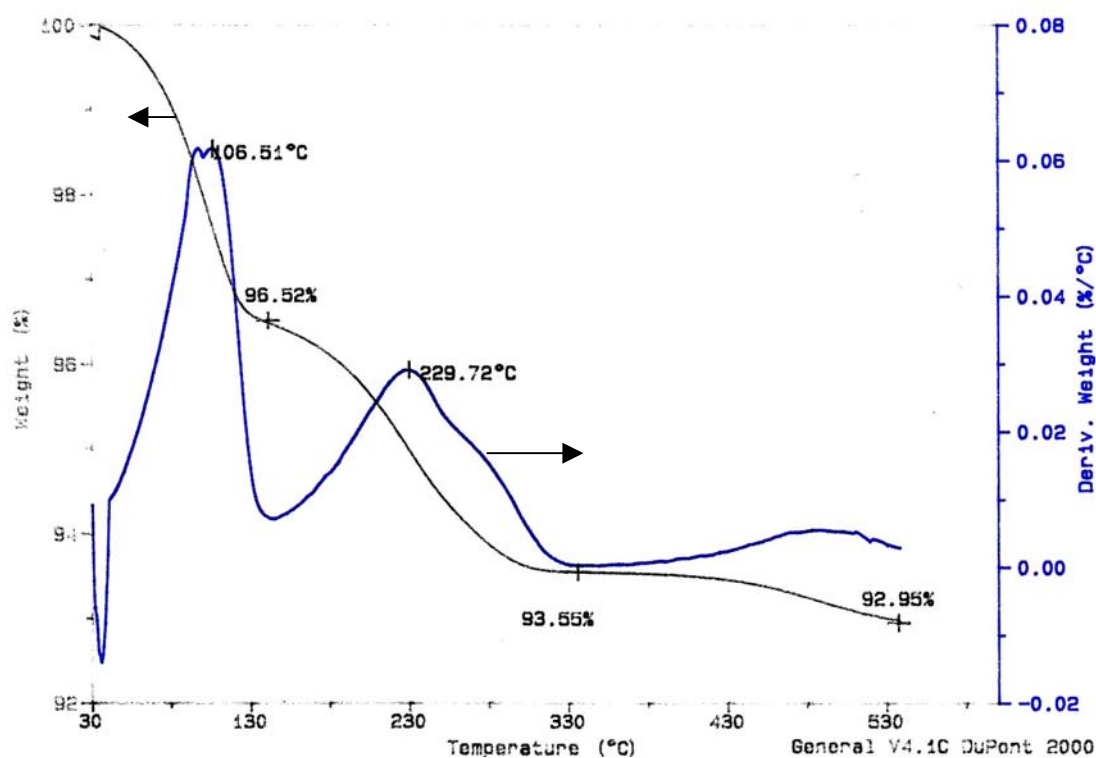


Figure 5.1 TGA result of bulk tungstophosphoric acid

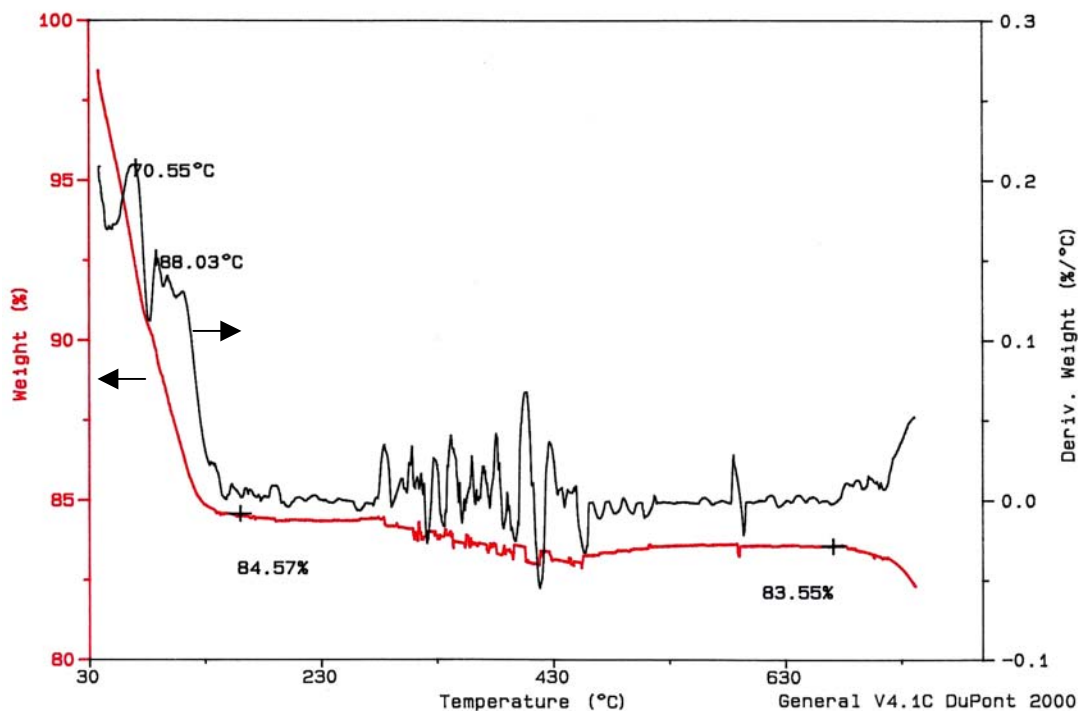


Figure 5.2 TGA result of bulk molybdophosphoric acid

5.1.2 Determination of Surface Area and Pore Diameter

All the surface areas and average pore diameters of the catalysts and the support, were calculated according to the N_2 -Adsorption data at 77 K by using BET equation by a computerized surface area analyzer.

The order of magnitude of surface areas of bulk tungstophosphoric acid and molybdophosphoric acid were found from N_2 adsorption as $1.0 \text{ m}^2/\text{g}$ and $5.0 \text{ m}^2/\text{g}$, as expected because the hydrogen forms of the heteropoly acid compounds have low surface areas [7]. The average pore diameters were found as 35.4 Å for bulk tungstophosphoric acid and 48.9 Å for molybdophosphoric acid.

The surface areas of the activated carbon before and after acidification steps were found as $1030 \text{ m}^2/\text{g}$ and $884 \text{ m}^2/\text{g}$, respectively. Acid used in the acidification step might decompose the structure of some pores in the activated

carbon; therefore the surface area of the acidified carbon came out to be smaller than that of original activated carbon. There was not a significant change in the average pore diameter of original activated carbon; it was found as 14.4 Å, and for acidified carbon a value of 14.6 Å was found.

Finally, the surface areas of supported catalysts were calculated. For 25-wt% TPA/AC catalyst, the surface area was found as 424 m²/g and for 31-wt% TPA/AC catalyst, this value was found as 501 m²/g. The average pore diameter of former one was found as 14.0 Å, and a value of 14.4 Å was found for 31-wt% TPA/AC catalyst.

5.1.3 Determination of Porosity of Activated Carbon

The porosity can be calculated from

$$\epsilon = \frac{\rho_s - \rho_b}{\rho_s} \quad (5.1)$$

where ρ_s represents solid density and ρ_b represents bulk density.

Bulk density, from mercury porosimetry, was found as 1.05 g/cm³ and solid density, from helium pycnometry, was found as 2.85 g/cm³. When these values were put into equation 5.1, porosity is obtained as follows:

$$\rightarrow \epsilon = \frac{2.85 - 1.05}{2.85} = 0.63$$

5.1.4 Determination of Calcination Temperature of Catalysts

25-wt% TPA/AC catalyst was calcined at two different temperatures, 120°C and 180°C and the calcination of 31-wt% TPA/AC catalyst was done at 130°C, as stated in the experimental part. These temperatures were not selected

arbitrarily, they were decided according to the TGA results of 25-wt% TPA/AC and 31-wt% TPA/AC, which were given in Figures 5.3 and 5.4, respectively. In TGA result of 25-wt% TPA/AC, a significant change in the weight of the catalyst was observed around 120°C and 180°C. Probably, at those temperatures, water of crystallization molecules were released. Also, around 80°C, a significant change in the weight was observed because, probably at this temperature the moisture of the catalyst was removed.

In TGA result of 31-wt% TPA/AC, again a significant change in the weight of the catalyst was observed around 65°C and 130°C. Probably, at the former temperature, the moisture of the compound was removed and at 130°C water of crystallization molecules were removed.

In both catalysts, higher temperatures were not selected for calcination because at higher temperatures (>350°C), the structure of Keggin-type heteropoly acids decomposes [40, 77].

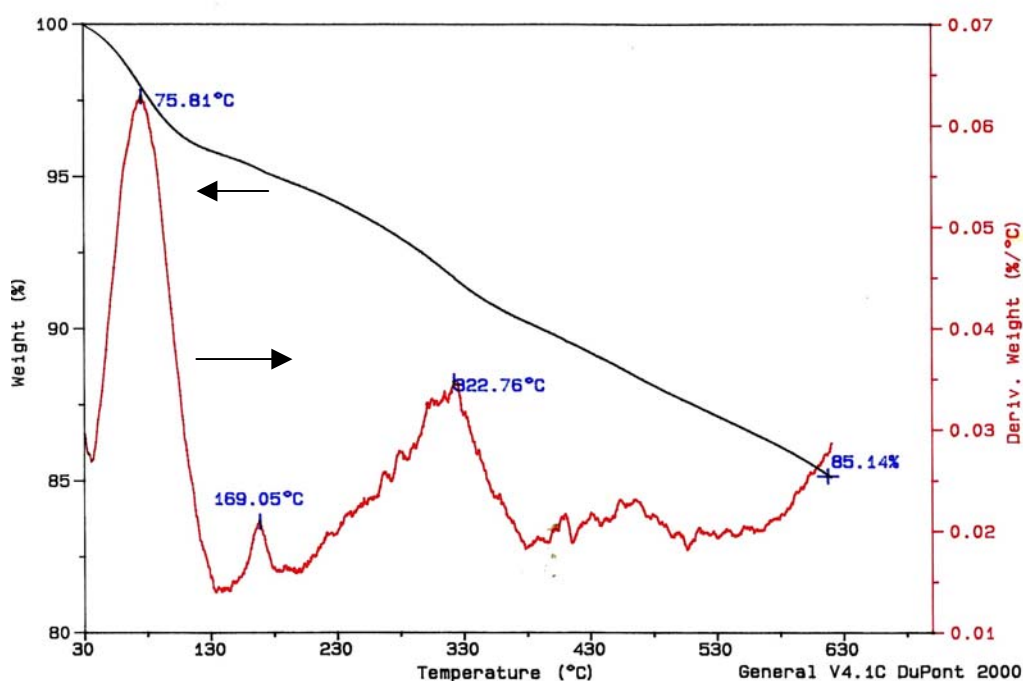


Figure 5.3 TGA result of 25-wt% TPA/AC catalyst

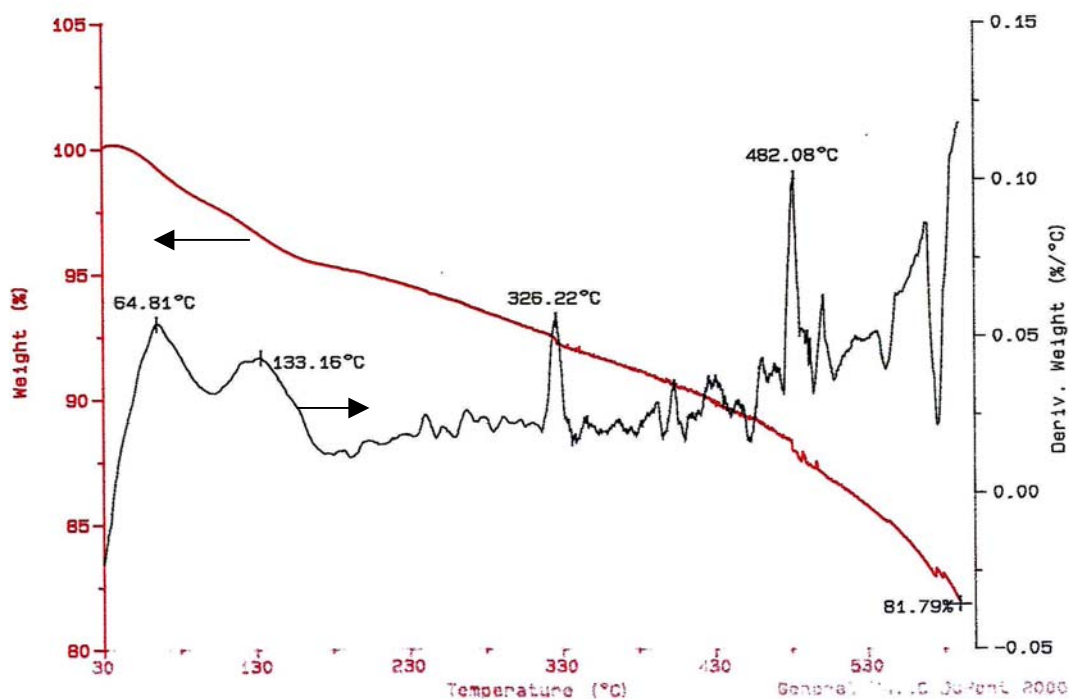


Figure 5.4 TGA result of 31-wt% TPA/AC catalyst

5.2 CATALYTIC REACTIONS

5.2.1 Catalytic Activity of Bulk Heteropoly Acid

In the first part of the experiments, the effect of temperature on the conversion of 2M2B to TAE and reaction rate in the presence of bulk tungstophosphoric acid was investigated. The temperature range was taken between 80°C - 97°C and 0.2 g of tungstophosphoric acid was loaded to the reactor. To check the reproducibility of this experiment, a second run, with fresh catalyst, was carried out keeping all the other working conditions such as initial feed concentration, temperature range, catalyst loading, etc. same. The experimental data, in tabulated form, for this set of experiments are given in Appendix C.1 and C.2. Variations of conversion of 2M2B to TAE and the reaction rate with temperature are given in Figure 5.5 and 5.6, respectively.

In this study, the conversion of 2M2B to TAE is defined as follows:

$$X_{A,f} = \frac{x_{TAE}}{(x_{2M2B} + x_{TAE})} \quad (5.2)$$

The way of determination of conversion values from gas chromatography data is given in Appendix A.2. Since the ethanol concentration was assumed to be constant throughout the reactions, it was not included in Equation 5.2.

The rate of reaction was calculated from the following equation:

$$-R_A = \frac{X_{Af} F_{Ao}}{m} \quad (5.3)$$

where, X_{Af} , F_{Ao} and m correspond to conversion, initial molar flow rate and mass of the catalyst, respectively. In the calculation of rate of reaction differential reactor assumption was done. Derivation of reaction rate is given, in details, in Appendix B.3.

In this study, rate calculations are based on differential reactor assumption. However, conversion values obtained here were in the order of magnitude of 0.2, which were much higher than the values for a differential reactor. In fact, in some experiments fractional conversions reached values quite close to equilibrium conversions (Figure 5.5). Also some variations of temperature were possible along the reactor. In such cases, uniform rate assumption along the reactor fails. So the rate values reported in Figures 5.6 and 5.8 actually correspond to the average values along the reactor.

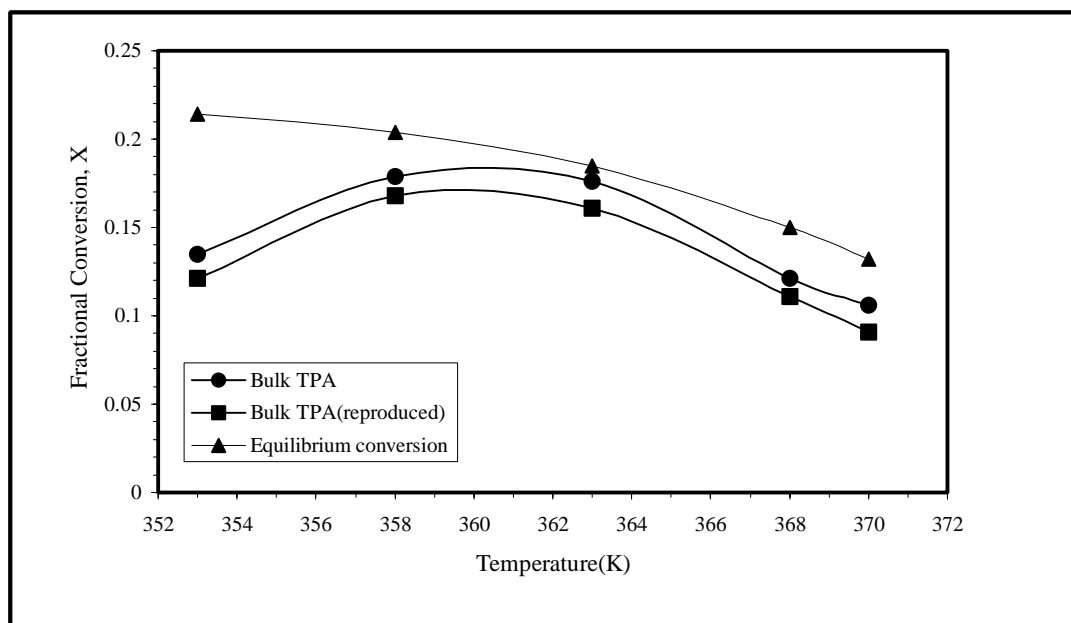


Figure 5.5 Variation of conversion with temperature in the presence of bulk tungstophosphoric acid (Exp.#: 1-2)

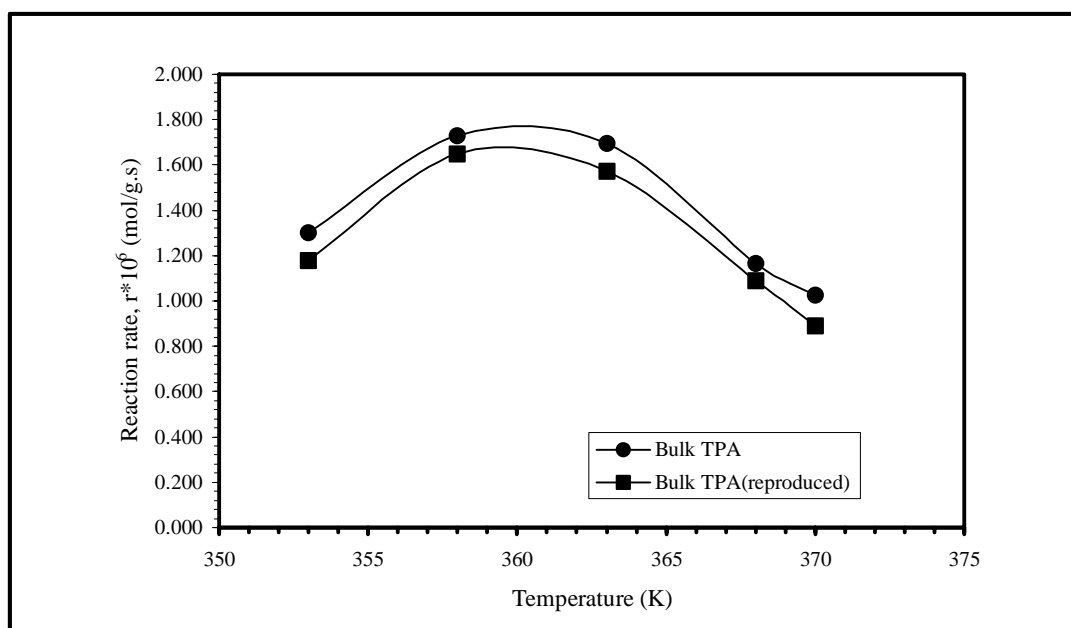


Figure 5.6 Variation of reaction rate with temperature in the presence of bulk tungstophosphoric acid (Exp.#: 1-2)

The conversion increased from 13.5% to 17.8% when the temperature was raised from 80°C (353K) to 85°C (358K) and slightly decreased to 17.6%. When the temperature was raised up to 97°C (370K), the conversion decreased to 10.6% as presented in Figure 5.5. These results show that the catalyst activity

was high between 85°C (358K) and 90°C(363K) and then it decreased drastically. This might due to the fact that, when the reaction temperature was increased above 85°C(358K), the reverse reaction (conversion of *tert*-ether to isoolefin) might suppress the forward reaction (conversion of isoolefin to *tert*-ether).

To check the reproducibility, the same experiment was repeated under the same conditions with fresh catalyst and the same trend was observed in catalytic activity of bulk TPA as shown in Figure 5.5. The results were slightly different from the results of previous run due to the experimental errors such as change in the flow rate of the carrier gas.

The experimental results were compared with the calculated equilibrium conditions corresponding to each temperature. The equilibrium for reaction j in the gas phase can be expressed as,

$$K_j = \prod (a_i)^{\nu_i} = \prod (\phi_i)^{\nu_i} \prod (y_i)^{\nu_i} \quad (5.4)$$

Here, a_i , ϕ_i , y_i and ν_i correspond to activity, fugacity coefficient, vapor mole fraction and stoichiometric coefficient of species i , respectively, in j th reaction. The equilibrium calculations were done by using expressions from literature [29,74]. These expressions and the details of the equilibrium calculations are given in Appendix B.2. Results of equilibrium calculations were tabulated in Table 5.1 and the results given in Figure 5.5 showed that, the overall conversion of 2M2B to TAEE could not reach the equilibrium in both runs. Only at 90°C (363K), the reaction approached to the equilibrium.

Table 5.1 Equilibrium Conversion Values at Different Temperatures

TEMPERATURE (K)	EQUIL. CONVERSION, X_{eqb}
353	0.214
358	0.204
363	0.185
368	0.150
370	0.132

5.2.2 Catalytic Activity of Supported Heteropoly Acid

In this part, firstly, the effect of temperature on conversion of 2M2B to TAE and reaction rate was investigated in the presence supported heteropoly acid catalysts, 25-wt% TPA/AC (T_{calc} : 120°C), 25-wt% TPA/AC (T_{calc} : 180°C) and 31-wt% TPA/AC. Here, the total amount of catalyst (TPA+support) loaded to the reactor was 0.2 g. The experimental data, in tabulated form, are given in Appendix C.3, C.4 and C.5.

Variations of conversion and reaction rate with temperature are given in Figures 5.7 and 5.8, respectively in order to show the change in the catalytic activity when the loading level of catalyst and calcination temperature was changed.

Since the conversion increased when the loading amount was raised from 25-wt% to 31-wt%, the reaction rate also increased as presented in Figure 5.8.

The calcination temperature also had a significant effect on conversion and reaction rate as shown in Figures 5.7 and 5.8. When the 25-wt% TPA/AC catalyst was calcined at 180°C, more water of crystallization molecules might be removed from the solid catalyst as compared to the 25-wt% TPA/AC catalyst calcined at 120°C and because of this reason the catalyst which was calcined at 180°C showed higher activity.

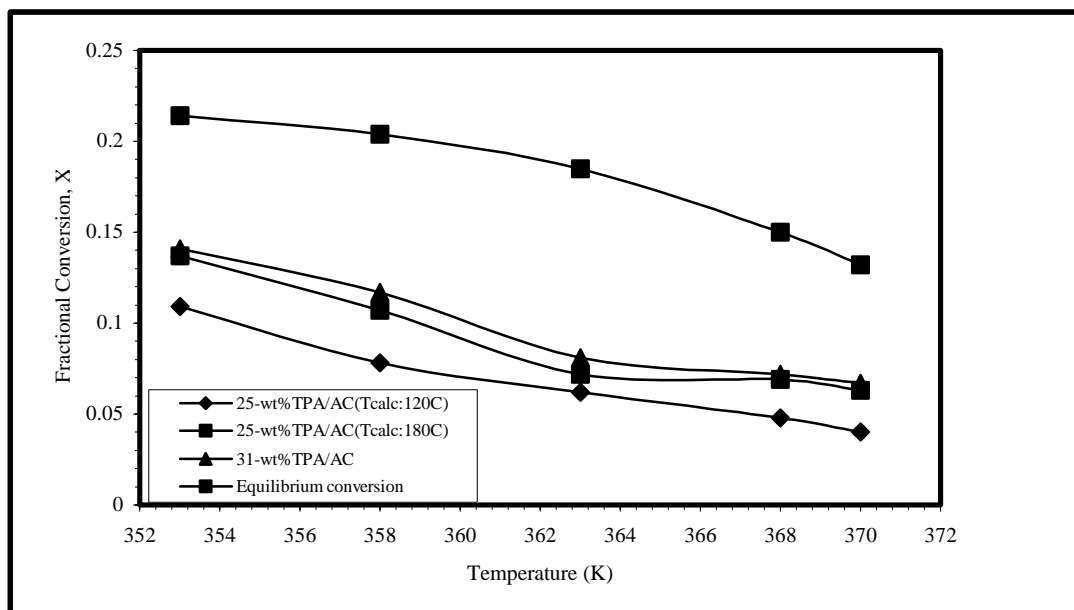


Figure 5.7 Variation of conversion with temperature in the presence of three different supported catalysts (Exp.#: 3-5)

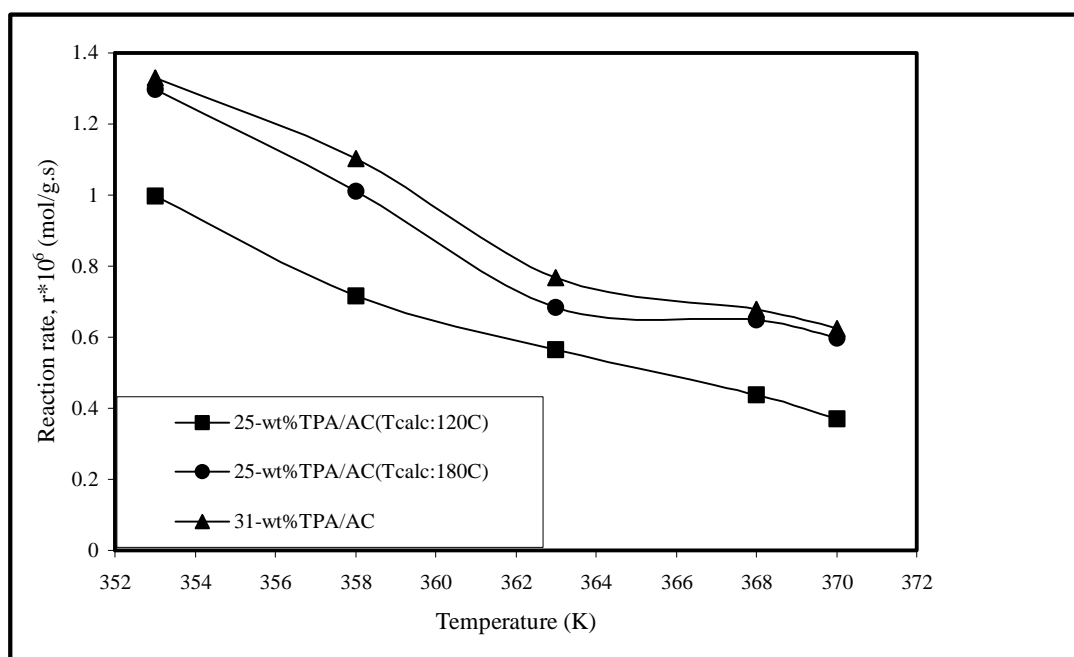


Figure 5.8 Variation of reaction rates with temperature in the presence of three different supported catalysts (Exp.#:3-5)

In the presence of supported catalyst, the experimental conversions could not reach the equilibrium conversion as observed in bulk tungstophosphoric acid (Figure 5.5).

After these experiments, in order to check the reproducibility, same experiments were repeated with 25-wt% TPA/AC catalyst by keeping all the working conditions same. The results are given in Figure 5.9 and Figure 5.10 and the experimental data for this reproducibility study are given in Appendices C.6 and C.7.

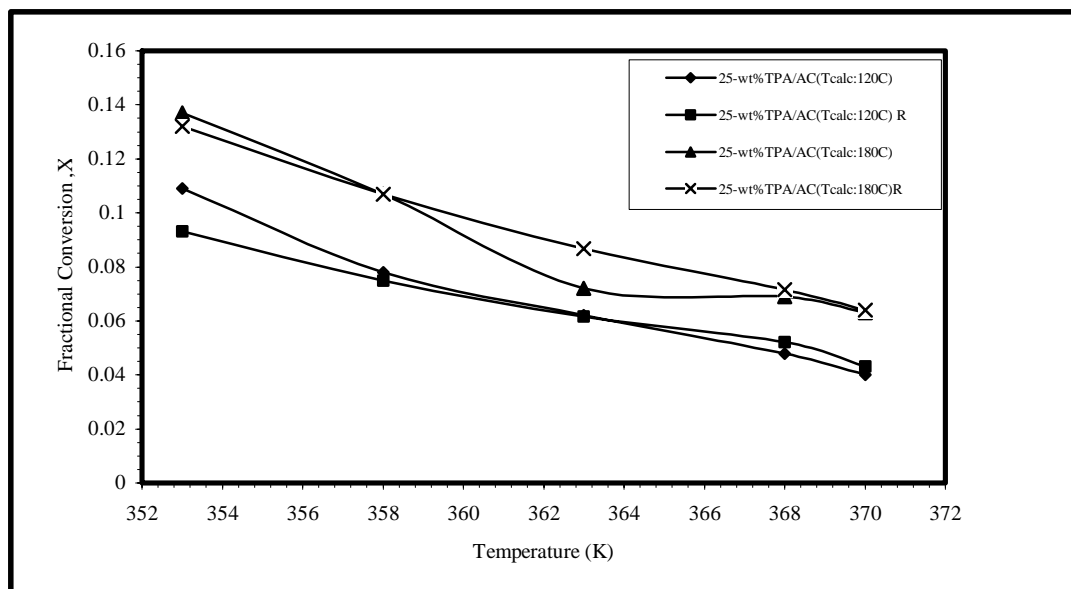


Figure 5.9 Variation of conversion with temperature in the presence of 25-wt% TPA/AC (reproducibility check)

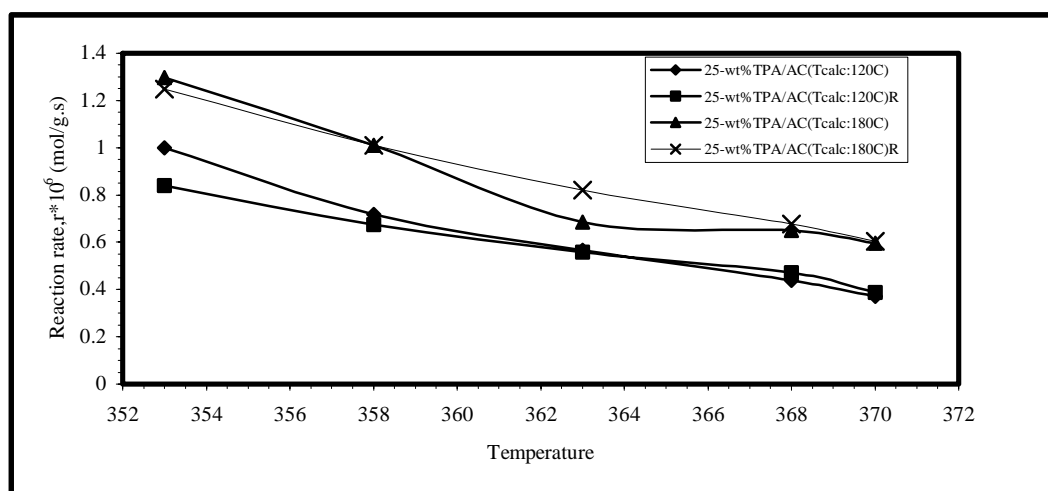


Figure 5.10 Variation of reaction rate with temperature in the presence of 25-wt% TPA/AC (reproducibility check) (Exp.#: 6-7)

The results did not deviate too much from each other, which showed their reproducibility, except the result obtained at 80°C (353K) for 25-wt%TPA/AC (T_{calc} : 120°C) catalyst and at 90°C (363K) for 25-wt%TPA/AC (T_{calc} : 180°C) catalyst. The deviation at these temperatures might be due to the experimental errors.

The comparison of the catalytic activity of bulk tungstophosphoric acid and supported tungstophosphoric acid catalyst was given in Figure 5.11. The results showed that at 80°C, bulk TPA, 25-wt% TPA/AC (T_{calc} : 180°C) and 31-wt% TPA/AC catalyst showed approximately the same activity. But, in general, it was observed that the catalytic activity of the supported ones was less than the catalytic activity of the bulk TPA when the total amount of support+TPA loaded to the reactor was taken as 0.2 g. Therefore in the next step, the amount of tungsten found in the structure of tungstophosphoric acid was taken as constant to see the change in the catalytic activity of supported catalysts[50] .

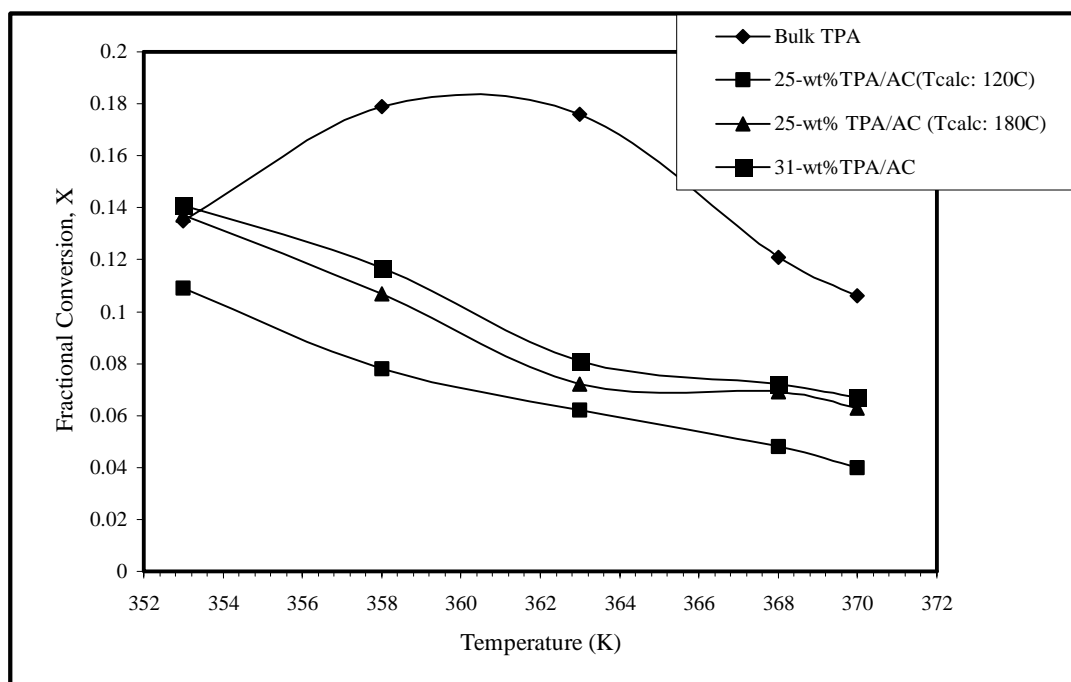


Figure 5.11 Comparison of bulk and supported tungstophosphoric acid catalysts ($w_{\text{total}}=0.2$ g) (Exp.#: 1,3-5)

When the tungsten concentration was kept constant, the loading level to the reactor did not remain constant. 0.8 g. of 25-wt% TPA/AC catalyst and 0.644 g. of 31-wt% TPA/AC catalyst were loaded to the reactor. The result was given in Figure 5.12 and the experimental data, in tabulated form, are given in Appendices C.8, C.9 and C.10. Higher conversions were obtained as compared to the results of the previous experiments (Run 3,4,5).

The catalysts showed a decreasing tendency in their catalytic activity as observed in the previous experiments (Run 3,4,5). Higher conversions (above 15%) were obtained at 80°C (353K), whereas they decreased (around 6%) as the temperature was raised to 97°C (370K). In addition, the experimental conversion could not reach the equilibrium conversion like in the previous experiments.

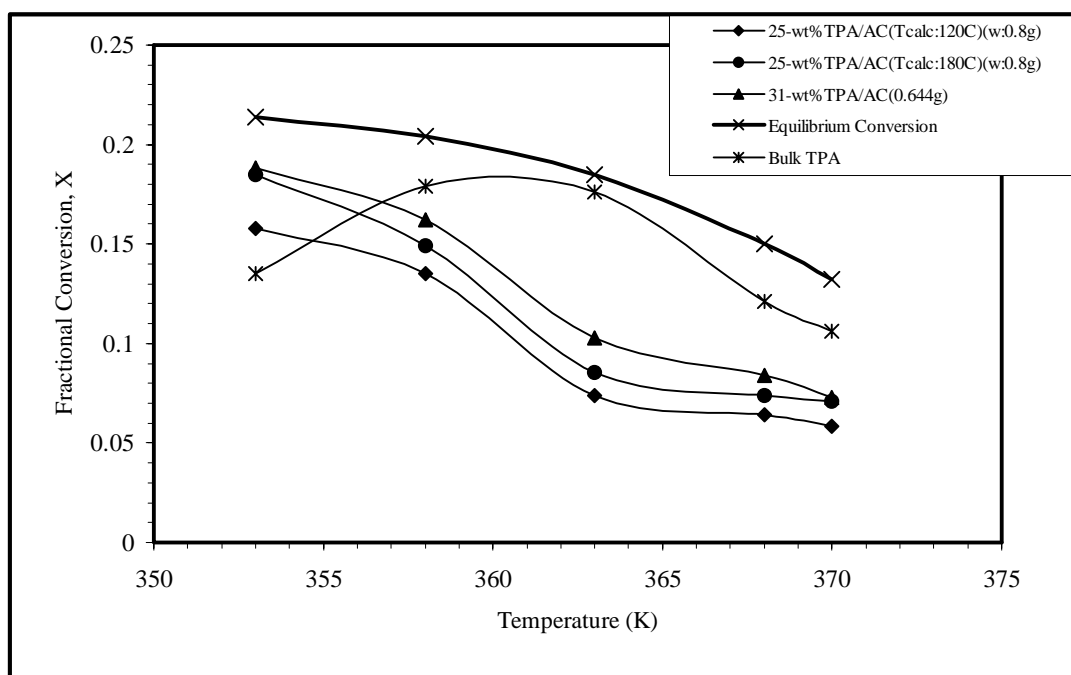


Figure 5.12 Variation of conversion with temperature at different levels of catalyst loading to reactor (Exp.#: 8-10)

Finally, the catalytic activity of supported catalysts (at constant tungsten concentration) was higher than that of bulk tungstophosphoric acid at 80°C (353 K) and decreased gradually, as observed in Figure 5.12.

The differences in the behavior of the catalysts, both in the conversion and in the reaction rate, can be explained as follows:

- a. As given in the previous sections, the backward reaction ($\text{TAE} \rightarrow 2\text{M}2\text{B}$) might suppress the forward reaction ($2\text{M}2\text{B} \rightarrow \text{TAE}$) with increasing temperature, therefore the conversion and the average reaction rate decreased with increasing temperature.
- b. There might be a shift in the mechanism of the reaction with increasing temperature; the adsorption equilibrium constant of either one of the reactants might decrease or increase with temperature, and
- c. By supporting, the reaction mechanism might change partially or completely with respect to the mechanism of bulk catalyst.

To see the possibility of b and c, the same experiments should be done with different feed concentrations in order to get the reaction mechanism in the presence of these catalysts.

5.2.3 Comparison of Catalysts

In order to make a decision on the catalytic activity of bulk and supported tungstophosphoric acid, reference experiments were done at 90°C, keeping all the other working conditions same, with macroreticular acidic resin, Amberlyst-15 which was used as the commercial catalyst for etherification reactions

between C₄-C₅ iso-olefins and alcohols [16,25,27,30,34], and with bulk molybdophosphoric acid (MPA), another Keggin type of heteropoly acid. The results are given in Tables 5.2 and 5.3, respectively and the experimental data are given, in tabulated form, in Appendices C.11 and C.12.

Table 5.2 Comparison of conversion values obtained at 90°C (w=0.2g)

CATALYST	CONVERSION, %
Bulk TPA	17.6
Amberlyst-15	15.6
Bulk MPA	12.4
31-wt% TPA/AC	8.1
25-wt%TPA/AC(T _{calc.} :180°C)	7.2
25-wt%TPA/AC(T _{calc.} :120°C)	6.2

Table 5.3 Comparison of reaction rates obtained at 90°C (w=0.2g)

CATALYST	RATE, r*10⁶ (mol/g cat. s)
Bulk TPA	1.696
Amberlyst-15	1.500
Bulk MPA	1.174
31-wt% TPA/AC	0.768
25-wt%TPA/AC(T _{calc.} :180°C)	0.684
25-wt%TPA/AC(T _{calc.} :120°C)	0.566

Bulk tungstophosphoric acid showed higher activity than Amberlyst-15 as expected due to its high acidity (superacid) [5-7,45]. This showed that bulk heteropoly acids could be a good candidate, instead of Amberlyst-15, for gas-phase etherification reactions between iso-olefins and alcohols. Also the results showed that, its activity was higher than that of bulk molybdophosphoric acid because as stated by Kozhevnikov [5,6,39] and Misono *et.al.*[7], the acidity of bulk TPA was higher than the acid strength of bulk MPA. In general, it is expected that, when the surface area of the catalyst increased, its activity also

increased but as it can be seen from Tables 5.1 and 5.2, the supported tungstophosphoric acid catalysts showed the least activity among the others in spite of their high surface area ($\sim 400\text{-}500\text{ m}^2/\text{g}$). Therefore, other factors should be taken into consideration: (i) the total amount (TPA+support) of catalyst loaded to the reactor might be insufficient as stated in the previous section, or (ii) the acid strength of tungstophosphoric acid might be reduced when loaded on activated carbon [6].

5.2.4 Deactivation of Bulk and Supported Heteropoly Acid

In this section, deactivation of bulk tungstophosphoric acid and 25-wt% TPA/AC (T_{calc} : 120°C) were investigated. In each experiment, 0.2 g. of catalyst were loaded to the reactor and the temperature range was taken between 80°C - 97°C , as in the previous experiments. Two runs were done with each catalyst to find the degree of deactivation. The results are given in Figure 5.14 and Figure 5.15. The experimental data are given in Appendices C.13 and C.14, in tabulated form.

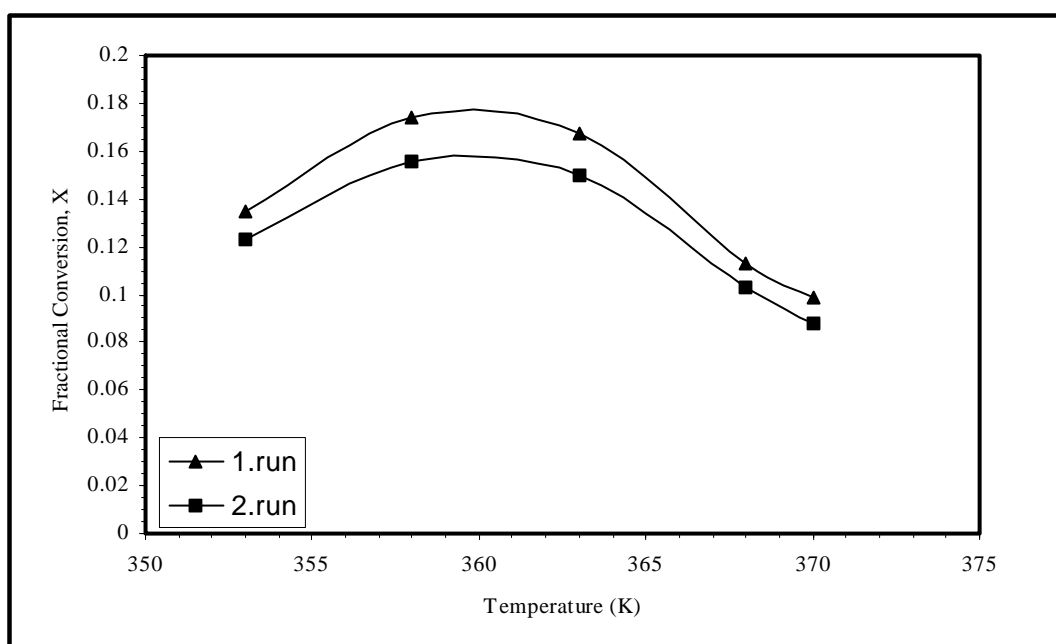


Figure 5.13 Deactivation of bulk TPA (Exp.#:13)

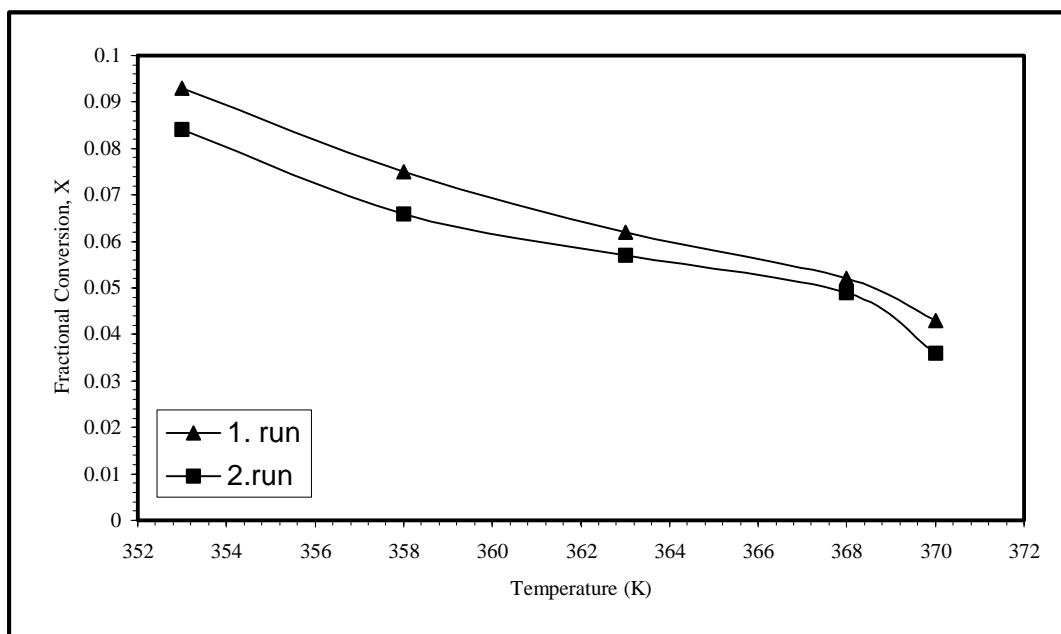


Figure 5.14 Deactivation of 25-wt%TPA/AC(T_{calc} : 120°C)(Exp.#:14)

The results showed that, when both bulk and supported heteropoly acid catalysts were reused (second run), the conversions were slightly different from the conversions obtained in the first run. That is, the deactivation of the catalysts was small under the reaction conditions. When bulk and supported TPA catalysts were used again, without the heat treatment, their activity decreased approximately 10% with respect to the activity of fresh catalyst.

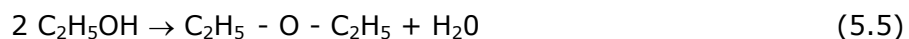
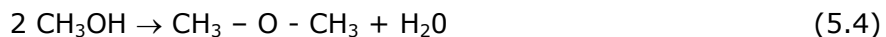
5.2.5 Catalytic Activity of Alcohol-treated Supported Heteropoly Acid

In this section, 0.644 g of 31-wt% TPA/AC catalyst was put into ethanol and waited overnight, loaded to the reactor and the etherification reaction was carried out at 90°C. The experimental data are given in Appendix C.15.

As given in section 5.2.2, 10.3% conversion was obtained with 31-wt% TPA/AC catalyst. On the other hand, 8.1% conversion was obtained when ethanol-treated 31-wt% TPA/AC catalyst was used. This showed that, the support could not entrap whole heteropoly acid and some amount of it leaked to the solvent.

5.2.6 Side Product Formation Reactions

Beside the *tert*-ether formation, sometimes side products, such as dimethyl or diethyl ether, can be formed [78, 79] in trace amounts in the main product according to the following reactions,



If the alcohol used in the etherification reaction was methanol, the possible side product was dimethyl ether and if ethanol was used, diethyl ether was formed as the possible side product.

In this section, to see whether there was a side product formation or not, two set of experiments were performed in the presence of bulk TPA at a fixed temperature of 90°C. Only methanol was fed to the system in one experiment and ethanol was used in the other one. It was observed that, there was not any side product formation at this temperature.

CHAPTER 6

CONCLUSIONS AND RECOMMENDATIONS

In this study, applicability of pure heteropoly acid and its supported form, to the etherification reaction of isoamylene (2-methyl-2-butene) with ethyl alcohol in a continuous differential reactor was studied. Major conclusions reached as a result of this work are,

1. The catalytic activity of bulk tungstophosphoric acid increases when the temperature is raised from 80°C to 85°C and then slightly decreases as the temperature increases up to 97°C. The conversion values obtained experimentally do not exceed the calculated equilibrium conversions. Only at 90°C, the reaction approached to the equilibrium.
2. The conversion and the rate of reaction decrease with increasing temperature in the presence of supported tungstophosphoric acid and their values are less than the values obtained in the presence of bulk TPA. When the loading level of TPA over activated carbon is increased from 25-wt% to 31-wt%, both the conversion and rate of reaction increase, as expected. The conversion values obtained here also do not reach the calculated equilibrium conversions.

3. Calcination temperature has significant effect on the catalytic performance of the catalyst. For 25-wt% TPA/AC catalyst, when the calcination temperature is raised from 120°C to 180°C, the conversion changes significantly.
4. When the level of supported TPA catalyst loaded to the reactor is increased, the catalytic activities of 31-wt% TPA/AC and 25-wt% TPA/AC (T_{calc} : 180°C) are higher than that of bulk TPA at 80°C but again decrease gradually as the temperature is increased.
5. When the experiments done with bulk TPA and 25-wt% TPA/AC were repeated with the same but fresh catalysts, approximately the same results were obtained which showed their reproducibility.
6. At 90°C, the highest activity belongs to bulk TPA among the others such as Amberlyst-15, bulk molybdophosphoric acid, etc. due to its lower surface area. This means that, the surface area does not have direct effect on the catalytic activity.
7. Deactivation occurs in bulk and supported tungstophosphoric acid (25-wt% TPA/AC) when they are reused, without any further treatment.
8. At 90°C, 31-wt% TPA/AC catalyst yielded a conversion value of 10.3% but the same catalyst gave 8.1% conversion after it was treated with ethanol. This shows that, there was a leakage of HPA into the solvent.
9. At 90°C, there is not any side product formation, either dimethyl ether or diethyl ether, in the presence of bulk TPA.

REFERENCES

- [1] Ravello, A., "How Should Environmentally Benign Gasolines Be Formulated", Chemical Reactor Technology for Environmentally Safe Reactors and Products, 1993, p. 1-6.
- [2] Smylie, M., Chinkin, R., and Whitten, G.Z., "Assesing the Effects of Reformulated Gasoline on Air Quality", NPRA Annual Meeting, 1991, Paper AM-91-21.
- [3] Harting, G.L., Shannon, H., "Oxygenates As Gasoline Blending Components", Chemical Reactor Technology for Environmentally Safe Reactors and Products, 1993, p. 7-15.
- [4] Ignatius, J., Jarvelin, H., Lindqvist, P., "Use TAME and Heavier Ethers to Improve Gasoline Properties", Hydrocarbon Processing, February, 1995, p. 51-53.
- [5] Kozhevnikov, I.V., "Heteropoly Acids and Related Compounds as Catalysts for Fine Chemical Synthesis", Catal., Rev. – Sci. Eng., 37(2), 1995, p. 311-352.
- [6] Kozhevnikov, I.V., "Catalysis by Heteropoly Acids and Multi-component Polyoxometalates in Liquid-Phase Reactions", Chem. Rev., 98, 1998, p. 171-198.
- [7] Mizuno, M., Misono, M., "Heterogeneous Catalysis" Chem. Rev., 98, 1998, p. 199-217.
- [8] Ancillotti, F., Fattore, V., "Oxygenate Fuels: Market Expansion and Catalytic Aspect of Synthesis", Fuel Processing Technology, 57, 1998, p. 163-194.
- [9] Schipper, P.H., Sapre, A.V., Le, Q.N., "Chemical Aspects of Clean Fuels Production", Chemical Reactor Technology for Environmentally Safe Reactors and Products, 1993, p. 147-182.
- [10] Brockwell, H.L., Sarathy, P.R., Trotta, R., "Synthesize Ethers", Hydrocarbon Processing, September, 1991, p. 133-141.
- [11] Varışlı, D., "The Simultaneous Production of Tert-Amyl Alcohol and Tert-Amyl Ethyl Ether in a Reactive Distillation Column", MS. Thesis, 2003, Middle East Technical University, Ankara.

- [12] Colombo, F., Cori, L., Dalloro, L., and Delogu, P., "Equilibrium Constant for the Methyl tert-Butyl Ether Liquid-Phase Synthesis by use of UNIFAC", *Ind. Eng. Chem. Res.*, 22, 1983, p. 219-223.
- [13] Rehfinger, A., Hoffmann, U., "Kinetics of MTBE Liquid Phase Synthesis Catalyzed by Ion Exchange Resin-I. Intrinsic Rate Expression in Liquid Phase Activities", *Chem. Eng. Science*, 45, 1990, p. 1605-1617.
- [14] Izquierdo, J.F., Cunill, F., Vila, M., Iborra, M., "Equilibrium Constants for MTBE and ETBE Liquid-Phase Syntheses Using C₄ Olefinic Cut", *Ind. Eng. Chem. Res.*, 33, 1994, p. 2830-2835.
- [15] Zhang, T. and Datta, R., "Integral Analysis of MTBE Synthesis Kinetics", *Ind. Eng. Chem. Res.*, 34, 1995, p. 730-740.
- [16] Ancillotti, F., Mauri, M.M., Pescarollo, E., and Romagnoni, L., "Mechanisms in the Reaction Between Olefins and Alcohols Catalyzed by Ion Exchange", *J. Mol. Catal.*, 4, 1978, p. 37-48.
- [17] Ahmed, F.E., "Toxicology and Human Health Effects Following Exposure to Oxygenated or Reformulated Gasoline", *Toxicology Letters*, 121, 2001, p. 89-113.
- [18] World Health Organization of the United Nations, "Environmental Health Criteria 206: Methyl Tertiary-Butyl Ether", 1998, WHO, Geneva, Switzerland.
- [19] Dekant, W., Bernauer, U., Rosner, E., and Amberg, A., "Toxicokinetics of Ethers Used As Fuel Oxygenates", *Toxicology Letters*, 24, 2001, p. 37-45.
- [20] Vainiotalo, S., Peltonen, Y., Ruonakangas, A., and Pfaffli, P., "Customer Exposure to MTBE, TAME, C₆ Alkyl Methyl Ethers and Benzene During Gasoline Refueling", *Environ. Health Perspect.*, 107, 1999, p. 133-140.
- [21] Rosenkranz, H.S., and Klopman, G., "Prediction of the Lack of Genotoxicity and Carcinogenicity in Rodents After Two Gasoline Additives: Methyl- and Ethyl-t-Butyl Ethers", *In Vivo Toxicol.*, 4, 1991, p. 49-54.
- [22] Sneesby, M.G., Tadé, M.O., Datta, R., and Smith, T.N., "ETBE Synthesis via Reactive Distillation. 1. Steady-State Simulation and Design Aspects", *Ind. Eng. Chem. Res.*, 36, 1997, p. 1855-1869.
- [23] Tau, L., and Davis, B.H., "Acid Catalyzed Formation of Ethyl Tertiary Butyl Ether (ETBE)", *Applied Catalysis*, 53, 1989, p. 263-271.
- [24] Caprino, L., and Tonga, G.I., "Potential Health Effects of Gasoline and Its Constituents: A Review of Current Literature (1990-1997) on Toxicology Data", *Environ. Health Perspect.*, 106, 1998, p. 115-125.
- [25] Krause, A.O.I., and Hammarström, L.G., "Etherification of Isoamylenes with Methanol", *Applied Catalysis*, 30, 1987, p. 313-324.
- [26] Rihko, L.K., Linnekoski, J.A., and Krause, A.O.I., "Reaction Equilibria in the Synthesis of 2-Methoxy-2-Methyl Butane and 2-Ethoxy-2-Methyl Butane in the Liquid Phase", *J. Chem. Eng. Data*, 39, 1994, p. 700-704.

- [27] Ancillotti, F., Massi Mauri, M., and Pescarollo, E., "Ion Exchange Resin Catalyzed Addition of Alcohols to Olefins", *J. Catal.*, 46, 1977, p. 49-57.
- [28] Rihko, L.K., and Krause, A.O.I., "Reactivity of Isoamylenes with Ethanol", *Applied Catalysis A: General*, 101, 1993, p. 283-295.
- [29] Kitchaiya, P., and Datta, R., "Ethers from Ethanol. 2. Reaction Equilibria of Simultaneous Tert-Amyl Ethyl Ether Synthesis and Isoamylenes Isomerization", *Ind. Eng. Chem. Res.*, 34, 1995, p. 1092-1101.
- [30] Linnekoski, J.A., Krause, A.O.I., and Struckmann, L.K., "Etherification and Hydration of Isoamylenes with Ion Exchange Resin", *Applied Catalysis A: General*, 170, 1998, p. 117-126.
- [31] Oktar, N., Murtezaoglu, K., Dogu, G., Gonderten, I., and Dogu, T., "Etherification Rates of 2-Methyl-2Butene and 2-Methyl-1-Butene with Ethanol for Environmentally Clean Gasoline Production", *Journal of Chemical Technology and Biotechnology*, 74, 1999, p. 155-161.
- [32] Kunin, R., Meitzner, E.F., Oline, J.A., Fisher, S.A., and Frisch, N., "Characterization of Amberlyst 15-Macroporous Sulfonic Acid Cation Exchange Resin", *Ind. Eng. Chem. Prod. Res. Dev.*, 1, 1962, p. 140-144.
- [33] Dogu, T., Aydın, E., Boz, N., Murtezaoglu, K., Dogu, G., "Diffusion Resistances and Contribution of Surface Diffusion in TAME and TAAE Production Using Amberlyst-15", *Int. Journal of Chemical Reactor Engineering*, 2003.
- [34] Panneman, H.J., Beenackers, A.A.C.M., "Synthesis of Methyl Tert-Butyl Ether catalyzed by Acidic Ion-Exchange Resins. Influence of the Proton Activity", *Ind. Eng. Chem. Res.*, 34, 1995, p. 4318-4325.
- [35] Adams, J.M., Clement, D.E., Graham, S.H., "Synthesis of Methyl Tert-Butyl Ether From Methanol and Isobutene Using a Clay Catalyst", *Clays & Clay Minerals*, 30, 1982, p. 129-134.
- [36] Chu, P., and Kuhl, G.H., "Preparation of Methyl Tert-Butyl Ether (MTBE) over Zeolite Catalysts", *Ind. Eng. Chem. Res.*, 26, 1987, p. 365-369.
- [37] Izumi, Y., Hasebe, R., and Urabe, K., "Catalysis by Heterogeneous Supported Heteropoly Acid", *J. Catal.*, 84, 1983, p. 402-409.
- [38] Cavani, F., "Heteropolycompound-based catalysts: A blend of acid and oxidizing properties", *Catalysis Today*, 41, 1998, p. 73-86.
- [39] Kozhevnikov, I.V., "Advances in Catalysis by Heteropolyacids", *Russ. Chem. Rev.*, 56(9), 1987, p. 811-825.
- [40] Misono, M., "Heterogeneous Catalysis by Heteropoly Compounds of Molybdenum and Tungsten", *Cat. Rev. -Sci. Eng.*, 29(2&3), 1987, p.269-321.
- [41] Hodnett, B.K., and Moffat, J.B., "Application of Temperature-Programmed Desorption to the Study of Heteropoly Compounds: Desorption of Water and Pyridine", *J. Catal.*, 88, 1984, p. 253-263.

- [42] Misono, M., Okuhara, T., Ichiki, T., Arai, T., and Kanda, Y., "Pseudoliquid Behavior of Heteropoly Compound Catalysts. Unusual Pressure Dependencies of the Rate and Selectivity for Ethanol Dehydration", *J. Am. Chem. Soc.*, 109, 1987, p. 5535-5536.
- [43] Takahashi, K., Okuhara, T., and Misono, M., "Phase Transition-Like Phenomenon Observed For Pseudoliquid Phase of Heteropoly Acid Catalysts", *Chem. Lett.*, 1985, p. 841-842.
- [44] Misono, M., "Acidic and Catalytic Properties of Heteropoly Compounds", *Materials Chemistry & Physics*, 17, 1987, p. 103-120.
- [45] Misono, M., and Okuhara, T., "Solid Superacid Catalysts", *CHEMTECH*, November, 1993, p. 23-29.
- [46] Kozhevnikov, I.V., and Matveev, K.I., "Homogeneous Catalysts Based on Heteropoly Acids(Review)", *Applied Catalysis*, 5, 1983, p. 135-150.
- [47] Mizuno, N., and Misono, M., "Heteropolyanions in Catalysis", *J. Mol. Catal.*, 86, 1994, p. 319-342.
- [48] Brückman, K., Che, M., Haber, J., and Tatibouet, J.M., "On the Physicochemical and Catalytic Properties of $H_5PV_2Mo_{10}O_{40}$ Supported on Silica ", *Catalysis Letters*, 25, 1994, p. 225-240.
- [49] Schwegler, M.A., Vinke, P., van der Eijk, M., and van Bekkum, H., "Activated Carbon as a Support for Heteropolyanion Catalysts", *Applied Catalysis A: General*, 80, 1992, p. 41-57.
- [50] Chimienti, M.E., Pizzio, L.R., Caceres, C.V., and Blanco, M.N., "Tungstophosphoric and Tungstosilicic Acids on Carbon as Acidic Catalysts", *Applied Catalysis A: General*, 208, 2001, p. 7-19.
- [51] Baba, T., Ono, Y., Ishimoto, T., Moritaka, S., Tanooka, S., "Heteropoly Acids Supported on Acidic Ion-Exchange Resin as Highly Active Solid-Acid Catalysts", *Bull. Chem. Soc. Jpn.*, 58, 1985, p. 2155-2156.
- [52] Soled, S., Miseo, S., McVicker, G., Gates, W.E., Gutierrez, A., and Paes, J., "Preparation of Bulk and Supported Heteropolyacid Salts", *Catalysis Today*, 36, 1997, p. 441-450.
- [53] Tatematsu, S., Hibi, T., Okuhara, T., and Misono, M., "Preparation Process and Catalytic Activity of $Cs_xH_{3-x}PW_{12}O_{40}$ ", *Chem. Lett.*, 1984, p. 865-868.
- [54] Izumi, Y., Urabe, K., and Onaka, M., "Development of Catalyst Materials for Acid-Catalyzed Reactions in the Liquid Phase", *Catalysis Today*, 35, 1997, p. 183-188.
- [55] Baba, T., and Ono, Y., "HPAs and Their Salts Supported on Acidic Ion-Exchange Resin as Highly Active Solid Acid Catalyst", *Applied Catalysis*, 22, 1986, p. 321-324.
- [56] Hayashi, H., and Moffat, J.B., "Methanol Conversion Over Metal Salts of 12-Tungstophosphoric Acid", *J.Catal.*, 81, 1983, p. 61-66.

- [57] Nishimura, T., Okuhara, T., and Misono, M., "High Catalytic Activity of an Insoluble Acidic Cesium Salt of Dodecatungstophosphoric Acid for Liquid-Phase Alkylation", *Applied Catalysis*, 73, 1991, p. L7-L11.
- [58] Okuhara, T., Nishimura, T., Watanabe, H., and Misono, M., "Insoluble Heteropoly Compounds as Highly Active Catalysts for Liquid-Phase Reactions", *J. Mol. Catal.*, 74, 1992, p. 247-256.
- [59] Misono, M., and Nojiri, N., "Recent Progress in Catalytic Technology in Japan", *Applied Catalysis*, 64, 1990, p. 1-30.
- [60] Hu, C., Hashimoto, M., Okuhara, T., and Misono, M., "Catalysis by Heteropoly Compounds", *J. Catal.*, 143, 1993, p. 437-448.
- [61] Shikata, S., Okuhara, T., and Misono, M., "Catalysis by Heteropoly Compounds. Part XXVI. Gas Phase Synthesis of MTBE over Heteropolyacids", *J. Mol. Catal. A: Chemical*, 100, 1995, p. 49-59.
- [62] Baronetti, G., Briand, L., Sedran, U., Thomas, H., "Heteropolyacid-Based Catalysis. Dawson Acid for MTBE Synthesis in Gas Phase", *Applied Catalysis A: General*, 172, 1998, p. 265-272.
- [63] Bielanski, A., Dziembaj, R., Malecka-Lubanska, A., Pozniczek, J., Hasik, M., and Drozdek, M., "Polyaniline Supported Heteropolyacid ($H_4SiW_{12}O_{40}$) as the Catalyst for MTBE Synthesis", *J. Catal.*, 185, 1999, p. 363-370.
- [64] Shikata, S., Nakata, S., Okuhara, T., and Misono, M., "Catalysis by Heteropoly Compounds. 32. Synthesis of MTBE Catalyzed by Heteropolyacids Supported on Silica", *J. Catal.*, 166, 1997, p. 263-271.
- [65] Knifton, J.F., and Edwards, J. C., "Methyl Tert-Butyl Ether Synthesis From Tert-Butanol via Inorganic Solid Acid Catalysis", *Applied Catalysis A: General*, 183, 1999, p. 1-13.
- [66] Kozhevnikov, I.V., Sinnema, A., van der Weerd, A.J.A., and van Bekkum, H., "Hydration and Acetoxylation of Dihydromyrcene Catalyzed by Heteropolyacid", *J. Mol. Catal. A: Chemical*, 120, 1997, p. 63-70.
- [67] Sato, S., Sugara, K., Furuta, H., and Nozaki, F., "Kinetic Studies of Liquid-Phase Acetal Formation Catalyzed by Keggin-type Heteropolyacid", *J. Mol. Catal. A: Chemical*, 114, 1996, p. 209-216.
- [68] Nomiya, K., Sugaya, Y., Sasa, S., and Miwa, M., "Catalysis by 12-Heteropolymolybdc Acid. II. Friedel-Crafts Type Reaction of Aromatic Compounds", *Bull. Chem. Soc. Jpn.*, 53, 1980, p. 2089-2090.
- [69] Izumi, Y., Ogawa, M., and Urabe, K., "Alkali Metal Salts and Ammonium Salts of Keggin-type Heteropolyacids as Solid Acid Catalysts for Liquid-Phase Friedel-Crafts Reactions", *Applied Catalysis A: General*, 132, 1995, p. 127-140.
- [70] Izumi, Y., "Hydration/Hydrolysis by Solid Acids", *Catalysis Today*, 33, 1997, p. 371-409.

- [71] Dupont, P., and Lefebvre, F., "Esterification of Propanoic Acid by Butanol and 2-Ethylhexanol Catalyzed by Heteropoly Acids Pure or Supported on Carbon", *J. Mol. Cat. A: Chemical*, 114, 1996, p. 299-307.
- [72] Oktar, N., "Kinetics for the Production of Tertiary Ethers Used As Gasoline Additives", Ph.D. Thesis, 2001, Gazi University Institute of Science and Technology, Ankara.
- [73] Pizzio, L.R., Caceres, C.V., and Blanco, M.N., "Acid Catalysts Prepared by Impregnation of Tungstophosphoric Acid Solutions on Different Supports", *Applied Catalysis A: General*, 167, 1998, p. 283-294.
- [74] Jensen, K.L., and Datta, R., "Ethers from Ethanol. 1. Equilibrium Thermodynamic Analysis of the Liquid-Phase ETBE Reaction", *Ind. Eng. Chem. Res.*, 34, 1995, p. 392-399.
- [75] Yaws, C.L., "Thermodynamic and Physical Property Data", Gulf Publishing Company, 1992, Houston-Texas, USA.
- [76] Hayashi, H., and Moffat, J.B., "The Properties of Heteropoly Acids and the Conversion of Methanol to Hydrocarbons", *J. Catal.*, 77, 1982, p. 473-484.
- [77] Na, K., Okuhara, T., and Misono, M., "Skeletal Isomerization of n-Butane over Cesium Hydrogen Salts of 12-Tungstophosphoric Acid", *J. Chem. Soc. Faraday Trans.*, 91(2), 1995, p. 367-373.
- [78] Rihko, L.K., Kiviranta-Paakkönen, P.K., and Krause, A.O.I., "Kinetic Model for the Etherification of Isoamylenes with Methanol", *Ind. Eng. Chem. Res.*, 36, 1997, p. 614-621.
- [79] Subramaniam, C., and Bhatia, S., "Liquid Phase Synthesis of MTBE Catalyzed by Ion Exchange Resin", *Can. J. Chem. Eng.*, 65, 1987, p. 613-620.

APPENDIX A

GAS CHROMATOGRAPH CALIBRATION FACTORS

During the analysis of reactants and products, to evaluate the peak read from the computer that is connected to the gas chromatography or integrator, and to calculate concentrations of the species using these peaks, it is necessary to calculate the calibration factors for gas chromatography. By this way, the errors due to injection and the probable errors coming from the detector can be eliminated.

In this study, the calibration factors for 2M2B and TAME were calculated to obtain quantitative results from the GC trace. The calibration factor of ethanol was taken as a unit, and the ratio between each of these species and ethanol were found.

Firstly, 2M2B-EtOH and TAME-EtOH mixtures were prepared concerning the composition range of experiments and these mixtures were injected to the column at different amounts. According to the results, it is concluded that the differences in concentration and injection amount do not affect the value of calibration factor of that species.

A.1 Sample Calculation for Finding Calibration Factors

To find out the calibration factor, for each species, mixtures of different volume fractions were prepared, and different amounts of samples from these mixtures were injected to the gas chromatograph. The calculation procedure for calibration factor is given in the following:

A_A : Area belongs to C₅ reactive olefin, 2M2B

A_B : Area belongs to EtOH

A_C : Area belongs to TAME

y_i : Volume fraction belongs to ith component

x_i : Molar fraction belongs to ith component

α_i : Relative calibration factor belongs to ith component

$$A_A\beta_A + A_B\beta_B = 1$$

$$x_A = \frac{A_A\beta_A}{A_A\beta_A + A_B\beta_B} = \frac{\frac{A_A\beta_A}{A_B\beta_B}}{\frac{A_A\beta_A}{A_B\beta_B} + \frac{A_B\beta_B}{A_B\beta_B}} \quad \text{and} \quad \alpha_I = \frac{\beta_A}{\beta_B}$$

$$x_A = \frac{\frac{A_A}{A_B}\alpha_A}{\frac{A_A}{A_B}\alpha_A + 1} \quad \text{and} \quad \alpha_I = \frac{x_A}{\frac{A_A}{A_B}(1 - x_A)}$$

$$\frac{x_A}{x_B} = \frac{y_A}{y_B} \times \frac{\frac{\rho_A}{M_A}}{\frac{\rho_B}{M_B}} \quad x_A + x_B = 1.0$$

Solving these equations simultaneously, calibration factor for species A can be found. Results of calibration experiments using 2M2B and EtOH are given in Table A.1. The calibration factor for TAE and EtOH was calculated in the same way.

Table A.1 The evaluation of calibration factor α for 2M2B

Injection amount, μl	y_A / y_B	AA	AB	AA/AB	x_B	x_A	α
1	0,20	481	1167	0.412	0.900	0.100	0.270
1	0.20	489	1163	0.420	0.900	0.100	0.265
3	0.20	1489	3301	0.451	0.900	0.100	0.247
3	0.20	1349	3082	0.438	0.900	0.100	0.254
5	0.20	2463	5177	0.476	0.900	0.100	0.234
5	0.20	2401	5004	0.479	0.900	0.100	0.232
1	0.10	241	1223	0.197	0.949	0.051	0.275
1	0.10	244	1269	0.192	0.949	0.051	0.282
3	0.10	752	3517	0.214	0.949	0.051	0.254
3	0.10	742	3486	0.213	0.949	0.051	0.255
5	0.10	1295	5681	0.228	0.949	0.051	0.238
5	0.10	1226	5512	0.222	0.949	0.051	0.244
$\alpha_{2M2B,avg}$:							0.256

A.2 Sample Calculation for Finding Concentration from GC

The mole fraction of components was calculated by using the following method.

$$A_A \beta_A + A_B \beta_B + A_C \beta_C = 1.0$$

$$x_{A'} = \frac{A_A \beta_A}{A_A \beta_A + A_B \beta_B + A_C \beta_C}$$

$$x_{A'} = \frac{\frac{A_A \beta_A}{A_B \beta_B}}{\frac{A_A \beta_A}{A_B \beta_B} + \frac{A_B \beta_B}{A_B \beta_B} + \frac{A_C \beta_C}{A_B \beta_B}} \quad \text{and defining } \alpha_i = \frac{\beta_i}{\beta_B}$$

$$x_{A'} = \frac{\left(\frac{A_A}{A_B} \right) \times \alpha_A}{\left(\frac{A_A}{A_B} \times \alpha_A + 1 + \frac{A_C}{A_B} \times \alpha_C \right)}$$

The mole fraction of other components is calculated in the same way. The final form of the equations are given in the following:

$$x_{B'} = \frac{1}{\left(\frac{A_A}{A_B} \times \alpha_A + 1 + \frac{A_C}{A_B} \times \alpha_C \right)}$$

$$x_{C'} = \frac{\left(\frac{A_C}{A_B} \right) \times \alpha_C}{\left(\frac{A_A}{A_B} \times \alpha_A + 1 + \frac{A_C}{A_B} \times \alpha_C \right)}$$

and the overall conversion, X_{Af} can be calculated from the following expression:

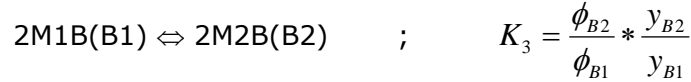
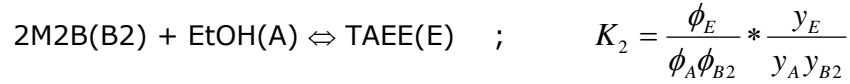
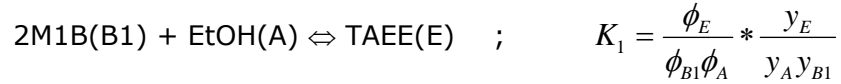
$$X_{Af} = \frac{A_C \times \alpha_C}{\left(A_A \times \alpha_A + A_C \times \alpha_C \right)}$$

APPENDIX B

CALCULATIONS

B.1 Calculation of Vapor-Phase Equilibrium Constants

Reactions considered to calculate equilibrium constants are as follows;



The equilibrium constants, K_1 , K_2 and K_3 were calculated from literature[74]:

$$\frac{\Delta G^\circ_T(l)}{RT} = \frac{\Delta G^\circ_T(g)}{RT} + \frac{1}{R} \sum_{j=1}^n \nu_j \left(\int_{T_{bj}}^T \frac{\Delta H^\circ_{\nu j T}}{T^2} dT \right) \quad (B.1.1)$$

where T_{bj} is the boiling point of the i th component, ν_j is the stoichiometric coefficient, (+) for products and (-) for reactants and T is the reaction temperature given in Kelvin.

$$\Delta H_{vjT}^{\circ} = I_{Hj} + \Delta a_j T + \frac{\Delta b_j}{2} T^2 + \frac{\Delta c_j}{3} T^3 + \frac{\Delta d_j}{4} T^4 \quad (\text{B.1.2})$$

where a, b, c and d are constants of heat capacity equation:

$$C_p = a + bT + cT^2 + dT^3 \quad \text{and}$$

I_{Hj} is the integration constant, obtainable at $T = T^{\circ} = 298 \text{ K}$ (The values of $\Delta H_{vj,298K}^{\circ}$ are given in Table B.1) and,

$$\Delta a_j \equiv a_j(g) - a_j(l); \quad \Delta b_j \equiv b_j(g) - b_j(l)$$

$$\Delta c_j \equiv c_j(g) - c_j(l); \quad \Delta d_j \equiv d_j(g) - d_j(l)$$

The values of gas-phase and liquid-phase heat capacity equation constants were found from the literature [29, 75]. They were given in Table B.2 and B.3, respectively.

Table B.1 Enthalpy of vaporization values at 298 K [75]

	$\Delta H_{vj,298K}^{\circ}$
2M2B	27.138
2M1B	25.862
EtOH	43.107
TAAE	36.668

Table B.2 Gas-phase heat capacity equation constants [75]

	a	b	c	d
2M2B	-1.333	414.007×10^{-3}	-203.899×10^{-6}	361.092×10^{-10}
2M1B	-0.289	434.72×10^{-3}	-232.81×10^{-6}	469.361×10^{-10}
EtOH	6.296	231.501×10^{-3}	-118.558×10^{-6}	222.183×10^{-10}
TAAE	20.789	615.467×10^{-3}	-266.738×10^{-6}	300.499×10^{-10}

Table B.3 Liquid-phase heat capacity equation constants [29]

	a	b	c	d
2M2B	132.9	-0.1475	7.511×10^{-4}	-8.817×10^{-8}
2M1B	126.5	-0.0609	5.084×10^{-4}	1.692×10^{-7}
EtOH	29.01	0.2697	-5.658×10^{-4}	2.079×10^{-6}
TAAE	107.1	0.5065	-3.764×10^{-4}	5.803×10^{-7}

To solve equation B.1.1, the liquid phase equilibrium constants of the same reactions should be calculated. Kitchaiya and Datta [29] obtained the following liquid-phase equilibrium constant correlations:

$$\ln K_1 = 22.809 + \frac{3136.3}{T} - 5.8227 \ln T + 0.0179T - 6.395 \times 10^{-6} T^2 - 1.672 \times 10^{-8} T^3$$

$$\ln K_2 = 26.779 + \frac{2078.6}{T} - 6.5925 \ln T + 0.0231T - 1.126 \times 10^{-5} T^2 - 1.414 \times 10^{-8} T^3$$

$$\ln K_3 = -3.97 + \frac{1057.7}{T} + 0.7698 \ln T - 0.0052T + 4.865 \times 10^{-6} T^2 - 2.58 \times 10^{-9} T^3$$

and from

$$K(\lambda) = \exp\left\{-\frac{\Delta G_T^\circ(\lambda)}{RT}\right\}; \lambda = \text{phase at which reaction occurs} \quad (\text{B.1.3})$$

the value of $\Delta G_T^\circ(l)$ was calculated at the reaction temperatures. From equation B.1.2, the value of ΔH_{vj}° was calculated at the reaction temperatures. After calculating the value of $\Delta G_T^\circ(g)$ in equation B.1.1, the values of gas-phase equilibrium constants, K_1 , K_2 and K_3 were calculated by using equation B.1.3. The results are given in Table B.1.

Table B.4 Vapor and Liquid-Phase Equilibrium Constants

Temp. (K)	K ₁ (l)	K ₂ (l)	K ₃ (l)	K ₁ (g)	K ₂ (g)	K ₃ (g)
353	10.137	1.1254	9.0079	1.0134	0.1332	7.6073
358	8.5454	0.9919	8.6152	0.7427	0.1015	7.3185
363	7.2276	0.8762	8.2486	0.5489	0.0779	7.0467
368	6.1324	0.7757	7.9061	0.4093	0.0603	6.7916
370	5.7471	0.7391	7.7753	0.3647	0.0545	6.6943

B.2 Calculation of Vapor-Phase Equilibrium Conversions

Again the same reactions given in section B.1 were taken into consideration to calculate equilibrium conversions

When these reactions were in equilibrium, material balances could be written as,

$$F_{B1} = F_{B10} (1-x_{B1})$$

$$F_{B2} = F_{B20} (1-x_{B2})$$

$$F_E = F_{B10} x_{B1} + F_{B20} x_{B2}$$

$$F_A = F_{A0} - F_{B10} x_{B1} - F_{B20} x_{B2}$$

$$\text{Overall; } \Sigma = F_{A0} + F_{B10} + F_{B20} - F_{B10} x_{B1} - F_{B20} x_{B2}$$

The equilibrium constants (calculated in the previous section) were written by using these material balance equations:

$$K_1 = \frac{\phi_E}{\phi_{B1}\phi_A} * \frac{(F_{B10}x_{B1} + F_{B20}x_{B2})(F_0 - (F_{B10}x_{B1} + F_{B20}x_{B2}))}{(F_{B10}(1-x_{B1}))(F_{A0} - (F_{B10}x_{B1} + F_{B20}x_{B2}))}$$

where $F_0 = F_{A0} + F_{B10} + F_{B20}$

$$K_2 = \frac{\phi_E}{\phi_{B2}\phi_A} * \frac{(F_{B10}x_{B1} + F_{B20}x_{B2})(F_0 - (F_{B10}x_{B1} + F_{B20}x_{B2}))}{(F_{B20}(1-x_{B2}))(F_{A0} - (F_{B10}x_{B1} + F_{B20}x_{B2}))}$$

$$K_3 = \frac{\phi_{B2}}{\phi_{B1}} * \frac{F_{B20}(1-x_{B2})}{F_{B10}(1-x_{B1})}$$

$\frac{\phi_E}{\phi_{B1}\phi_A}$, $\frac{\phi_E}{\phi_{B2}\phi_A}$, $\frac{\phi_{B2}}{\phi_{B1}} \rightarrow 1$ and dividing each term by F_0 gave,

$$K_1 = \frac{(y_{B10}x_{B1} + y_{B20}x_{B2})(1 - (y_{B10}x_{B1} + y_{B20}x_{B2}))}{(y_{B10}(1-x_{B1}))(y_{A0} - (y_{B10}x_{B1} + y_{B20}x_{B2}))}$$

$$K_2 = \frac{(y_{B10}x_{B1} + y_{B20}x_{B2})(1 - (y_{B10}x_{B1} + y_{B20}x_{B2}))}{(y_{B20}(1-x_{B2}))(y_{A0} - (y_{B10}x_{B1} + y_{B20}x_{B2}))}$$

$$K_3 = \frac{y_{B20}(1-x_{B2})}{y_{B10}(1-x_{B1})}$$

where $y_{B20} = (y_{B0})(0.85)$ and $y_{B10} = (y_{B0})(0.15)$ [Since 2M2B used in the reactions was a mixture of 85 mol % 2M2B + 15 mol% 2M1B]. Solving K_1 and K_2 simultaneously, at a given reaction temperature, gave us the value of x_{B1} and x_{B2} and from

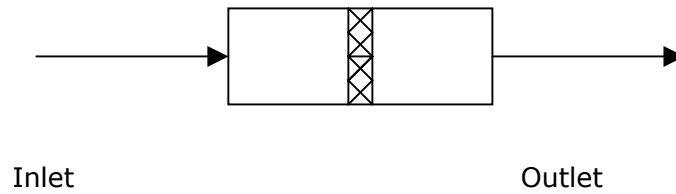
$$x_{eq.} = 0.15x_{B1} + 0.85x_{B2}$$

the equilibrium conversion values were calculated and found that they were decreasing with increasing temperature since these etherification reactions were exothermic. The conversion values are given in Table B.2.

Table B.5 Equilibrium Conversion vs. Temperature

Temp. (K)	X_{B1}	X_{B2}	Eq. Conv., $x_{eq.}$
353	0.39	0.183	0.214
358	0.36	0.176	0.204
363	0.31	0.163	0.185
368	0.25	0.132	0.150
370	0.21	0.118	0.132

B.3 Calculation of Reaction Rate in a Packed Continuous Differential Reactor



2-methyl-2-butene; F_{B0}

$$F_{Bf} = F_{B0}(1 - X_{Af})$$

Ethanol; F_{A0}

$$F_A = F_{A0} - F_{B0} X_{Af}$$

TAAE; $F_{E0} = 0$

$$F_E = F_{B0} X_{Af}$$

For 2M2B, the steady-state material balance equation is,

$$dF_{B0} - dF_{Bf} + (-R_A)dV = 0 \tag{B.3.1}$$

$$\Rightarrow dF_{B0} - dF_{B0}(1 - X_{Af}) + (-R_A)dV = 0$$

$$\Rightarrow \int \frac{dV}{F_{B0}} = \int \frac{dX_A}{(-R_A)}$$

$-R_A$ values can be taken as constant since the reaction rate does not change so much throughout the reactor. Therefore, reaction rate expression given above can be simplified to the expression given below,

$$-R_A = \frac{F_{B0} X_A}{V} \quad (\text{B.3.2})$$

In this type of reactors, the reaction rate ($-R_A^*$) can be expressed in terms of catalyst amount:

$$\begin{aligned} -R_A^* &= \frac{-R_A}{(1-\epsilon_b)\rho_{cat.}} \\ -R_A &= (-R_A^*)(1-\epsilon_b)\rho_{cat.} = \frac{F_{B0} X_{Af}}{V} \\ \Rightarrow -R_A^* &= \frac{X_{Af} F_{B0}}{V(1-\epsilon_b)\rho_{cat.}} = \frac{X_{Af} F_{B0}}{m} \end{aligned}$$

therefore the reaction rate is obtained in terms of mol/g cat. s.

B.4 Calculation of Volume Fraction from Experimental Data

$$(2M2B)_{\text{volume fraction}} = \theta_{2M2B} = \frac{\left(y_{2M2B} \times \frac{MW_{2M2B}}{\rho_{2M2B}} \right)}{\left(y_{2M2B} \times \frac{MW_{2M2B}}{\rho_{2M2B}} \right) + \left(y_{EtOH} \times \frac{MW_{EtOH}}{\rho_{EtOH}} \right)}$$

B.5 Calculation of Molar Flow Rate

The inlet molar flow rates of reactants, 2M2B and Ethanol, can be expressed as follow,

$$F_{2M2B,0} = v \times C_{2M2B,0} \quad , \quad F_{EtOH,0} = v \times C_{EtOH,0}$$

where v is the total volumetric flow rate and is set to 0.0477 ml/min in all our experiments and $C_{2M2B,0}$ and $C_{EtOH,0}$ are the initial molar concentrations.

B.6 Calculation of Initial Molar Concentration (Theoretical)

$$C_{i0} = \left(\frac{V_i}{V_t} \right) \times \left(\frac{\rho_i}{MW_i} \right) \times 1000$$

where V_i is the amount of the reactant put into the feed mixture given in milliliters, V_t is the total amount of feed mixture given also in milliliters. In our experiments, initial molar concentration (theoretical) of 2M2B and ethanol were found as 2.82 M and 12.02 M, respectively.

APPENDIX C

EXPERIMENTAL DATA

Before each experiment, by-pass data were taken in order to calculate initial feed concentrations (experimental) and in all other calculations these experimental feed concentrations were used.

C.1 Experimental Data for 1st Experiment (Bulk TPA)

C_{B0} : 2.82 M, C_{A0} : 12.02 M, the calculation procedure of this initial concentrations are given in Appendix B.6. Since ethanol was excess in amount, its concentration was assumed as constant.

Table C.1 By-pass data of 1st Experiment (w=0.2 g)

A_{2M2B}	A_{EtOH}	A_{2M2B}/A_{EtOH}	x_{2M2B}	x_{EtOH}
2060	2615	0.788	0.168	0.832
2089	2668	0.783	0.167	0.833
1936	2415	0.802	0.170	0.830
Average			0.168	0.832

$$\text{Experimental } C_{B0} = C_{A0} \times \frac{x_{2M2B}}{x_{EtOH}} = 12.02 \times \frac{0.168}{0.832} = 2.43M$$

Table C.2 Experimental data for 1st Experiment

T _{rxn} ,K	A _B	A _A	A _E	A _B *a _B	A _A *a _A	A _E *a _E	X _{Af}	Rate
353	2720	3930	319.9	696.32	3930	101.7282	0.127	1.231E-06
353	2140	3200	269.8	547.84	3200	85.7964	0.135	1.307E-06
353	1995	2960	252.3	510.72	2960	80.2314	0.136	1.311E-06
353	2260	3155	294.6	578.56	3155	93.6828	0.139	1.346E-06
Average:							0.135	1.299E-06
358	2095	3350	373	536.32	3350	118.614	0.181	1.749E-06
358	2950	4450	534	755.2	4450	169.812	0.184	1.772E-06
358	2830	4376	498	724.48	4376	158.364	0.179	1.732E-06
358	3070	4616	513	785.92	4616	163.134	0.172	1.660E-06
Average:							0.179	1.728E-06
363	1530	2375	239.7	391.68	2375	76.2246	0.163	1.5729E-06
363	1988	3004	315.6	508.928	3004	100.3608	0.165	1.590E-06
363	1660	2695	291.3	424.96	2695	92.6334	0.179	1.728E-06
363	1505	2410	295.7	385.28	2410	94.0326	0.196	1.894E-06
Average:							0.176	1.696E-06
368	1567	2300	162.1	401.152	2300	51.5478	0.114	1.099E-06
368	1450	2125	158.2	371.2	2125	50.3076	0.119	1.152E-06
368	1570	2326	189.4	401.92	2326	60.2292	0.130	1.258E-06
368	1650	2364	178.9	422.4	2364	56.8902	0.119	1.146E-06
Average:							0.121	1.164E-06
370	1565	2292	141	400.64	2292	44.838	0.101	9.718E-07
370	1525	2214	145.8	390.4	2214	46.3644	0.106	1.025E-06
370	1734	2503	173.7	443.904	2503	55.2366	0.111	1.068E-06
370	1364	2095	131.8	349.184	2095	41.9124	0.107	1.035E-06
Average:							0.106	1.025E-06

C.2 Experimental Data for 2nd Experiment (Bulk TPA-reproduced)

C_{B0}: 2.82 M, C_{A0}: 12.02 M

Table C.3 By-pass data of 2nd Experiment (w=0.2 g)

A _{2M2B}	A _{EiOH}	A _{2M2B} /A _{EiOH}	X _{2M2B}	X _{EiOH}
1971	2410	0.818	0.173	0.827
2269	2614	0.868	0.182	0.818
2065	2493	0.828	0.175	0.825
2094	2423	0.864	0.181	0.819
Average			0.178	0.822

$$\text{Experimental } C_{B0} = C_{A0} \times \frac{x_{2M2B}}{x_{EiOH}} = 12.02 \times \frac{0.178}{0.822} = 2.60M$$

Table C.4 Experimental data for 2nd Experiment

T _{rxn} ,K	A _B	A _A	A _E	A _B *a _B	A _A *a _A	A _E *a _E	X _{Af}	Rate
353	1337	1933	142.6	342.272	1933	45.3468	0.117	1.147E-06
353	1542	2019	170.1	394.752	2091	54.0918	0.121	1.180E-06
353	1553	1990	175.7	397.568	2190	55.8726	0.123	1.207E-06
353	1818	2300	201.8	465.408	2450	64.1724	0.121	1.187E-06
Average:							0.120	1.180E-06
358	1335	2077	210.4	341.76	2077	66.9072	0.164	1.605E-06
358	1442	2081	242.2	369.152	2081	77.0196	0.173	1.692E-06
358	1446	2083	239.3	370.176	2083	76.0974	0.171	1.671E-06
358	1476	2103	235.6	377.856	2103	74.9208	0.165	1.622E-06
Average:							0.168	1.647E-06
363	1524	2190	230.4	390.14	2190	73.2672	0.15810	1.550E-06
363	1418	1995	220.1	363.01	1995	69.9918	0.16164	1.584E-06
363	1490	2186	232.6	381.44	2186	73.9668	0.16242	1.592E-06
363	1555	2337	237.2	398.08	2337	75.4296	0.15930	1.561E-06
Average:							0.160	1.572E-06
368	1628	2199	165.6	416.768	2199	52.6608	0.112	1.099E-06
368	1520	2089	151.2	389.12	2089	48.0816	0.110	1.078E-06
368	1598	2095	168.7	409.088	2095	53.6466	0.116	1.136E-06
368	1465	2008	139.6	375.04	2008	44.3928	0.106	1.037E-06
Average:							0.111	1.088E-06
370	1464	3037	115.1	374.784	3037	36.6018	0.089	8.720E-07
370	1436	3075	116.8	367.616	3075	37.1424	0.092	8.994E-07
370	1578	2914	128.5	403.968	2914	40.863	0.092	9.003E-07
370	1564	3046	125.6	400.384	3046	39.9408	0.091	8.890E-07
Average:							0.091	8.902E-07

C.3 Experimental Data for 3rd Experiment (25-wt% TPA/AC, T_{calc.}:120°C)

C_{B0}: 2.82 M, C_{A0}: 12.02 M

Table C.5 By-pass data of 3rd Experiment (w=0.2 g)

A _{2M2B}	A _{EiOH}	A _{2M2B} /A _{EiOH}	X _{2M2B}	X _{EiOH}
2274	2941	0.773	0.165	0.835
2361	3019	0.782	0.167	0.833
2408	3127	0.770	0.165	0.835
2307	2958	0.780	0.166	0.834
Average			0.166	0.834

$$\text{Experimental } C_{B0} = C_{A0} \times \frac{x_{2M2B}}{x_{EiOH}} = 12.02 \times \frac{0.166}{0.834} = 2.39M$$

Table C.6 Experimental data for 3rd Experiment

T _{rxn} ,K	A _B	A _A	A _E	A _B *a _B	A _A *a _A	A _E *a _E	X _{Af}	Rate
353	1415	2127	127.2	362.24	2127	40.4496	0.100	9.221E-07
353	1494	2337	148.4	382.464	2337	47.1912	0.110	1.008E-06
353	1507	2355	150.5	385.792	2345	47.859	0.110	1.013E-06
353	1347	2023	139.8	344.832	2023	44.4564	0.114	1.048E-06
Average:							0.109	9.980E-07
358	1528	2222	102.1	391.168	2222	32.4678	0.077	7.036E-07
358	1577	2263	103.5	403.712	2263	32.913	0.075	6.920E-07
358	1627	2395	111.2	416.512	2395	35.3616	0.078	7.184E-07
358	1624	2342	116.9	415.744	2342	37.1742	0.082	7.535E-07
Average:							0.078	7.169E-07
363	1923	2773	94.5	492.29	2773	30.0351	0.058	5.279E-07
363	1457	2149	77.0	372.99	2149	24.486	0.062	5.655E-07
363	1633	2310	88.4	418.048	2310	28.1112	0.063	5.784E-07
363	1626	2404	90.4	416.256	2404	28.7472	0.065	5.930E-07
Average:							0.062	5.662E-07
368	1693	2385	64.2	433.408	2385	20.4156	0.045	4.130E-07
368	1365	1979	58	349.44	1979	18.444	0.050	4.602E-07
368	1708	2396	72.3	437.248	2396	22.9914	0.050	4.586E-07
368	1672	2363	64.8	428.032	2363	20.6064	0.046	4.216E-07
Average:							0.048	4.384E-07
370	1574	2195	54.5	402.944	2195	17.331	0.041	3.786E-07
370	1678	2416	55.5	429.568	2416	17.649	0.039	3.623E-07
370	1473	2100	50	377.088	2100	15.9	0.040	3.714E-07
370	1612	2248	54.1	412.672	2248	17.2038	0.040	3.674E-07
Average:							0.040	3.699E-07

C.4 Experimental Data for 4th Experiment (25-wt% TPA/AC, T_{calc.}:180°C)

C_{B0}: 2.82 M, C_{A0}: 12.02 M

Table C.7 By-pass data of 4th Experiment (w=0.2 g)

A _{2M2B}	A _{EiOH}	A _{2M2B} /A _{EiOH}	X _{2M2B}	X _{EiOH}
1380	1745	0.791	0.168	0.832
1016	1350	0.753	0.162	0.838
1138	1448	0.786	0.167	0.833
1388	1814	0.765	0.164	0.836
Average			0.165	0.835

$$\text{Experimental } C_{B0} = C_{A0} \times \frac{x_{2M2B}}{x_{EiOH}} = 12.02 \times \frac{0.165}{0.835} = 2.38M$$

Table C.8 Experimental data for 4th Experiment

T _{rxn} ,K	A _B	A _A	A _E	A _B *a _B	A _A *a _A	A _E *a _E	X _{Af}	Rate
353	1556	2251	155.3	398.336	2251	49.3854	0.110	1.043E-06
353	1188	1813	145.7	304.128	1813	46.3326	0.132	1.251E-06
353	1402	2097	192.7	358.912	2097	61.2786	0.146	1.380E-06
353	1076	1681	165.6	275.456	1681	52.6608	0.160	1.518E-06
Average:							0.137	1.298E-06
358	1680	2421	161.6	430.08	2421	51.3888	0.107	1.010E-06
358	1480	2203	132.5	378.88	2203	42.135	0.100	9.468E-07
358	1048	1501	95.4	268.288	1501	30.3372	0.102	9.610E-07
358	1656	2364	180.2	423.936	2364	57.3036	0.119	1.126E-06
Average:							0.107	1.011E-06
363	1768	2395	101.2	452.61	2395	32.1816	0.066	6.280E-07
363	1588	2316	93.0	406.53	2316	29.574	0.068	6.415E-07
363	1512	2185	100.4	387.072	2185	31.9272	0.076	7.208E-07
363	1634	2358	112.6	418.304	2358	35.8068	0.079	7.459E-07
Average:							0.072	6.841E-07
368	1479	2060	80.7	378.624	2060	25.6626	0.063	6.005E-07
368	1443	1954	83.7	369.408	1954	26.6166	0.067	6.358E-07
368	1488	2121	87.9	380.928	2121	27.9522	0.068	6.467E-07
368	1532	2175	100.8	392.192	2175	32.0544	0.076	7.148E-07
Average:							0.069	6.494E-07
370	1552	2099	65.2	397.312	2099	20.7336	0.050	4.692E-07
370	1520	2230	82	389.12	2230	26.076	0.063	5.941E-07
370	1437	1968	83.7	367.872	1968	26.6166	0.067	6.383E-07
370	1476	2074	92.4	377.856	2074	29.3832	0.072	6.826E-07
Average:							0.063	5.960E-07

C.5 Experimental Data for 5th Experiment (31-wt% TPA/AC)

C_{B0}: 2.82 M, C_{A0}: 12.02 M

Table C.9 By-pass data of 5th Experiment (w=0.2 g)

A _{2M2B}	A _{EiOH}	A _{2M2B} /A _{EiOH}	X _{2M2B}	X _{EiOH}
2080	2830	0.735	0.158	0.842
2007	2816	0.713	0.154	0.846
2174	2963	0.734	0.158	0.842
2125	2918	0.728	0.157	0.843
Average			0.157	0.843

$$\text{Experimental } C_{B0} = C_{A0} \times \frac{x_{2M2B}}{x_{EiOH}} = 12.02 \times \frac{0.157}{0.843} = 2.24M$$

Table C.10 Experimental data for 5th Experiment

T _{rxn} ,K	A _B	A _A	A _E	A _B *a _B	A _A *a _A	A _E *a _E	X _{Af}	Rate
353	1182	2024	154.3	302.592	2024	49.0674	0.140	1.321E-06
353	1440	2372	192.3	368.64	2372	61.1514	0.142	1.347E-06
353	1460	2198	198.6	373.76	2198	63.1548	0.145	1.369E-06
353	1196	2007	150	306.176	2007	47.7	0.135	1.276E-06
Average:							0.140	1.329E-06
358	1502	2276	160.3	384.512	2276	50.9754	0.117	1.108E-06
358	1458	2288	160.5	373.248	2288	51.039	0.120	1.139E-06
358	1504	2293	160.1	385.024	2293	50.9118	0.117	1.106E-06
358	1577	2391	160.3	403.712	2391	50.9754	0.112	1.062E-06
Average:							0.117	1.104E-06
363	1322	2122	96.7	338.43	2122	30.7506	0.083	7.880E-07
363	1424	2087	100.8	364.54	2087	32.0544	0.081	7.646E-07
363	1542	2380	99.5	394.752	2380	31.641	0.074	7.020E-07
363	1413	2174	107.5	361.728	2174	34.185	0.086	8.168E-07
Average:							0.081	7.678E-07
368	1426	2193	86.9	365.056	2193	27.6342	0.070	6.657E-07
368	1670	2476	101	427.52	2476	32.118	0.070	6.610E-07
368	1444	2275	90.6	369.664	2275	28.8108	0.072	6.840E-07
368	1532	2298	99.3	392.192	2298	31.5774	0.075	7.049E-07
Average:							0.072	6.789E-07
370	1526	2299	89.2	390.656	2299	28.3656	0.068	6.404E-07
370	1540	2255	82.9	394.24	2255	26.3622	0.063	5.929E-07
370	1742	2572	100.3	445.952	2572	31.8954	0.067	6.314E-07
370	1378	2004	79.8	352.768	2004	25.3764	0.067	6.348E-07
Average:							0.066	6.249E-07

C.6 Experimental Data for 6th Experiment (25-wt% TPA/AC, T_{calc.}:120°C)

C_{B0}: 2.82 M, C_{A0}: 12.02 M

Table C.11 By-pass data of 6th Experiment (w=0.2 g)

A _{2M2B}	A _{EiOH}	A _{2M2B} /A _{EiOH}	X _{2M2B}	X _{EiOH}
2005	2570	0.780	0.166	0.834
2265	2895	0.782	0.167	0.833
2119	2755	0.769	0.165	0.835
2161	2769	0.780	0.167	0.833
Average			0.166	0.834

$$\text{Experimental } C_{B0} = C_{A0} \times \frac{x_{2M2B}}{x_{EiOH}} = 12.02 \times \frac{0.166}{0.834} = 2.39M$$

Table C.12 Experimental data for 6th Experiment

T _{rxn} ,K	A _B	A _A	A _E	A _B *a _B	A _A *a _A	A _E *a _E	X _{Af}	Rate
353	1624	2295	129.8	415.744	2295	41.2764	0.090	8.140E-07
353	1398	2006	109.9	357.888	2006	34.9482	0.089	8.019E-07
353	1328	1991	115.8	339.968	1991	36.8244	0.098	8.809E-07
353	1450	2040	123.1	371.2	2040	39.1458	0.095	8.598E-07
Average:							0.093	8.392E-07
358	1688	2391	110.8	432.128	2391	35.2344	0.075	6.795E-07
358	1490	2128	100.1	381.44	2128	31.8318	0.077	6.942E-07
358	1950	2691	124.4	499.2	2691	39.5592	0.073	6.618E-07
358	1524	2213	97.9	390.144	2213	31.1322	0.074	6.661E-07
Average:							0.075	6.754E-07
363	1548	2085	75.8	396.29	2085	24.1044	0.057	5.168E-07
363	1602	2231	86.2	410.11	2231	27.4116	0.063	5.647E-07
363	1526	2092	80.4	390.656	2092	25.5672	0.061	5.537E-07
363	1712	2425	96.7	438.272	2425	30.7506	0.066	5.909E-07
Average:							0.062	5.565E-07
368	1635	2209	71.3	418.56	2209	22.6734	0.051	4.632E-07
368	1596	2195	67.1	408.576	2195	21.3378	0.050	4.474E-07
368	1755	2364	80.2	449.28	2364	25.5036	0.054	4.842E-07
368	1816	2483	83	464.896	2483	26.394	0.054	4.842E-07
Average:							0.052	4.697E-07
370	1481	2014	49.8	379.136	2014	15.8364	0.040	3.614E-07
370	1569	2111	60.2	401.664	2111	19.1436	0.045	4.100E-07
370	1536	2100	56.7	393.216	2100	18.0306	0.044	3.952E-07
370	1812	2512	65.2	463.872	2512	20.7336	0.043	3.856E-07
Average:							0.043	3.881E-07

C.7 Experimental Data for 7th Experiment (25-wt% TPA/AC, T_{calc.}:180°C)

C_{B0}: 2.82 M, C_{A0}: 12.02 M

Table C.13 By-pass data of 7th Experiment (w=0.2 g)

A _{2M2B}	A _{EiOH}	A _{2M2B} /A _{EiOH}	x _{2M2B}	x _{EiOH}
1830	2145	0.853	0.179	0.821
1515	1996	0.759	0.163	0.837
1638	2084	0.786	0.168	0.832
1488	1941	0.767	0.164	0.836
Average			0.168	0.832

$$\text{Experimental } C_{B0} = C_{A0} \times \frac{x_{2M2B}}{x_{EiOH}} = 12.02 \times \frac{0.165}{0.835} = 2.38M$$

Table C.14 Experimental data for 7th Experiment

T _{rxn} ,K	A _B	A _A	A _E	A _B *a _B	A _A *a _A	A _E *a _E	X _{Af}	Rate
353	1578	2237	156.9	403.968	2237	49.8942	0.110	1.040E-06
353	1494	2251	185.8	382.464	2251	59.0844	0.134	1.266E-06
353	1540	2306	208.5	394.24	2306	66.303	0.144	1.362E-06
353	1493	2295	196.5	382.208	2295	62.487	0.141	1.329E-06
Average:							0.132	1.249E-06
358	1592	2268	146.4	407.552	2268	46.5552	0.103	9.698E-07
358	1746	2595	190.5	446.976	2595	60.579	0.119	1.129E-06
358	1834	2591	173.7	469.504	2591	55.2366	0.105	9.958E-07
358	1935	2890	173.1	495.36	2890	55.0458	0.100	9.461E-07
Average:							0.107	1.010E-06
363	1358	2009	95.6	347.65	2009	30.4008	0.080	7.607E-07
363	1465	2075	118.8	375.04	2075	37.7784	0.092	8.657E-07
363	1114	1618	84.1	285.184	1618	26.7438	0.086	8.111E-07
363	1398	1998	110.7	357.888	1998	35.2026	0.090	8.472E-07
Average:							0.087	8.212E-07
368	1226	1763	80	313.856	1763	25.44	0.075	7.093E-07
368	1564	2121	93.6	400.384	2121	29.7648	0.069	6.546E-07
368	1458	1991	89.8	373.248	1991	28.5564	0.071	6.723E-07
368	1288	1876	79.2	329.728	1876	25.1856	0.071	6.713E-07
Average:							0.072	6.769E-07
370	1704	2380	86.5	436.224	2380	27.507	0.059	5.611E-07
370	1855	2568	106.1	474.88	2568	33.7398	0.066	6.275E-07
370	1592	2209	88.6	407.552	2209	28.1748	0.065	6.117E-07
370	1790	2457	100.6	458.24	2457	31.9908	0.065	6.173E-07
Average:							0.064	6.044E-07

C.8 Experimental Data for 8th Experiment (25-wt% TPA/AC, T_{calc.}:120°C)

C_{B0}: 2.82 M, C_{A0}: 12.02 M

Table C.15 By-pass data of 8th Experiment (w=0.8 g)

A _{2M2B}	A _{EiOH}	A _{2M2B} /A _{EiOH}	X _{2M2B}	X _{EiOH}
2084	2722	0.766	0.164	0.836
2417	3102	0.779	0.166	0.834
2285	2955	0.773	0.165	0.835
2385	2994	0.797	0.169	0.831
Average			0.166	0.834

$$\text{Experimental } C_{B0} = C_{A0} \times \frac{x_{2M2B}}{x_{EiOH}} = 12.02 \times \frac{0.166}{0.834} = 2.39M$$

Table C.16 Experimental data for 8th Experiment

T _{rxn} ,K	A _B	A _A	A _E	A _B *a _B	A _A *a _A	A _E *a _E	X _{Af}	Rate
353	1728	2826	261.4	442.368	2826	83.1252	0.158	3.757E-07
353	1920	3056	278.8	491.52	3056	88.6584	0.153	3.629E-07
353	1630	2438	255.6	417.28	2438	81.2808	0.163	3.872E-07
353	1584	2366	237.8	405.504	2366	75.6204	0.157	3.733E-07
Average:							0.158	3.748E-07
358	1850	2950	224.2	473.6	2950	71.2956	0.131	3.108E-07
358	1652	2598	210	422.912	2598	66.78	0.136	3.239E-07
358	1618	2468	218.8	414.208	2468	69.5784	0.144	3.416E-07
358	1680	2638	202.6	430.08	2638	64.4268	0.130	3.094E-07
Average:							0.135	3.214E-07
363	1582.5	2187	106.4	405.12	2187	33.8193	0.077	1.830E-07
363	1704	2388	113.9	436.22	2388	36.2043	0.077	1.820E-07
363	1588.5	2262	102.2	406.656	2262	32.4837	0.074	1.757E-07
363	1972	2884	116.4	504.832	2884	37.0152	0.068	1.622E-07
Average:							0.074	1.757E-07
368	1692	2283	90.3	433.152	2283	28.7154	0.062	1.477E-07
368	1802	2472	105.4	461.312	2472	33.5172	0.068	1.609E-07
368	1788	2596	97.8	457.728	2596	31.1004	0.064	1.511E-07
368	1824	2734	98.2	466.944	2734	31.2276	0.063	1.489E-07
Average:							0.064	1.521E-07
370	1966	2788	101	503.296	1394	32.118	0.060	1.425E-07
370	1507.5	2101.5	73.8	385.92	1401	23.4684	0.057	1.361E-07
370	1540.5	2079	77.4	394.368	1386	24.6132	0.059	1.395E-07
370	1686	2460	82.2	431.616	1230	26.1396	0.057	1.356E-07
Average:							0.058	1.384E-07

C.9 Experimental Data for 9th Experiment (25-wt% TPA/AC, T_{calc.}:180°C)

C_{B0}: 2.82 M, C_{A0}: 12.02 M

Table C.17 By-pass data of 9th Experiment (w=0.8 g)

A _{2M2B}	A _{EiOH}	A _{2M2B} /A _{EiOH}	X _{2M2B}	X _{EiOH}
2007	2550	0.787	0.168	0.832
1531	1950	0.785	0.167	0.833
2311	2989	0.773	0.165	0.835
2228	2781	0.801	0.170	0.830
Average			0.168	0.832

$$\text{Experimental } C_{B0} = C_{A0} \times \frac{x_{2M2B}}{x_{EiOH}} = 12.02 \times \frac{0.168}{0.832} = 2.43M$$

Table C.18 Experimental data for 9th Experiment

T_{rxn}, K	A_B	A_A	A_E	$A_B \cdot a_B$	$A_A \cdot a_A$	$A_E \cdot a_E$	X_{Af}	Rate
353	1704	2500	308.6	436.224	2500	98.1348	0.184	4.433E-07
353	1324	2144	243.2	338.944	2144	77.3376	0.186	4.484E-07
353	1352	2042	239.8	346.112	2042	76.2564	0.181	4.358E-07
353	1302	2012	244	333.312	2012	77.592	0.189	4.558E-07
Average:							0.185	4.458E-07
358	1366	2010	191.4	349.696	2010	60.8652	0.148	3.578E-07
358	1524	2476	218.2	390.144	2476	69.3876	0.151	3.645E-07
358	1586	2342	231.2	406.016	2342	73.5216	0.153	3.701E-07
358	1628	2458	217	416.768	2458	69.006	0.142	3.429E-07
Average:							0.149	3.588E-07
363	1772	2602	131.8	453.63	2602	41.9124	0.085	2.042E-07
363	1878	2662	143.4	480.77	2662	45.6012	0.087	2.091E-07
363	1716	2510	127.0	439.296	2510	40.386	0.084	2.032E-07
363	1472	2190	112.2	376.832	2190	35.6796	0.086	2.088E-07
Average:							0.085	2.063E-07
368	1768	2416	113.2	452.608	2416	35.9976	0.074	1.778E-07
368	1564	2152	98.4	400.384	2152	31.2912	0.072	1.750E-07
368	1584	2202	105.6	405.504	2202	33.5808	0.076	1.846E-07
368	1442	2090	90.2	369.152	2090	28.6836	0.072	1.740E-07
Average:							0.074	1.779E-07
370	1620	2304	101	414.72	2304	32.118	0.072	1.735E-07
370	1606	2196	96.4	411.136	2196	30.6552	0.069	1.675E-07
370	1704	2270	103.8	436.224	2270	33.0084	0.070	1.698E-07
370	1528	2178	95.2	391.168	2178	30.2736	0.072	1.734E-07
Average:							0.071	1.710E-07

C.10 Experimental Data for 10th Experiment (31-wt% TPA/AC)

C_{B0} : 2.82 M, C_{A0} : 12.02 M

Table C.19 By-pass data of 10th Experiment (w=0.644 g)

A_{2M2B}	A_{EtOH}	A_{2M2B}/A_{EtOH}	x_{2M2B}	x_{EtOH}
2198	2905	0.757	0.162	0.838
2176	2916	0.746	0.160	0.840
2175	3046	0.714	0.155	0.845
2191	2994	0.732	0.158	0.842
Average			0.159	0.841

$$\text{Experimental } C_{B0} = C_{A0} \times \frac{x_{2M2B}}{x_{EtOH}} = 12.02 \times \frac{0.159}{0.841} = 2.27M$$

Table C.20 Experimental data for 10th Experiment

T _{rxn} ,K	A _B	A _A	A _E	A _B *a _B	A _A *a _A	A _E *a _E	X _{Af}	Rate
353	1165	2024	218.9	298.24	2024	69.6102	0.189	5.301E-07
353	1206	2005	212.6	308.736	2005	67.6068	0.180	5.032E-07
353	1061	1954	199.0	271.616	1954	63.282	0.189	5.293E-07
353	1185	2045	230.6	303.36	2045	73.3308	0.195	5.453E-07
Average:							0.188	5.266E-07
358	1254	2062	191.5	321.024	2062	60.897	0.159	4.467E-07
358	1192	1940	186.2	305.152	1940	59.2116	0.163	4.552E-07
358	1275	2192	201.7	326.4	2192	64.1406	0.164	4.601E-07
358	1133	1965	174.4	290.048	1965	55.4592	0.161	4.496E-07
Average:							0.162	4.538E-07
363	1346	2026	122.4	344.576	2026	38.9232	0.101	2.843E-07
363	1482	2284	141.0	379.392	2284	44.838	0.106	2.961E-07
363	1590	2310	127.7	407.04	2310	40.6086	0.091	2.541E-07
363	1284	2165	132.2	328.704	2165	42.0396	0.113	3.176E-07
Average:							0.103	2.885E-07
368	1305	2011	100.8	334.08	2011	32.0544	0.088	2.452E-07
368	1406	2166	93.2	359.936	2166	29.6376	0.076	2.131E-07
368	1350	2208	106.5	345.6	2208	33.867	0.089	2.500E-07
368	1364	2050	98.6	349.184	2050	31.3548	0.082	2.308E-07
Average:							0.084	2.353E-07
370	1420	2227	88.9	363.52	2227	28.2702	0.072	2.021E-07
370	1610	2334	96.8	412.16	2334	30.7824	0.069	1.947E-07
370	1332	1989	85.5	340.992	1989	27.189	0.074	2.069E-07
370	1418	2141	93.4	363.008	2141	29.7012	0.076	2.119E-07
Average:							0.073	2.045E-07

C.11 Experimental Data for 11th Experiment (Amberlyst-15)C_{B0}: 2.82 M, C_{A0}: 12.02 MTable C.21 By-pass data of 11th Experiment (w=0.2 g)

A _{2M2B}	A _{EiOH}	A _{2M2B} /A _{EiOH}	X _{2M2B}	X _{EiOH}
2075	2625	0.790	0.168	0.832
2198	2806	0.783	0.167	0.833
2398	3115	0.770	0.165	0.835
Average			0.167	0.833

$$\text{Experimental } C_{B0} = C_{A0} \times \frac{x_{2M2B}}{x_{EiOH}} = 12.02 \times \frac{0.167}{0.833} = 2.41M$$

Table C.22 Experimental data for 11th Experiment

T_{rxn}, K	A_B	A_A	A_E	$A_B \cdot a_B$	$A_A \cdot a_A$	$A_E \cdot a_E$	X_{Af}	Rate
363	1943	2870	236.2	497.408	2870	75.1116	0.131	1.256E-06
363	2760	4072	410.7	706.56	4072	130.6026	0.156	1.494E-06
363	2905	4380	424.5	743.68	4380	134.991	0.154	1.471E-06
363	2311	3577	360.0	591.616	3577	114.48	0.162	1.552E-06
363	2326	3651	364.2	595.456	3651	115.8156	0.163	1.559E-06
363	2033	3220	326.7	520.448	3220	103.8906	0.166	1.593E-06
363	1779	2775	282.1	455.424	2775	89.7078	0.165	1.576E-06
Average:							0.157	1.500E-06

C.12 Experimental Data for 12th Experiment (Bulk MPA)

C_{B0} : 2.82 M, C_{A0} : 12.02 M

Table C.23 By-pass data of 12th Experiment (w=0.2 g)

A_{2M2B}	A_{EtOH}	A_{2M2B}/A_{EtOH}	X_{2M2B}	X_{EtOH}
2004	2592	0.773	0.165	0.835
1350	1716	0.787	0.168	0.832
1407	1809	0.778	0.166	0.834
1508	1958	0.770	0.165	0.835
Average			0.166	0.834

$$\text{Experimental } C_{B0} = C_{A0} \times \frac{x_{2M2B}}{x_{EtOH}} = 12.02 \times \frac{0.166}{0.834} = 2.39M$$

Table C.24 Experimental data for 12th Experiment

T_{rxn}, K	A_B	A_A	A_E	$A_B \cdot a_B$	$A_A \cdot a_A$	$A_E \cdot a_E$	X_{Af}	Rate
363	1212	1758	119.4	310.272	1758	37.9692	0.109	1.036E-06
363	1492	2180	139.6	381.952	2180	44.3928	0.104	9.892E-07
363	1200	1774	140.8	307.2	1774	44.7744	0.127	1.208E-06
363	1228	1862	163.6	314.368	1862	52.0248	0.142	1.349E-06
363	1336	1948	145.6	342.016	1948	46.3008	0.119	1.133E-06
363	1400	2050	170.6	358.4	2050	54.2508	0.131	1.249E-06
363	1484	2206	181.8	379.904	2206	57.8124	0.132	1.255E-06
Average:							0.124	1.174E-06

C.13 Experimental Data for 13th Experiment (Bulk TPA)

C_{B0} : 2.82 M, C_{A0} : 12.02 M

Table C.25 By-pass data of 13th Experiment (w=0.2 g)

A_{2M2B}	A_{EtOH}	A_{2M2B}/A_{EtOH}	x_{2M2B}	x_{EtOH}
2471	3307	0.747	0.161	0.839
2572	3498	0.735	0.159	0.841
2564	3482	0.738	0.159	0.841
2434	3344	0.729	0.157	0.843
Average			0.159	0.841

$$\text{Experimental } C_{B0} = C_{A0} \times \frac{x_{2M2B}}{x_{EtOH}} = 12.02 \times \frac{0.159}{0.841} = 2.27M$$

Table C.26 Experimental data for 13th Experiment (1.run)

T_{rxn}, K	A_B	A_A	A_E	$A_B \cdot a_B$	$A_A \cdot a_A$	$A_E \cdot a_E$	X_{Af}	Rate
353	1482	2392	185.2	379.392	2392	58.8936	0.134	1.159E-06
353	1542	2504	200.7	394.752	2504	63.8226	0.139	1.201E-06
353	1475	2335	178.3	377.6	2335	56.6994	0.131	1.126E-06
353	1532	2437	190.9	392.192	2437	60.7062	0.134	1.156E-06
Average:							0.135	1.161E-06
358	1698	2783	290.4	434.688	2783	92.3472	0.175	1.512E-06
358	1589	2651	276	406.784	2651	87.768	0.177	1.531E-06
358	1556	2567	259.1	398.336	2567	82.3938	0.171	1.479E-06
358	1640	2732	275.2	419.84	2732	87.5136	0.172	1.488E-06
Average:							0.174	1.502E-06
363	1564	2508	245.4	400.384	2508	78.0372	0.163	1.407E-06
363	1534	2484	250.9	392.704	2484	79.7862	0.169	1.457E-06
363	1518	2437	240.3	388.608	2437	76.4154	0.164	1.418E-06
363	1644	2717	275.6	420.864	2717	87.6408	0.172	1.487E-06
Average:							0.167	1.442E-06
368	1488	2358	146.2	380.928	2358	46.4916	0.109	9.384E-07
368	1589	2439	163.1	406.784	2439	51.8658	0.113	9.756E-07
368	1562	2392	151.2	399.872	2392	48.0816	0.107	9.260E-07
368	1652	2570	187.6	422.912	2570	59.6568	0.124	1.067E-06
Average:							0.113	9.767E-07
370	1606	2464	139.3	411.136	2464	44.2974	0.097	8.391E-07
370	1508	2259	137.6	386.048	2259	43.7568	0.102	8.783E-07
370	1671	2606	148.7	427.776	2606	47.2866	0.100	8.588E-07
370	1580	2402	135.8	404.48	2402	43.1844	0.096	8.323E-07
Average:							0.099	8.521E-07

Table C.27 Experimental data for 13th Experiment (2.run)

T _{rxn} ,K	A _B	A _A	A _E	A _B *a _B	A _A *a _A	A _E *a _E	X _{Af}	Rate
353	1740	2712	186.4	445.44	2712	59.2752	0.117	1.013E-06
353	1368	2301	128.7	350.208	2301	40.9266	0.105	9.027E-07
353	1456	2292	179.8	372.736	2292	57.1764	0.133	1.147E-06
353	1426	2257	180	365.056	2257	57.24	0.136	1.169E-06
Average:							0.123	1.058E-06
358	1446	2323	210.7	370.176	2323	67.0026	0.153	1.322E-06
358	1558	2491	225.9	398.848	2491	71.8362	0.153	1.317E-06
358	1508	2385	229.6	386.048	2385	73.0128	0.159	1.372E-06
358	1464	2345	225.8	374.784	2345	71.8044	0.161	1.387E-06
Average:							0.156	1.350E-06
363	1480	2308	208.7	378.88	2308	66.3666	0.149	1.286E-06
363	1560	2493	218.8	399.36	2493	69.5784	0.148	1.280E-06
363	1605	2595	230.3	410.88	2595	73.2354	0.151	1.305E-06
363	1444	2299	205.2	369.664	2299	65.2536	0.150	1.294E-06
Average:							0.150	1.291E-06
368	1525	2387	129.9	390.4	2387	41.3082	0.096	8.255E-07
368	1690	2592	175.6	432.64	2592	55.8408	0.114	9.862E-07
368	1618	2501	161.7	414.208	2501	51.4206	0.110	9.528E-07
368	1472	2208	122.2	376.832	2208	38.8596	0.093	8.065E-07
Average:							0.103	8.928E-07
370	1659	2449	125.3	424.704	2449	39.8454	0.086	7.400E-07
370	1478	2231	113.8	378.368	2231	36.1884	0.087	7.531E-07
370	1580	2412	129.6	404.48	2412	41.2128	0.092	7.978E-07
370	1435	2137	110.1	367.36	2137	35.0118	0.087	7.507E-07
Average:							0.088	7.604E-07

C.14 Experimental Data for 14th Experiment (25-wt% TPA/AC, T_{calc.}:120°C)

C_{B0}: 2.82 M, C_{A0}: 12.02 M

Table C.28 By-pass data of 14th Experiment (w=0.2 g)

A _{2M2B}	A _{EiOH}	A _{2M2B} /A _{EiOH}	x _{2M2B}	x _{EiOH}
2274	2941	0.773	0.165	0.835
2361	3019	0.782	0.167	0.833
2408	3127	0.770	0.165	0.835
2307	2958	0.780	0.166	0.834
Average			0.166	0.834

$$\text{Experimental } C_{B0} = C_{A0} \times \frac{x_{2M2B}}{x_{EiOH}} = 12.02 \times \frac{0.166}{0.834} = 2.39M$$

Table C.29 Experimental data for 14th Experiment (1.run)

T_{rxn}, K	A_B	A_A	A_E	$A_B \cdot a_B$	$A_A \cdot a_A$	$A_E \cdot a_E$	X_{Af}	Rate
353	1624	2295	129.8	415.744	2295	41.2764	0.090	8.140E-07
353	1398	2006	109.9	357.888	2006	34.9482	0.089	8.019E-07
353	1328	1991	115.8	339.968	1991	36.8244	0.098	8.809E-07
353	1450	2040	123.1	371.2	2040	39.1458	0.095	8.598E-07
Average:							0.093	8.392E-07
358	1688	2391	110.8	432.128	2391	35.2344	0.075	6.795E-07
358	1490	2128	100.1	381.44	2128	31.8318	0.077	6.942E-07
358	1950	2691	124.4	499.2	2691	39.5592	0.073	6.618E-07
358	1524	2213	97.9	390.144	2213	31.1322	0.074	6.661E-07
Average:							0.075	6.754E-07
363	1548	2085	75.8	396.29	2085	24.1044	0.057	5.168E-07
363	1602	2231	86.2	410.11	2231	27.4116	0.063	5.647E-07
363	1526	2092	80.4	390.656	2092	25.5672	0.061	5.537E-07
363	1712	2425	96.7	438.272	2425	30.7506	0.066	5.909E-07
Average:							0.062	5.565E-07
368	1635	2209	71.3	418.56	2209	22.6734	0.051	4.632E-07
368	1596	2195	67.1	408.576	2195	21.3378	0.050	4.474E-07
368	1755	2364	80.2	449.28	2364	25.5036	0.054	4.842E-07
368	1816	2483	83	464.896	2483	26.394	0.054	4.842E-07
Average:							0.052	4.697E-07
370	1481	2014	49.8	379.136	2014	15.8364	0.040	3.614E-07
370	1569	2111	60.2	401.664	2111	19.1436	0.045	4.100E-07
370	1536	2100	56.7	393.216	2100	18.0306	0.044	3.952E-07
370	1812	2512	65.2	463.872	2512	20.7336	0.043	3.856E-07
Average:							0.043	3.881E-07

Table C.30 Experimental data for 14th Experiment (2.run)

T _{rxn} ,K	A _B	A _A	A _E	A _B *a _B	A _A *a _A	A _E *a _E	X _{Af}	Rate
353	1556	2129	115.1	398.336	2129	36.6018	0.084	7.849E-07
353	1562	2308	116.9	399.872	2308	37.1742	0.085	7.934E-07
353	1498	2083	110.6	383.488	2083	35.1708	0.084	7.836E-07
353	1414	2008	105	361.984	2008	33.39	0.084	7.877E-07
Average:							0.084	7.874E-07
358	1677	2319	93.8	429.312	2319	29.8284	0.065	6.060E-07
358	1794	2406	102.7	459.264	2406	32.6586	0.066	6.192E-07
358	1697	2317	89.9	434.432	2317	28.5882	0.062	5.759E-07
358	1596	2285	95.4	408.576	2285	30.3372	0.069	6.447E-07
Average:							0.066	6.115E-07
363	1520	2185	80.4	389.12	2185	25.5672	0.062	5.751E-07
363	1724	2351	78.6	441.344	2351	24.9948	0.054	4.999E-07
363	1318	2092	65.4	337.408	2092	20.7972	0.058	5.415E-07
363	1436	2125	69.2	367.616	2125	22.0056	0.056	5.268E-07
Average:							0.057	5.358E-07
368	1912	2513	77.5	489.472	2513	24.645	0.048	4.471E-07
368	1895	2785	79.6	485.12	2785	25.3128	0.050	4.626E-07
368	1925	2611	82	492.8	2611	26.076	0.050	4.687E-07
368	1662	2353	69.8	425.472	2353	22.1964	0.050	4.625E-07
Average:							0.049	4.602E-07
370	1949	2602	57.9	498.944	2602	18.4122	0.036	3.320E-07
370	1960	2675	61.3	501.76	2675	19.4934	0.037	3.488E-07
370	1696	2200	49.4	434.176	2200	15.7092	0.035	3.257E-07
370	1759	2412	52.7	450.304	2412	16.7586	0.036	3.347E-07
Average:							0.036	3.353E-07

C.15 Experimental Data for 15th Experiment (31-wt% TPA/AC)

C_{B0}: 2.82 M, C_{A0}: 12.02 M

Table C.31 By-pass data of 15th Experiment (w=0.644 g)

A _{2M2B}	A _{EiOH}	A _{2M2B} /A _{EiOH}	X _{2M2B}	X _{EiOH}
2105	2882	0.730	0.158	0.842
1997	2672	0.747	0.161	0.839
2002	2703	0.741	0.159	0.841
Average			0.159	0.841

$$\text{Experimental } C_{B0} = C_{A0} \times \frac{x_{2M2B}}{x_{EiOH}} = 12.02 \times \frac{0.159}{0.841} = 2.27M$$

Table C.32 Experimental data for 15th Experiment

T_{rxn}, K	A_B	A_A	A_E	$A_B \cdot a_B$	$A_A \cdot a_A$	$A_E \cdot a_E$	X_{Af}	Rate
363	1360	2073	98.4	348.16	2073	31.2912	0.082	2.310E-07
363	1589	2365	110.2	406.784	2365	35.0436	0.079	2.222E-07
363	1570	2268	112.1	401.92	2268	35.6478	0.082	2.282E-07
363	1405	2078	99.7	359.68	2078	31.7046	0.081	2.269E-07
363	1593	2360	108.6	407.808	2360	34.5348	0.078	2.187E-07
363	1563	2365	109.5	400.128	2365	34.821	0.080	2.243E-07
363	1440	2109	102.1	368.64	2109	32.4678	0.081	2.267E-07
Average:							0.081	2.254E-07

C.16 Experimental Data for 16th Experiment (Bulk TPA)

Reactant: pure methanol in 1.run, pure ethanol in 2.run

Table C.33 Experimental data of 16th Experiment (methanol)

T_{rxn}, K	A_B	A_A	A_E	$A_B \cdot a_B$	$A_A \cdot a_A$	$A_E \cdot a_E$	X_{Af}	Rate
363	-	1655	-	-	1655	-	-	-
363	-	1679	-	-	1679	-	-	-
363	-	1911	-	-	1911	-	-	-
363	-	1743	-	-	1743	-	-	-
363	-	1760	-	-	1760	-	-	-
363	-	1756	-	-	1756	-	-	-
363	-	1795	-	-	1795	-	-	-

Table C.34 Experimental data of 16th Experiment (ethanol)

T_{rxn}, K	A_B	A_A	A_E	$A_B \cdot a_B$	$A_A \cdot a_A$	$A_E \cdot a_E$	X_{Af}	Rate
363	-	2799	-	-	2799	-	-	-
363	-	2982	-	-	2982	-	-	-
363	-	2880	-	-	2880	-	-	-
363	-	2953	-	-	2953	-	-	-
363	-	2921	-	-	2921	-	-	-
363	-	2951	-	-	2951	-	-	-
363	-	2956	-	-	2956	-	-	-